AD-A124 007 PERFORMANCE ANALYSIS OF DIRECT-SEQUENCE SPREAD-SPECTRUM 1/2
MULTIPLE-ACCESS C..(U) ILLINOIS UNIV AT URBANA
COORDINATED SCIENCE LAB D E BORTH APR 80 R-880
UNCLASSIFIED DAAG29-78-C-0016 F/G 17/2 NL

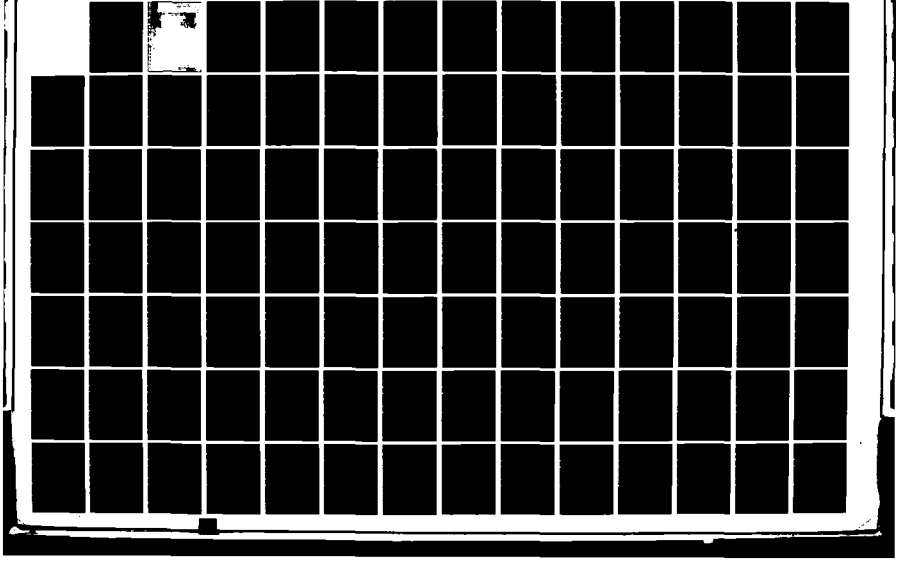

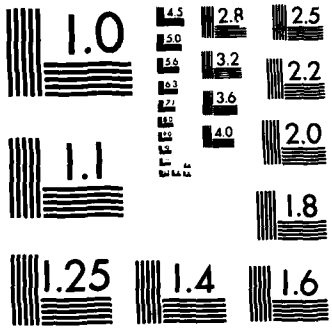

UNCLASSIFIED

SECURITY CLASSIFICATION OF THIS PAGE *(When Data Entered)*

REPORT DOCUMENTATION PAGE		READ INSTRUCTIONS BEFORE COMPLETING FORM
1. REPORT NUMBER	2. GOVT ACCESSION NO. AD-A124 007	3. RECIPIENT'S CATALOG NUMBER
4. TITLE *(and Subtitle)* PERFORMANCE ANALYSIS OF DIRECT-SEQUENCE SPREAD-SPECTRUM MULTIPLE-ACCESS COMMUNICATION VIA FADING CHANNELS		5. TYPE OF REPORT & PERIOD COVERED Technical Report
		6. PERFORMING ORG. REPORT NUMBER R-880; UILU-ENG 80-2212
7. AUTHOR(s) David Edward Borth		8. CONTRACT OR GRANT NUMBER(s) DAAG-29-78-C-0016
9. PERFORMING ORGANIZATION NAME AND ADDRESS Coordinated Science Laboratory University of Illinois at Urbana-Champaign Urbana, Illinois 61801		10. PROGRAM ELEMENT, PROJECT, TASK AREA & WORK UNIT NUMBERS
11. CONTROLLING OFFICE NAME AND ADDRESS Joint Services Electronics Program		12. REPORT DATE April 1980
		13. NUMBER OF PAGES 188
14. MONITORING AGENCY NAME & ADDRESS*(if different from Controlling Office)*		15. SECURITY CLASS. *(of this report)* UNCLASSIFIED
		15a. DECLASSIFICATION/DOWNGRADING SCHEDULE

16. DISTRIBUTION STATEMENT *(of this Report)*

Approved for public release; distribution unlimited

17. DISTRIBUTION STATEMENT *(of the abstract entered in Block 20, if different from Report)*

18. SUPPLEMENTARY NOTES

19. KEY WORDS *(Continue on reverse side if necessary and identify by block number)*

Spread-Spectrum Communication
Fading Channels
Multiple-Access Communication

20. ABSTRACT *(Continue on reverse side if necessary and identify by block number)*

The performance of biphase direct-sequence spread-spectrum multiple-access (SSMA) communication for a general class of fading channels is investigated. The channels considered are those for which the channel output consists of a strong stable specular signal plus a faded version of this signal. Such channels are the result of a transmission medium which gives rise to a major stable communication path and a number of additional weaker communication paths. The fading channel is modeled as a general wide-sense-stationary uncorrelated-scattering (WSSUS) channel -- a model which is general enough

(over)

DD FORM 1 JAN 73 1473

UNCLASSIFIED

SECURITY CLASSIFICATION OF THIS PAGE *(When Data Entered)*

20. ABSTRACT (cont'd)

to exhibit both time and frequency selectivity and to impose no restrictions on the fading rate. A discussion of the important parameters of the WSSUS channel is given and two important classes of WSSUS channels are developed from the general fading channel model: time-selective fading channels and frequency-selective fading channels. In analyzing the performance of direct-sequence SSMA communications via fading channels two measures of system performance that are considered are average signal-to-noise ratio at the receiver output and the average probability of error.

PERFORMANCE ANALYSIS OF DIRECT-SEQUENCE SPREAD-SPECTRUM MULTIPLE-ACCESS COMMUNICATION VIA FADING CHANNELS

by

David Edward Borth

This work was supported in part by the Joint Services Electronics Program under Contract DAAG-29-78-C-0016.

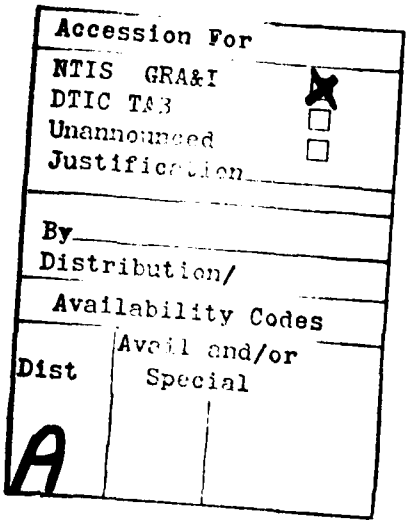

PERFORMANCE ANALYSIS OF DIRECT-SEQUENCE SPREAD-SPECTRUM MULTIPLE-ACCESS COMMUNICATION VIA FADING CHANNELS

BY

DAVID EDWARD BORTH

B.S., University of Illinois, 1974
M.S., University of Illinois, 1975

THESIS

Submitted in partial fulfillment of the requirements
for the degree of Doctor of Philosophy in Electrical Engineering
in the Graduate College of the
University of Illinois at Urbana-Champaign, 1979

Thesis Adviser: Professor Michael B. Pursley

Urbana, Illinois

PERFORMANCE ANALYSIS OF DIRECT-SEQUENCE SPREAD-SPECTRUM MULTIPLE-ACCESS COMMUNICATION VIA FADING CHANNELS

David Edward Borth, Ph.D.
Department of Electrical Engineering
University of Illinois at Urbana-Champaign, 1979

Abstract

The performance of biphase direct-sequence spread-spectrum multiple-access (SSMA) communication for a general class of fading channels is investigated. The channels considered are those for which the channel output consists of a strong stable specular signal plus a faded version of this signal. Such channels are the result of a transmission medium which gives rise to a major stable communication path and a number of additional weaker communication paths. The fading channel is modeled as a general wide-sense-stationary uncorrelated-scattering (WSSUS) channel -- a model which is general enough to exhibit both time and frequency selectivity and to impose no restrictions on the fading rate. A discussion of the important parameters of the WSSUS channel is given and two important classes of WSSUS channels are developed from the general fading channel model: time-selective fading channels and frequency-selective fading channels. In analyzing the performance of direct-sequence SSMA communications via fading channels two measures of system performance that are considered are average signal-to-noise ratio at the receiver output and the average probability of error.

For the general WSSUS model, results are obtained for the average signal-to-noise ratio at the receiver output in terms of the spread-spectrum signature sequences and the covariance function for the fading process. The results are then specialized to both time-selective and frequency-selective fading channels. For these two classes of channels, expressions are obtained for the correlation receiver output signal-to-noise ratio in terms of the aperiodic autocorrelation functions of the signature sequences, the covariance function of the fading process, and the additive white Gaussian noise spectral density. Numerical evaluations are presented for specific examples of each of these two types of channels. The effects of fading on single-user direct-sequence spread-spectrum and phase-shift-keyed systems is discussed and it is shown that the spread-spectrum system yields markedly improved performance over the phase-shift-keyed system when frequency-selective fading channels are considered. Analytical expressions for the average signal-to-noise ratio are derived for a SSMA system with random signature sequences, and the use of these expressions in preliminary system design is discussed.

An expression is derived for the probability of error at the output of a correlation receiver in terms of expectations over the faded signal and the multiple-access interference. Due to analytical difficulties in evaluating the expectations, however, a moment space bounding technique is used to derive bounds on the probability of error. For a single user direct-sequence spread-spectrum system, exact expressions for the probability of error are given for both time-selective and frequency-selective fading channels. These expressions are compared with the results obtained from Nth moment space bounds.

TABLE OF CONTENTS

CHAPTER 1

INTRODUCTION

1.1. Spread-Spectrum Multiple-Access Communication Systems

The advent of the synchronous communication satellite in 1963 [Spilker, 1977] has made possible the realization of practical multiple-access communication systems. This realization of multiple-access communication systems has been achieved principally because of the wide coverage area, small duration of outage times, and simplicity of antenna systems afforded by the use of synchronous orbit satellites. To date, three major types of multiple-access schemes are either being utilized by, or are being proposed for use with, synchronous satellites: frequency-division multiple-access, time-division multiple-access, and code-division multiple-access [Pritchard, 1977]. Frequency-division multiple-access (FDMA) achieves its multiple-access capability through the use of a separate carrier frequency for each user. Its principal advantages are that it is compatible with existing analog trunk systems and that the satellite design for a FDMA system is very simple. Time-division multiple-access (TDMA) achieves its multiple-access capability through the use of a dedicated time-slot for each user. The principal advantages of such a system are that it fits in naturally with digital communication systems and that it exhibits increased capacity over FDMA. The third multiple-access scheme, code-division multiple-access (CDMA), achieves its multiple-access capability primarily through coding. Unlike FDMA and TDMA, however, CDMA requires no precise time or frequency coordination

among the various users. CDMA techniques have been considered for use in a wide variety of applications including the NASA tracking and data-relay system (TDRS) ([Stampfl and Jones, 1970], [Chen and Burnett, 1977]), systems to provide communication to aircraft [Lebow, et. al., 1971], air traffic control systems [Stiglitz, 1973], systems to control remotely-piloted vehicles [Malm and Schreder, 1973], and numerous satellite communication systems (e.g., [Drouilhet and Bernstein, 1969], [Kochevar, 1977], and [Pritchard, 1978]). In fact, a recent survey article of 29 satellite communication systems lists five proposed military satellite communication systems that will use CDMA [Pritchard, 1978].

The most common form of CDMA is spread-spectrum multiple-access (SSMA) which is characterized by the use of a unique code sequence assigned to each user and modulated onto the carrier along with the digital data. By a spread-spectrum system, we mean any system by which a data signal is modulated onto a wideband carrier so that the resultant transmitted signal has a bandwidth which is much larger than the data signal bandwidth [Scholtz, 1977]. The reason for using SSMA is that, in addition to its multiple-access capabilities, other desirable qualities are simultaneously provided including increased immunity from interference and jamming, low detectability, compatability with other (non-spread-spectrum) systems operating in the same frequency band, and, with the proper choice of modulation method, increased immunity from the effects of fading and multipath distortion [Cahn, 1973]. The most commonly used forms of SSMA are: direct sequence SSMA (DS/SSMA), in which a high rate code is used to phase modulate, together with the data signal, the carrier-signal;

frequency-hopped SSMA (FH/SSMA), in which a code sequence is used to control a frequency-synthesized carrier signal onto which data is modulated, and hybrid SSMA, which can be a combination of DS/SSMA and FH/SSMA. By way of example, DS/SSMA will be used in the NASA TDRS system [Chen and Burnett, 1977], FH/SSMA has been used in the TATS modulation system for the Lincoln Experimental Satellites [Drouilhet and Bernstein, 1969], and hybrid SSMA will be used in the proposed Joint Tactical Information Distribution System (JTIDS), a military communication, navigation, and identification system [Smith, 1978].

For the remainder of this thesis we shall be concerned only with DS/SSMA, also known in the literature as phase-coded SSMA [Pursley, 1974] or pseudonoise SSMA [Anderson and Wintz, 1969]. In particular, we shall be concerned with analysis of the communication performance of an asynchronous DS/SSMA communication system operating over a fading channel. Such a system has been previously analyzed elsewhere for communication over additive white Gaussian noise (AWGN) channels (e.g., [Pursley, 1974], [Pursley, 1977], [Yao, 1977]). In the next section we shall present a review of some of the results obtained on the performance of DS/SSMA communications via AWGN channels.

1.2. DS/SSMA Communications via AWGN Channels

In this section we will initially review the results obtained by Pursley (1974, 1979) for the communications performance of an asynchronous DS/SSMA communication system operating over an additive white Gaussian noise (AWGN) channel. The purpose of this review is threefold: to review

the principles of operation of a DS/SSMA communication system, to introduce notation that will be useful in the analysis of DS/SSMA communications via fading channels, and to provide a basis of comparison of performance for DS/SSMA communications via fading channels. Later in this section we shall present a brief review of other published literature on the performance of DS/SSMA systems over AWGN channels.

We shall consider the DS/SSMA system model shown in Fig. 1 for K users. The k-th users' data signal $b_k(t)$ is a sequence of unit amplitude, positive and negative, rectangular pulses of duration T, given by

$$b_k(t) = \sum_{\ell=-\infty}^{\infty} b_{k,\ell} p_T(t-\ell T), \tag{1.1}$$

where $b_{k,\ell} \in \{+1,-1\}$ denotes the k-th user's information sequence and $p_\tau(t) = 1$ for $0 \leq t < \tau$ and $p_\tau(t) = 0$ otherwise. Each user is assigned a code waveform $a_k(t)$ which consists of a periodic sequence of unit amplitude, positive and negative, rectangular pulses of duration T_c. The code waveform for the k-th user may therefore be written as

$$a_k(t) = \sum_{j=-\infty}^{\infty} a_j^{(k)} p_{T_c}(t-jT_c), \tag{1.2}$$

where $(a_j^{(k)})$ is the discrete periodic signature sequence assigned to the k-th user. We assume that each signature sequence has period $N = T/T_c$ so that there is one code period per data symbol.

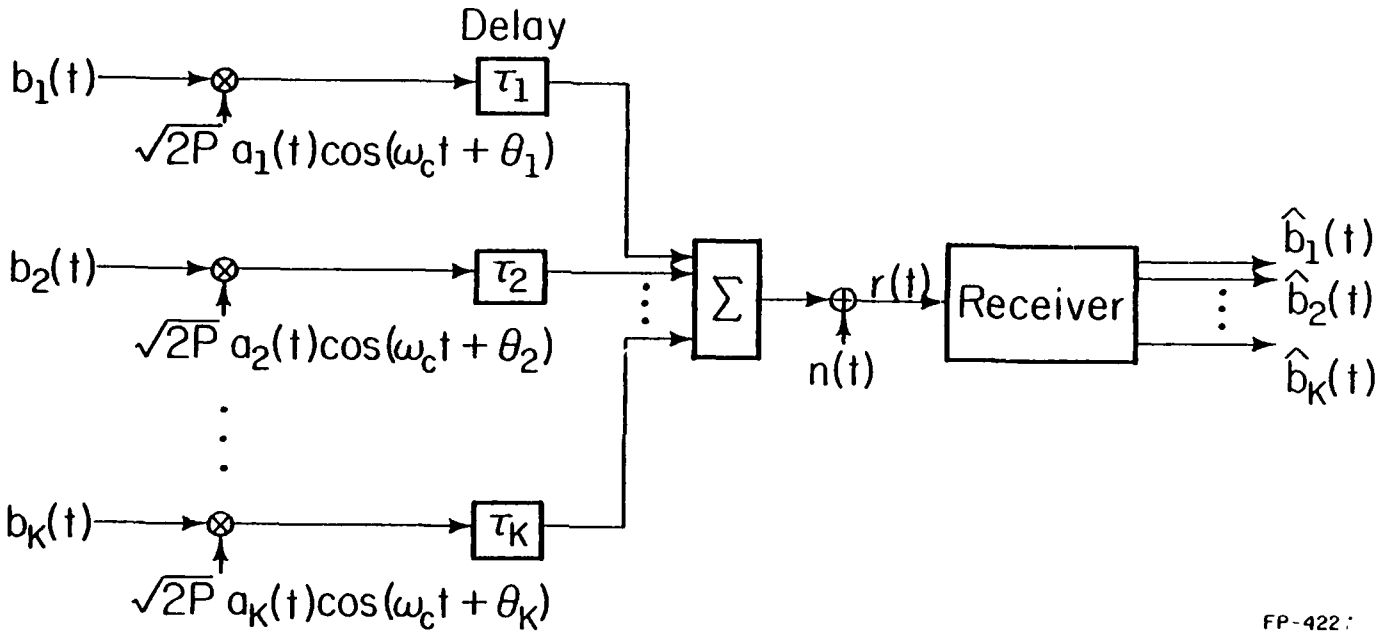

Figure 1. DS/SSMA system model with AWGN channel.

The data signal $b_k(t)$ is modulated onto the phase-coded carrier $c_k(t)$, which is given by

$$c_k(t) = \sqrt{2P}\, a_k(t)\cos(\omega_c t + \theta_k) \tag{1.3}$$

so that the transmitted signal for the k-th user is

$$s_k(t) = \sqrt{2P}\, a_k(t)b_k(t)\cos(\omega_c t + \theta_k)\ . \tag{1.4}$$

Here P represents the common signal power, ω_c represents the common center frequency, and θ_k represents the phase of the k-th carrier.

For asynchronous systems, the received signal r(t) at the input to the receiver in Figure 1 is given by

$$r(t) = n(t) + \sum_{k=1}^{K} \sqrt{2P}\, a_k(t-\tau_k)b_k(t-\tau_k)\cos(\omega_c t+\varphi_k) \tag{1.5}$$

where $\varphi_k \triangleq \theta_k - \omega_c\tau_k$, τ_k accounts for the nominal propagation time for the k-th signal, and n(t) is additive white Gaussian noise with a two-sided spectral density $N_0/2$.

If the received signal r(t) is the input to a correlation receiver matched to $s_i(t)$, the output Z_i at the sample moment t = T is given by [Pursley, 1977] as

$$\begin{aligned} Z_i &= \int_0^T r(t)a_i(t)\cos\,\omega_c t dt \\ &= \sqrt{P/2}\,\{b_{i,0}T + \sum_{\substack{k=1 \\ k\neq i}}^{K} [b_{k,-1}R_{k,i}(\tau_k)+b_{k,0}\hat{R}_{k,i}(\tau_k)]\cos\,\varphi_k\} \\ &\quad + \int_0^T n(t)a_i(t)\cos\,\omega_c t dt. \end{aligned} \tag{1.6}$$

Since we are concerned with relative phase shifts modulo 2π and relative time delays modulo T, we have assumed in (1.6), without loss of generality, that $\theta_i = 0$ and $\tau_i = 0$. Furthermore, as in [Pursley, 1977], in writing (1.6), we have neglected the double frequency components. The two terms $R_{k,i}$ and $\hat{R}_{k,i}$ appearing in (1.6) are the continuous-time partial cross-correlation functions of the code waveforms, defined by

$$R_{k,i}(\tau) = \int_0^{\tau} a_k(t-\tau)a_i(t)dt \tag{1.7}$$

$$\hat{R}_{k,i}(\tau) = \int_{\tau}^{T} a_k(t-\tau)a_i(t)dt \tag{1.8}$$

for $0 \le \tau \le T$. For convenience, we shall denote the continuous-time partial autocorrelation functions $R_{k,k}$ and $\hat{R}_{k,k}$ by R_k and $\hat{R}_k$, respectively. For values of τ in the range $0 \le \ell T_c \le \tau \le (\ell+1)T_c \le T$, the two cross-correlation functions $R_{k,i}$ and $\hat{R}_{k,i}$ can be written as

$$R_{k,i}(\tau) = C_{k,i}(\ell-N)T_c + [C_{k,i}(\ell+1-N)-C_{k,i}(\ell-N)](\tau-\ell T_c) \tag{1.9}$$

$$\hat{R}_{k,i}(\tau) = C_{k,i}(\ell)T_c + [C_{k,i}(\ell+1) - C_{k,i}(\ell)](\tau-\ell T_c) \tag{1.10}$$

where $C_{k,i}$ is the discrete aperiodic cross-correlation function for the sequences $(a_j^{(k)})$ and $(a_j^{(i)})$ defined by

$$C_{k,i}(\ell) = \begin{cases} \sum_{j=0}^{N-1-\ell} a_j^{(k)} a_{j+\ell}^{(i)}, & 0 \le \ell \le N-1 \\ \sum_{j=0}^{N-1+\ell} a_{j-\ell}^{(k)} a_j^{(i)}, & 1-N \le \ell < 0 \\ 0 & |\ell| \ge N. \end{cases} \tag{1.11}$$

The discrete aperiodic autocorrelation function $C_{k,k}$ will be denoted by C_k.

Up to this point, we have not indicated any means of measuring the DS/SSMA system performance. Three performance measures that have been considered in the past are average signal-to-noise ratio [Pursley, 1974], [Pursley, 1977], worst case performance [Pursley, 1977], and average probability of error [Yao, 1977]. For DS/SSMA systems with AWGN channels, the work of Yao (1977), coupled with the results of Pursley and Sarwate (1977b) on the efficient computation of signal-to-noise ratio establishes that for systems of interest, the signal-to-noise ratio is an accurate measure of performance which is relatively easy to compute. Using the average signal-to-noise ratio (SNR) at the output of the i-th correlation receiver as the measure of system performance, as in [Pursley, 1977], the phase angles, time delays, and data symbols for the k-th signal ($k \neq i$) are modeled as mutually independent random variables which are uniformly distributed on $[0,2\pi]$, $[0,T]$, and $\{+1,-1\}$, respectively. SNR_i is then defined by

$$SNR_i \triangleq E\{Z_i | b_{i,0} = +1\} / (Var\{Z_i | b_{i,0} = +1\})^{\frac{1}{2}}, \tag{1.12}$$

where, without loss of generality, we have assumed $b_{i,0} = +1$. From (1.6) we find that

$$E\{Z_i | b_{i,0} = +1\} = \sqrt{P/2}\ T \tag{1.13}$$

and

$$Var\{Z_i | b_{i,0} = +1\} = \left(\frac{P}{4T}\right) \sum_{\substack{k=1 \\ k\neq i}}^{K} \int_0^T [R_{k,i}^2(\tau) + \hat{R}_{k,i}^2(\tau)]d\tau + \tfrac{1}{2}N_0T$$

$$= \left(\frac{P}{4T}\right) \sum_{\substack{k=1 \\ k\neq i}}^{K} \sum_{\ell=0}^{N-1} \int_{\ell T_c}^{(\ell+1)T_c} [R_{k,i}^2(\tau) + \hat{R}_{k,i}^2(\tau)]d\tau + \tfrac{1}{2}N_0T. \tag{1.14}$$

Using (1.9) and (1.10) in (1.14), (1.14) reduces to

$$\mathrm{Var}\{Z_i | b_{i,0} = +1\} = \frac{PT^2}{12N^3}\left(\sum_{\substack{k=1 \\ k\neq i}}^{K} r_{k,i}\right) + \tfrac{1}{2}N_0 T \tag{1.15}$$

where

$$r_{k,i} \triangleq 2\mu_{k,i}(0) + \mu_{k,i}(1) \tag{1.16}$$

and

$$\mu_{k,i}(n) \triangleq \sum_{\ell=1-N}^{N-1} C_{k,i}(\ell)\, C_{k,i}(\ell+n), \tag{1.17}$$

which is a function of the discrete aperiodic cross-correlation functions $C_{k,i}$. In [Pursley and Sarwate, 1977b], it was shown that $\mu_{k,i}(n)$ can be also expressed by

$$\mu_{k,i}(n) = \sum_{\ell=1-N}^{N-1} C_k(\ell)\, C_i(\ell+n) \tag{1.18}$$

which is a function of the discrete aperiodic <u>autocorrelation</u> functions of the code signature sequences. From (1.12), (1.13), and (1.15), the average signal-to-noise ratio at the output of the i-th correlation receiver is found to be

$$\mathrm{SNR}_i = \left\{(6N^3)^{-1} \sum_{\substack{k=1 \\ k\neq i}}^{K} r_{k,i} + \frac{N_0}{2\mathcal{E}}\right\}^{-\frac{1}{2}} \tag{1.19}$$

where $\mathcal{E} \triangleq PT$ is the signal energy per bit.

In addition to the results obtained by Pursley (1974, 1977) indicated

above, many other results have been obtained on the performance of DS/SSMA communications via AWGN channels. In 1977, Yao (1977) presented several approaches for evaluating bounds on the average probability of error (P_e) of a DS/SSMA system using an isomorphism theorem from the theory of moment spaces. Under a certain set of conditions (K large, N large, and $N \gg K$), Yao verified that P_e could be approximated quite well by the expression $P_e = 1-\Phi(SNR_i)$, where Φ is the standard Gaussian cumulative distribution function and SNR_i is given by (1.19). Further discussion of Yao's work may be found in Chapter 4 of this thesis. Also in 1977, Roefs and Pursley (1977) evaluated the performance of a DS/SSMA system employing binary random sequences as signature sequences. They found that the expression obtained for the average signal-to-noise ratio using random binary signature sequences,

$$SNR = \left\{ \frac{N_0}{2\mathcal{E}} + \frac{K-1}{3N} \right\}^{-\frac{1}{2}}, \qquad (1.20)$$

was a very accurate approximation to SNR_i for typical system values of $\mathcal{E}/N_0$, N, and K and thus is useful in the preliminary design of a DS/SSMA system. In 1978, the results of [Pursley, 1977] were extended to the quadriphase DS/SSMA system case ([Pursley and Garber, 1978], [Garber, 1978a]). Generally speaking, the results obtained for the quadriphase DS/SSMA system case are very similar to the biphase DS/SSMA system case with the exception that a broader class of signature sequences can be employed by the quadriphase system, offering promise of improved performance over AWGN channels. Other results that have been obtained on the performance of DS/SSMA communication systems over AWGN channels deal primarily with properties of the signature sequence correlation functions

appearing in (1.19) (e.g., see [Roefs, 1977], [Pursley and Sarwate, 1977a], [Pursley and Roefs, 1979], [Sarwate and Pursley, 1979]). A tutorial treatment of many of these properties as well as an extensive bibliography of other papers treating correlation properties of signature sequences may be found in [Sarwate and Pursley, 1979].

1.3 Direct Sequence Spread Spectrum Communications via Fading Channels

In Section 1.1 we noted that one of the reasons for considering SSMA as a multiple-access technique was that, with the proper choice of modulation method, SSMA could be designed to reduce the effects of fading. In fact, one of the earliest applications of spread spectrum techniques was in communicating over multipath channels by employing a pseudonoise modulated frequency-shift keyed (FSK) signal [Price and Green, 1958]. In this section we shall review some of the literature on the performance of direct sequence spread-spectrum (DS/SS) communications via fading channels.

One of the earliest studies on the performance of DS/SSMA over multipath channels was one conducted by Massey and Uhran (1969) for NASA in 1969. This study was concerned with the design of good sets of signature sequences which would permit reliable communication over multipath channels. Essentially this study culminated in the realization that the odd cross-correlation function of the signature sequences, defined in [Pursley, 1977], is just as important as the periodic cross-correlation function for communication over multipath channels or for asynchronous DS/SSMA communications. Some of these results have also been reported in [Massey and Uhran, 1975]. Kadar and Schreiber

(1971) considered the effects of a single fading path together with a single nonfading path on the performance of a DS/SS system employing a post-detection correlation receiver. Their primary result was an expression for the signal-to-interference ratio, neglecting thermal noise, at the output of the post-detection correlation receiver. Cahn (1973) presented "heuristic" analyses of the effects of direct-plus-specular multipath and direct-plus-diffuse multipath on the performance of a single-user DS/SS communication system. Cahn assumed that the fading components of the received signal were Gaussian and hence could be treated as additional noise in deriving an expression for the probability of error at the output of a correlation receiver. Jacobs (1974), in a tutorial paper considered the effects of a direct-plus-specular multipath channel model on a DS/SS system. Finally, Chang (1979), considered the effects of fading on the performance of a digital matched filter in a communication system employing amplitude shift keying (ASK) together with a maximal-length shift register signature sequence.

Within the past several years, there have appeared several studies on the effects of fading on DS/SSMA communication systems ([Orr, 1977], [Welch, 1978], [Gardner and Orr, 1979]). All of these studies have concentrated on determining the system signal-to-noise ratio and/or probability of error for multiple-user DS/SS systems communicating via a class of channels known as nondispersive, slow-fading channels (see Chapter 2).

The literature survey given above is intended to indicate the amount and direction of research that has already been performed on DS/SS communications via fading channels. It is also intended to

indicate some of the deficiencies in the analysis of DS/SSMA communications over fading channels. In particular, in all of the analyses presented to date, little, if any attention has been given to detailed consideration of the fading channel model being used. While the assumptions of direct-plus-specular fading or nondispersive fading may be valid for some physical channels, the channels over which spread-spectrum systems are employed often exhibit radically different channel characteristics. For example, because the bandwidth occupied by a DS/SSMA system is typically quite large, the channel used may exhibit frequency selectivity due to the presence of a distribution of channel paths over which the signal propagates. Clearly, such a characteristic is not incorporated in either the direct-plus-specular channel model or the nondispersive fading channel models. Furthermore, the published results noted above have either made certain very specialized assumptions in deriving the results above or have not used correlation receivers in the DS/SSMA system model. In this thesis we will analyze the performance of the DS/SSMA system model shown in Figure 1 for a broad class of fading channels. In the next section an outline of the thesis research is given.

1.4 Outline of the Thesis

Chapter 2 describes a comprehensive model of a fading channel in terms of the statistical properties of the channel with the viewpoint of characterizing typical fading channels over which DS/SSMA systems might be used. This characterization includes development of the important wide-sense-stationary uncorrelated-scattering (WSSUS) channel model and three subclasses of the WSSUS channel model: the time-selective

fading channel model, the frequency-selective fading channel model, and the nondispersive fading channel model.

Chapter 3 analyzes the performance of DS/SSMA communications via fading channels using the average signal-to-noise ratio at the output of a correlation receiver as the system performance measure. In this analysis, the DS/SSMA system model of Chapter 1 is used together with the WSSUS fading channel model of Chapter 2. After analysis of system performance over doubly-spread channels is considered, performance of the DS/SSMA system over time-selective and frequency-selective fading channels is analyzed. A comparison of the performance of single-user phase-shift keyed (PSK) and DS/SS communication systems over fading channels is given. An analysis of the performance of a DS/SSMA system using random binary sequences as the signature sequences is also given.

Chapter 4 analyzes the performance of DS/SSMA communications via fading channels using probability of error at the output of a correlation receiver as the system performance measure. Bounds on the probability of error are obtained using an isomorphism theorem from the theory of moment spaces. The "Gaussian approximation" for the probability of error, $P_e \approx 1 - \Phi(SNR_i)$, for DS/SSMA communications via fading channels is discussed.

In Chapter 5, a summary of the major results of this thesis is given.

CHAPTER 2

INTRODUCTION TO FADING CHANNELS

2.1. A Description of Fading

In many analyses of the performance of various types of communication systems, the communication channel is frequently modeled as a linear time-invariant system whose transfer function consists of a frequency-independent magnitude less than unity proportional to the propagation loss and a delay term proportional to the propagation delay between the channel modulator and the channel demodulator. In addition, the channel is usually considered to be corrupted by additive stationary Gaussian noise. While this simple additive white Gaussian noise model is quite accurate for channels such as deep space communication channels, it is often an overly-simplified model for high-frequency (HF) long distance communications achieved via the ionosphere and for microwave communications beyond the horizon achieved through the use of tropospheric scatter. In the latter two channels, the received signal has been experimentally shown to undergo a process known as fading. Fading is a term generally used to describe any linear channel whose performance is other than that of the ideal channel described above. A fading channel may exhibit such properties as selective frequency response, intersymbol interference in digital communications, spreading of signals in the frequency domain, a time-varying amplitude response, or any combination of these attributes. The description of a comprehensive model for a fading channel is given in this chapter. The remainder of this section will describe fading from a phenomenological point of view and give special examples of fading channels.

In addition to the two examples of fading channels given above, the HF ionospheric channel and the microwave tropospheric scatter channel, there exist several other types of channels which exhibit fading. One example is a very high frequency (VHF) communication link between an aircraft and a synchronous satellite relay [Bond and Meyer, 1966]. Such a link has been analyzed and has been shown to exhibit fading due to the presence of a secondary propagation path between the satellite, the earth's surface, and the airplane, in addition to the primary propagation path between the airplane and the satellite. Another example of a fading channel, this time an artificially created one, is the communications channel temporarily created by an experiment known as the West Ford Project [Lebow, et. al., 1964]. In this project, 20 Kg of 2 cm long copper dipoles were injected into an orbit about the earth and transhorizon communications were conducted at 8GHZ using this orbiting dipole belt as a scattering mechanism. Fading was predicted prior to the experiment and confirmed experimentally during the course of the experiment. A third example of a fading channel is that of line-of-sight microwave communication links. Although such links are designed to provide reliable point-to-point communications, occasionally these links undergo severe fading due to the formation of tropospheric inversion layers permitting multiple transmission paths between the transmitting and receiving antennas [Jakes, 1978]. As a result of these multiple paths, the received signal is a vector sum of several delayed versions of the transmitted signal, and consequently, depending on the phase relationship of the received multiple signals, the channel exhibits

fading. Recently, Rummler (1978, 1979) has shown that the fading effects exhibited by line-of-sight microwave channels could be modeled well by a three-path channel model. A final example of another channel exhibiting fading, and one of much current interest, is that of communication at millimeter to optical wavelengths in line-of-sight paths through the non-ionized atmosphere [Strohbehn, 1968]. In this channel, fading is present due to random fluctuations in the dielectric constant of the atmosphere. These four examples serve to demonstrate that fading is not limited to just the two "classical" fading channels, the HF ionospheric and microwave tropospheric scatter channels.

Fading encountered over an HF ionospheric channel, for example, has been experimentally verified to be of two types -- short duration rapid fading over time spans less than a second and long duration slow fading over time spans from one second to an hour or longer. The statistics of the two fading processes are different; hence these two types of fading must be accounted for in the channel model. It will be shown in Section 2.3 that the two types of fading lead to a "quasi-wide-sense-stationary" fading channel model for practical radio channels.

The origin of the fading mechanism for most of the fading channels mentioned above may be traced to the scattering of an electromagnetic wave off a random medium. To see how this leads to fading, consider the following: let a single continuous sine wave be allowed to be scattered by a random medium. The scattered components may be resolved into in-phase and quadrature components. The instantaneous values of the two types of components may be shown to be uncorrelated. Using the central limit theorem, as the number of in-phase and quadrature components becomes

large, the sum of the in-phase components approaches a Gaussian random process. Similarly, the quadrature components add to form an identically distributed Gaussian random process. Hence, the in-phase and quadrature random processes collectively form a zero-mean complex Gaussian random process [Van Trees, Sec. A.3.1, 1971]. If the random medium is a single surface and is time-invariant, the received signal, after scattering, can be shown to have a Rayleigh-distributed amplitude and uniformly distributed phase, i.e., the signal is undergoing fading. Further discussion of the modelling of scattering of sinusoids off of random media as a complex Gaussian random process may be found in [Stein, 1966]; in the following we will accept the fact that scattering results in a zero-mean complex Gaussian random process, provided that a "sufficient number" of random scatterers exists for the particular geometry under consideration.

2.2. Statistical Model of Fading

In this section, we develop the most general model of the fading channel with the idea in mind that the model should be applicable to the analysis of DS/SSMA communications over fading channels. In subsequent sections, the model developed here will be simplified by making appropriate assumptions.

To begin with, since the signals under consideration are bandpass signals (i.e., narrow-band signals centered at some frequency ω_0), complex envelope notation is the most convenient method of describing these signals. To clarify the notation to be used, several standard properties ([Van Trees, 1971], [Stein, 1966], [Stein and Jones, 1967]) of bandpass signals are given below in complex envelope notation.

The transmitted signal may be represented in complex envelope notation as

$$s_0(t) = \mathrm{Re}[u_0(t)\exp(j2\pi f_0 t)], \tag{2.1}$$

where $u_0(t)$ is a lowpass signal having a Fourier transform $U_0(f)$,

$$u_0(t) = \int_{-\infty}^{\infty} U_0(f)\exp(j2\pi ft)df. \tag{2.2}$$

By narrowband signals, we mean that if we define the normalized bandwidth of $u_0(t)$ as

$$B_n = \frac{\int |U_0(f)|^2 df}{|U_0(0)|^2} \tag{2.3}$$

then

$$B_n \ll f_0. \tag{2.4}$$

Given a linear, time-invariant system with an impulse response $h(t)$ and a transfer function $H(f)$, where

$$h(t) = \int_{-\infty}^{\infty} H(f)e^{+j2\pi ft}df = \mathrm{Re}\{2h_e(t)\exp(j2\pi f_0 t)\} \tag{2.5}$$

and $H(f)$ is a bandpass function around f_0, the output $y(t)$ due to an input $s_0(t)$ given by (2.1) is

$$y(t) = \mathrm{Re}\left[y_e(t)e^{j\omega_0 t}\right] \tag{2.6}$$

where

$$y_e(t) = \int_{-\infty}^{\infty} h_e(t-\sigma)u_0(\sigma)d\sigma \ . \tag{2.7}$$

Equations (2.6) and (2.7) illustrate the advantage of using complex envelope notation for bandpass signals and systems; to evaluate the output of a bandpass system due to a bandpass signal input, we simply convolve the impulse response envelope with the input signal envelope, multiply by $\exp(j2\pi f_0 t)$ and take the real part of the resulting product.

For a linear time-varying bandpass system with impulse response $h(t,\tau)$ where

$$h(t,\tau) = \mathrm{Re}[2h_e(t,\tau)\exp(j2\pi(t-\tau))], \tag{2.8}$$

the expression corresponding to (2.7) is

$$y_e(t) = \int_{-\infty}^{\infty} h_e(t,u)u_0(u)du. \tag{2.9}$$

In (2.8), $h(t,\tau)$ denotes the output at time t due to an impulse at time τ.

Finally, we will need the following algebraic identity: Given two complex numbers X and Y, then

$$\mathrm{Re}[X]\mathrm{Re}[Y] = \tfrac{1}{2}\,\mathrm{Re}[XY] + \tfrac{1}{2}\,\mathrm{Re}[XY^*]. \tag{2.10}$$

Other properties of complex envelope notation will be developed as needed.

We now proceed to the development of the fading channel model. Consider the propagation model shown in Figure 2. In the figure, a signal $s_0(t)$ given by (2.1) is transmitted and scattered by a moving random medium which is assumed to be able to be modeled as a layered scatterer, where each layer has an incremental thickness dr. Associated with each layer is a propagation delay τ which is in addition to the nominal propagation delay t_0 between the transmitter and the receiver. The received signal due to scattering from the layer whose incremental

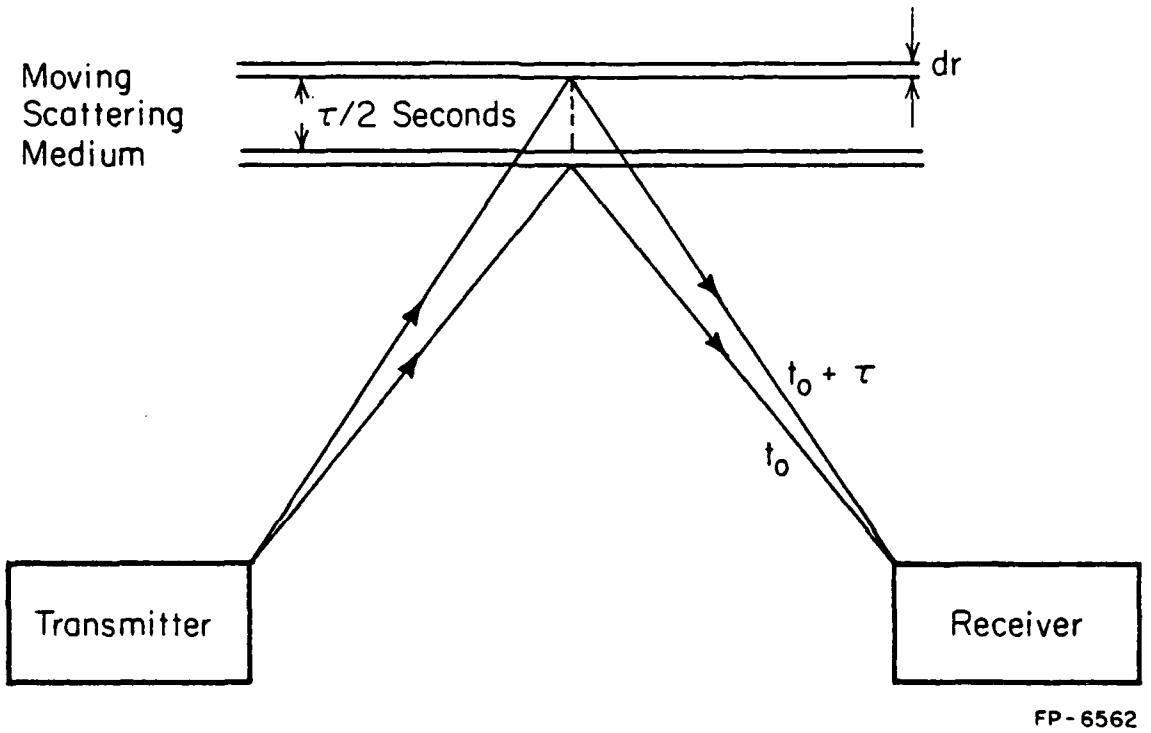

Figure 2. Propagation model of a fading channel.

propagation delay is τ is given by

$$s(t,\tau) = \mathrm{Re}[\beta(\tau, t-t_0)u_0(t-t_0-\tau)\exp(j2\pi f_0(t-t_0-\tau))]d\tau \qquad (2.11)$$

where $\beta(\tau,t)$ is the time-varying transmission coefficient for a wave scattering of a layer whose incremental propagation delay is τ. Several comments about the form of (2.11) are in order. First, (2.11) assumes that the thickness dr and its corresponding propagation delay $d\tau$ may be chosen small enough such that $\beta(\tau,t)$ is constant in its first argument over the delay $d\tau$. This allows the effect of scattering off a single layer to be modeled as a simple time-varying multiplicative factor as opposed to some form of superposition of responses. Second, it is important to note that the received signal $s(t,\tau)$ is a function of <u>two</u> arguments: the first denotes time and the second denotes the incremental propagation delay due to the layer that the transmitted signal is being scattered from. Hence the received signal is both time-varying due to the fact that the scattering volume was assumed to be moving, and layer dependent since the scattering medium was assumed to be able to be modelled as consisting of differential layers. Third, the time origins of the various terms of (2.11) should be noted. For a received signal at time t due to scattering from a layer having a <u>total</u> propagational delay of $t_0 + \tau$ associated with it, the signal would have to be transmitted at time $t-t_0-\tau$. Thus the arguments of $u_0(\cdot)$ and $\exp(j2\pi f(\cdot))$ are the transmitted time origin. The second argument of $\beta(\tau, t-t_0)$ refers to the nominal time at which the received signal was transmitted. Such a time origin is by no means unique; other authors have made the time origin of the scattering process

the actual time origin of the transmitted signal $t-t_0-\tau$ [Kailath, 1961] or the time at which the transmitted wave was scattered off a reasonably well-defined medium [Van Trees, Ch. 13, 1971]. All such time origins are essentially equivalent, although one choice of time origin may be more appealing to the intuition for a given type of scattering medium. Finally, the statistical nature of $\beta(\tau,t)$ must be determined. From our discussion in Section 2.1, we assume $\beta(\tau,t)$ to be a zero-mean complex Gaussian random process. Inherent in this assumption is the fact that $\beta(\tau,t)$ has a Rayleigh-fading envelope and a uniformly distributed phase, both of which are time varying due to the presence of a moving random medium. Hence, the term $\exp(j2\pi f_0\tau)$ may be absorbed into $\beta(\tau,t)$ in (2.11).

The total received signal is a superposition of the responses due to all the scattered layers:

$$s(t) = \int_{-\infty}^{\infty} s(t,\tau)d\tau = \mathrm{Re}\left[\int_{-\infty}^{\infty} \beta(\tau,t-t_0)u_0(t-t_0-\tau)\exp[j2\pi f_0(t-t_0)]d\tau\right]. \quad (2.12)$$

Equation (2.12) may also be written in the form

$$s(t) = \mathrm{Re}[u(t-t_0)\exp\, j(2\pi f_0(t-t_0))] \quad (2.13)$$

where

$$u(t) = \int_{-\infty}^{\infty} \beta(\tau,t)u_0(t-\tau)d\tau = \int_{-\infty}^{\infty} \beta(t-\tau,t)u_0(\tau)d\tau. \quad (2.14)$$

Comparing (2.13) and (2.14) with (2.6) and (2.9), it is readily seen that $\beta(\tau,t)$ represents a time-varying equivalent low-pass impulse response for the general fading channel. Applying an impulse at time α to (2.14), we obtain

$$u_I(t) = \int_{-\infty}^{\infty} \beta(\tau,t)\, \delta(t-\alpha-\tau)d\tau = \beta(t-\alpha,t). \qquad (2.15)$$

That is, $\beta(t-\alpha,t)$ is the response at time t to an impulse applied at time α.

Equation (2.12) represents the most general model of a fading channel that we will discuss here. Before proceeding further, experimental evidence justifying the use of this model as well as suggesting other models will be examined briefly. To begin with, if the random medium is slowly varying with time and can be modeled as consisting of a single layer, (2.12) reduces to

$$s(t) = \mathrm{Re}[\beta u_0(t-t_0)\exp\, j2\pi f_0(t-t_0)] \qquad (2.16)$$

where β is a zero-mean complex Gaussian random variable. The assumptions necessary for the transition from (2.12) to (2.16) will be examined in greater detail in Section 2.7. Letting the transmitted signal be a continuous sine wave at a frequency f_0, (2.16) becomes

$$s(t) = \mathrm{Re}[\beta \exp\, j2\pi f_0(t-t_0)]. \qquad (2.17)$$

It can be shown that the amplitude of a zero-mean complex Gaussian random variable is Rayleigh-distributed and the phase uniformly distributed. Hence (2.17) predicts that the amplitude of the received sine wave is Rayleigh distributed. Experimental evidence (e.g. [McNicol, 1949], [Grisdale, et.al., 1957]) for the HF ionospheric channel tends to support this prediction; at the same time, experimental data [McNicol, 1949] for many fading channels exhibit a Rician amplitude distribution. Rician fading is usually considered to be due to a specular component in the

received path, i.e., the presence of a fixed non-random scatterer in the transmitter-receiver propagation path. In this case (2.12) may be modified to include a deterministic component in the received signal:

$$s(t) = \mathrm{Re}[(Au(t-t_0) + \int_{-\infty}^{\infty} \beta(\tau, t-t_0)u_0(t-t_0-\tau))d\tau \exp(j2\pi f_0(t-t_0)] \quad (2.18)$$

where A is the transmission coefficient associated with the specular path. The presence of a specular component is necessary for coherent communications including DS/SSMA communication systems; accordingly (2.18) will be used in subsequent work.

The above comments are not meant to suggest that all fading is Rician or Rayleigh in nature; on the contrary, experimental data for the HF ionospheric channel and the mm-to-optical wave line-of-sight channel indicate that the amplitude of the received signal is lognormally distributed in many instances. Stein (1966) suggests that deviations from a Rayleigh amplitude distribution for the HF ionospheric channel may be due to an insufficient number of scatterers in a scattering "layer" to support the complex Gaussian random process hypothesis stated in Section 2.1. For the line-of-sight mm-to-optical wave channel, Strohbehn (1968) has shown that the channel may be modeled as consisting of a very large number of randomly moving slabs. The transmitted signal is then modulated by the product of the random transmission coefficients of each of the slabs. Assuming the transmission coefficients to be independent of each other, the logarithm of the overall channel amplitude transmission function is the sum of the logarithms of the slab transmission

functions and, using a central limit theorem argument, is thus normally distributed. The channel transmission function is then seen to be lognormally distributed in amplitude. Despite the fact that some channels may be modelled as exhibiting a lognormal amplitude distribution, for the remainder of this study, we assume that the fading channels of concern exhibit predominately Rician fading.

In determining the performance of communication systems over fading channels, frequent use is made of the second order statistical properties of the channel model. In particular, assuming $\beta(\tau,t)$ to be a zero-mean complex Gaussian process, given $u_0(t)$, $u(t)$ given by (2.14) is also a zero-mean complex Gaussian process which is completely characterized statistically by its covariance function. What is not commonly realized however, is that for a bandpass process represented by complex envelope notation, <u>two</u> covariance functions are needed to completely characterize the second order properties of the process. To see this, the covariance of $s(t)$ given by (2.12) is defined in the usual manner as

$$R_s(t_1,t_2) = E\{s(t_1)s(t_2)\}. \tag{2.19}$$

Using (2.12) and (2.10) in (2.19), we obtain

$$\begin{aligned} R_s(t_1,t_2) = \mathrm{Re}\Bigg[&\int_{-\infty}^{\infty}\int_{-\infty}^{\infty} \tfrac{1}{2}E\{\beta(\tau_1,t_1-t_0)\beta(\tau_2,t_2-t_0)\}u_0(t_1-t_0-\tau_1)u_0(t_2-t_0-\tau_2) \\ &\cdot\exp[j\pi f_0(t_1+t_2-2t_0)]d\tau_1 d\tau_2\Bigg] \\ + \mathrm{Re}\Bigg[&\int_{-\infty}^{\infty}\int_{-\infty}^{\infty} \tfrac{1}{2}E\{\beta(\tau_1,t_1-t_0)\beta^*(\tau_2,t_2-t_0)\}u_0(t_1-t_0-\tau_1)u_0^*(t_2-t_0-\tau_2) \\ &\cdot\exp[j2\pi f_0(t_1-t_2)]d\tau_1 d\tau_2\Bigg] . \end{aligned} \tag{2.20}$$

Note that to evaluate (2.20), two covariance functions are needed,

$$\tilde{\Lambda}(\tau_1,\tau_2;t_1,t_2) \triangleq \tfrac{1}{2}E\{\beta(\tau_1,t_1)\beta(\tau_2,t_2)\} \tag{2.21}$$

and

$$\Lambda(\tau_1,\tau_2;t_1,t_2) \triangleq \tfrac{1}{2}E\{\beta(\tau_1,t_1)\beta^*(\tau_2,t_2)\}. \tag{2.22}$$

$\Lambda(\cdot)$ given by (2.22) is defined to be the space-time cross-covariance function (or simply the covariance function) of the fading process [Stein, 1966]. In most applications, the narrow-band process $\beta(\tau,t)$ is so constituted that ([Bello, 1963], [Van Trees, 1971])

$$\tilde{\Lambda}(\tau_1,\tau_2;t_1,t_2) \equiv 0. \tag{2.23}$$

Examples of processes which do not satisfy (2.23) are given in ([Bello, 1961], [Brown and Crane, 1969]). It is easily seen that (2.23) is a <u>necessary</u> condition for stationary bandpass processes. For by representing the equivalent bandpass impulse response in complex envelope notation as

$$B(\tau,t) = \mathrm{Re}\{\beta(\tau,t)\exp(j2\pi f_0 t)\} \tag{2.24}$$

as in (2.8), the autocorrelation function of $B(\tau,t)$ is given by

$$\begin{aligned} R_B(\tau_1,t_1;\tau_2,t_2) &= \mathrm{Re}[\tfrac{1}{2}E\{\beta(\tau_1,t_1)\beta(\tau_2,t_2)\}\exp(j2\pi f_0(t_1+t_2))] \\ &\quad + \mathrm{Re}[\tfrac{1}{2}E\{\beta(\tau_1,t_1)\beta^*(\tau_2,t_2)\}\exp(j2\pi f_0(t_1-t_2))] \\ &= \mathrm{Re}[\tilde{\Lambda}(\tau_1,\tau_2;t_1,t_2)\exp(j2\pi f_0(t_1+t_2))] \\ &\quad + \mathrm{Re}[\Lambda(\tau_1,\tau_2;t_1,t_2)\exp(j2\pi f_0(t_1-t_2))]. \end{aligned} \tag{2.25}$$

In order for $R_B(\cdot)$ to be a function only of the time difference $t_1 - t_2$, $\tilde{\Lambda}(\cdot)$ must vanish in (2.25). A different proof of this result utilizing the spectra of the bandpass processes may be found in [Van Trees, Sec. A.3.1, 1971]. Grettenberg (1965) has proven that a necessary and sufficient condition for (2.23) to hold is that $\beta(\tau,t)$ and $e^{j\theta}\beta(\tau,t)$ be identically distributed for all real θ. A more direct proof of this latter result may be found in [Miller, Th. II.4.4, 1974].

In the sequel, it will be assumed that (2.23) holds for <u>all</u> complex envelope processes that we shall encounter. There are three reasons for this: First, in virtually all the literature on fading channels (e.g., [Bello, 1963], [Kennedy, 1969], [Stein, 1966], [Van Trees, 1971]) this assumption is made either explicitly or by modelling the equivalent bandpass impulse response as a stationary process. Second, if $\tilde{\Lambda}(\cdot)$ is non-zero, much of the appeal of the representation of bandpass processes by complex envelope notation is lost since two covariance processes must now be specified whereas the real bandpass process requires only one. Finally, and probably the most important reason from a practical standpoint is the fact that even if $\tilde{\Lambda}(\cdot)$ were non-zero, it is doubtful that a meaningful measurement of $\tilde{\Lambda}(\cdot)$ could be made over an actual fading channel, considering the difficulty in measuring $\Lambda(\cdot)$ [Bello, 1971].

One other covariance function associated with the general fading channel model given by (2.12) is the frequency-time cross-covariance [Stein, 1966] defined by

$$R_F(f_1,f_2;t_1,t_2) \triangleq \tfrac{1}{2}E\{H(f_1;t_1)H^*(f_2;t_2)\} \tag{2.26}$$

where

$$H(f;t) = \int_{-\infty}^{\infty} \beta(\tau;t)\exp(-j2\pi f\tau)\,d\tau \tag{2.27}$$

is the range Fourier transform of the equivalent low-pass impulse response $\beta(\tau,t)$ for the channel. Using (2.27) in (2.26) we obtain

$$R_F(f_1,f_2;t_1,t_2) = \int_{-\infty}^{\infty}\int_{-\infty}^{\infty} \Lambda(\tau_1,\tau_2;t_1,t_2)\exp(j2\pi(f_1\tau_1-f_2\tau_2))d\tau_1 d\tau_2 \qquad (2.28)$$

which is recognized to be the double Fourier transform of the space-time cross-covariance function.

In practice the very general fading channel model developed above is difficult to use in the performance analysis of communication systems due to the mathematical complexities involved. Furthermore, as has been shown by Bello (1963), a simpler model is warranted for most radio channels. In the next section, we will develop such a model.

2.3. The WSSUS Fading Channel

We now develop the wide-sense stationary uncorrelated scattering (WSSUS) fading channel model from the general fading channel model (2.12) presented in Section (2.2). In this development, we will also define the wide-sense stationary (WSS) channel and the uncorrelated scattering (US) channel.

In Section 2.1 we noted that some channels exhibit two types of fading: long-term fading and short-term fading. Short term fading over these channels is often such that the short term fading statistics are approximately stationary over time. Hence, it is convenient to define a subclass of the general fading channel model known as wide-sense stationary (WSS) channels. Bello (1963) defines the WSS channel as a channel whose correlation functions $R_F(\cdot)$ and $\Lambda(\cdot)$ are invariant under a translation in time. The space-time cross-covariance function given

by (2.22) satisfies

$$\Lambda(\tau_1,\tau_2;t_1,t_2) = \Lambda(\tau_1,\tau_2;t_1-t_2) \tag{2.29}$$

while the frequency-time cross-covariance function given by (2.26) satisfies

$$R_F(f_1,f_2;t_1,t_2) = R_F(f_1,f_2;t_1-t_2) \tag{2.30}$$

for the WSS channel.

While developing the general fading channel model in Section 2.2, we assumed that the scattering medium could be modeled as consisting of differential layers. A reasonable assumption for many channels is to assume that the complex Gaussian process $\beta(\tau,t)$ is independent of $\beta(\sigma,t)$ for $\tau \neq \sigma$. Note that this is equivalent to assuming that the effect of scatterers in one differential layer is independent of the effect of the scatterers in all other differential layers. The space-time cross-covariance function for such a channel is given by

$$\Lambda(\tau_1,\tau_2;t_1,t_2) = \Lambda(\tau_1;t_1,t_2)\delta(\tau_1 - \tau_2). \tag{2.31}$$

Channels whose space-time cross-covariance functions satisfy (2.31) are known as uncorrelated scattering (US) channels [Bello, 1963]. We remark in passing that the US channel is the wide-sense dual of the WSS channel using the definitions of duality given by Bello (1964).

Channels which exhibit both WSS channel characteristics and US channel characteristics are known as wide-sense stationary uncorrelated scattering (WSSUS) channels [Bello, 1963]. Using (2.29) and (2.31), the space-time cross-covariance function for a WSSUS channel is given by

$$\Lambda(\tau_1,\tau_2;t_1,t_2) = \rho(\tau_1,t_1-t_2)\delta(\tau_1-\tau_2), \tag{2.32}$$

where for convenience we have let $\rho(\tau_1,t_1-t_2) = \Lambda(\tau_1,\tau_2;t_1,t_2)$ for the special case of a WSSUS channel. Note that for WSSUS channels, two assumptions on $\Lambda(\cdot)$ are being made: (1) the scattering processes due to different layers are statistically uncorrelated and (2) the scattering processes in each layer are wide-sense stationary. Since $\beta(\tau,t)$ is a zero-mean complex Gaussian process which satisfies (2.23), wide-sense stationarit, of $\beta(\tau,t)$ implies strict-sense stationarity of $\beta(\tau,t)$ [Miller, 1974].

Although the above channel models simplify the determination of the performance of communication systems considerably, they would be of little value unless these models correspond to actual fading channels. Fortunately, most radio channels appear to exhibit WSSUS channel properties ([Bello, 1963], [Stein, 1966]). As noted in Section 2.1, radio channel fading is often characterized by the superposition of short-term fading on long-term fading. The short-term fading is usually found to exhibit stationary statistics while the long-term fading is often highly non-stationary, depending upon the time interval of interest. Bello (1963) has introduced the term quasi-wide-sense stationary uncorrelated scattering (QWSSUS) to describe such a channel. As might be expected, a QWSSUS channel has WSSUS channel characteristics over time intervals on the order of the duration of short-term fading. Over longer time intervals, the channel correlation functions no longer exhibit stationarity. However, Bello (1963) has noted that the performance of communication systems over QWSSUS channels may be evaluated by computing system

performance by modeling the channel as a WSSUS channel, and then averaging the short-time system performance over the long-term fading statistics of the channel. In light of this, for the remainder of this chapter, we will consider the WSSUS channel model only. An additional reason for considering this model is that the WSSUS channel is the simplest nondegenerate channel which exhibits both time- and frequency-selective behavior.

2.4. Doubly-Spread Channels

In the previous section, we developed the WSSUS fading channel model from the general fading channel model. In this section, we discuss the most general class of WSSUS channels, known either as doubly-spread channels [Van Trees, 1971] or doubly-dispersive channels [Kennedy, 1969]. Our goal is to characterize the various parameters of doubly-spread channels and to introduce notation often used in conjunction with discussions of fading channels.

A word about terminology is first in order. Doubly-spread channels are so called because they spread the time and frequency waveforms of a signal transmitted through the channel. Demonstration of this spreading in both domains must wait until discussion of the singly-spread degenerate channels which exhibit spreading in only one domain.

For the doubly-spread channel, the space-time cross-covariance function of the channel is given by (2.32). The scattering function $S_{DR}(\tau,f)$ of the channel is defined to be

$$S_{DR}(\tau,f) \triangleq \int_{-\infty}^{\infty} e^{-j2\pi ft}\rho(\tau,t)dt, \tag{2.33}$$

where $\rho(\tau,t)$ is defined implicitly by (2.32). Note that the scattering function is the temporal Fourier transform of $\rho(\tau,t)$.

The scattering function provides a means of characterizing the Doppler spread of the channel, as will be seen shortly. It should be noted that most of the results to this point and for the rest of this chapter could just as well have been developed in terms of the channel scattering function instead of the channel covariance function; see Kennedy (1969) for such an approach. Because the channel scattering function and the channel covariance function are Fourier transform pairs, such parallelism is to be expected.

If the scattering function is concentrated in one region of the τ,f plane, it may be characterized grossly in terms of its moments. We make the following definitions [Van Trees, 1971]:

The mean delay is defined to be

$$m_R \triangleq \frac{1}{2\sigma_b^2} \int\int_{-\infty}^{\infty} \tau \, S_{DR}(\tau,f) d\tau df. \tag{2.34}$$

The mean-square delay spread is defined to be

$$L \triangleq \frac{1}{2\sigma_b^2} \int\int_{-\infty}^{\infty} \tau^2 S_{DR}(\tau,f) d\tau df - m_R^2 \quad . \tag{2.35}$$

The mean Doppler shift is defined to be

$$m_D \triangleq \frac{1}{2\sigma_b^2} \int\int_{-\infty}^{\infty} f \, S_{DR}(\tau,f) d\tau df. \tag{2.36}$$

The mean-square Doppler spread is defined to be

$$B \triangleq \frac{1}{2\sigma_b^2} \int\int_{-\infty}^{\infty} f^2 S_{DR}(\tau,f) d\tau df - m_D^2 \quad . \tag{2.37}$$

In (2.34)-(2.37),

$$2\sigma_b^2 = \iint_{-\infty}^{\infty} S_{DR}(\tau,f)\,d\tau\,df \ . \tag{2.38}$$

In addition, we will define the duration T and the bandwidth W of a narrowband bandpass signal given by (2.1) to be

$$T = \frac{1}{E_t}\int_{-\infty}^{\infty} t^2 |u_0(t)|^2 dt \tag{2.39}$$

and

$$W = \frac{1}{E_t}\int_{-\infty}^{\infty} f^2 |U_0(t)|^2 df \tag{2.40}$$

where

$$E_t = \int_{-\infty}^{\infty} |u_0(t)|^2 dt \tag{2.41}$$

and $U_0(t)$ is defined by (2.2).

This definition of the mean-square properties L, B, T, and W is not unique; Kennedy (1969) defines these properties using Lerner's (1959) definition of the duration of a signal. The definitions given above are given only for completeness. For strictly time- or band-limited scattering functions and/or bandpass signals, simpler definitions will be used for L, B, T, and W.

An underspread channel is defined to be one for which [Van Trees, 1971]

$$BL < 1; \tag{2.42}$$

similarly, an overspread channel is defined to be one for which [Van Trees, 1971]

$$BL > 1 \ . \tag{2.43}$$

In reviewing the literature on doubly-spread channels, the terms correlation (or coherence) time and correlation (or coherence) bandwidth are often encountered in characterizing the channel [Kennedy, 1969]. The correlation time of a fading channel is defined to be the time separation τ_c beyond which samples of the received complex envelope are independent. Since the channel scattering process is assumed to be modeled as a zero-mean complex Gaussian process, given the transmitted signal, the received signal envelope is also a zero-mean complex Gaussian process. Thus independence of time samples is implied if the correlation function of the envelope is zero. Using (2.32) and (2.14), the correlation between time samples of the received signal envelope is

$$R_{TE}(t_1,t_2) \triangleq \tfrac{1}{2} E\{u(t_1)u^*(t_2)\} = \int_{-\infty}^{\infty} \rho_T(\tau,t_1-t_2)u_0(t_1-\tau)u_0^*(t_2-\tau)d\tau . \qquad (2.44)$$

By convention, we choose the correlation time for the channel to be the <u>smallest</u> time separation $\tau_c = t_1-t_2$ for which

$$R_{TE}(t_1,t_2) = 0. \qquad (2.45)$$

In a similar fashion, the correlation bandwidth of a fading channel is defined to be the frequency separation W_c beyond which samples of the Fourier transform of the received complex envelope are independent. From the comments above, the received signal envelope is a complex Gaussian process and it therefore follows that the Fourier transform of the received envelope is also a complex Gaussian process. Thus independence of frequency samples is implied if the correlation function of the Fourier transform of the received envelope is zero. From (2.14), the Fourier transform of the received envelope is

$$U(f) = \int_{-\infty}^{\infty}\int \beta(\tau,t)u_0(t-\tau)\exp(-j2\pi ft)d\tau dt. \tag{2.46}$$

Using (2.32), the correlation between frequency samples of the Fourier transform of the received signal envelope is given by

$$R_{FE}(f_1,f_2) \triangleq \tfrac{1}{2} E\{U(f_1)U^*(f_2)\}$$

$$= \int_{-\infty}^{\infty}\int\int \rho(\tau,t_1-t_2)u_0(t_1-\tau)u_0^*(t_2-\tau)\exp[j2\pi(f_2t_2-f_1t_1)]d\tau dt_1 dt_2 \tag{2.47}$$

By convention, we choose the correlation bandwidth for the channel to be the <u>smallest</u> frequency separation $W_c = f_1-f_2$ for which

$$R_{FE}(f_1,f_2) = 0 . \tag{2.48}$$

In Sections 2.5 and 2.6 simpler expressions are derived for the correlation functions of the received envelope for time separations and frequency separations, respectively.

Finally, we note that in the above, the doubly-spread channel was characterized in terms of its channel covariance function and the temporal Fourier transform of this quantity, the channel scattering function. Alternatively, we could have characterized the channel by the spatial Fourier transforms of these two quantities:

$$R_{DR}(\nu,t) \triangleq \int_{-\infty}^{\infty} \rho(\tau,t)\exp(-j2\pi\nu\tau)d\tau \tag{2.49}$$

and

$$P_{DR}(\nu,f) \triangleq \int_{-\infty}^{\infty} S_{DR}(\tau,f)\exp(-j2\pi\nu\tau)d\tau \tag{2.50}$$

The quantity $R_{DR}(f,\nu)$ defined in (2.49) is known as the two-frequency correlation function [Van Trees, 1971]; the quantity $P_{DR}(f,\nu)$ in (2.50) is defined to be the Doppler cross-power spectral density [Bello, 1963]. The usefulness of having the four quantities $\rho(\tau,t)$, $S_{DR}(\tau,f)$, $R_{DR}(\nu,t)$, and $P_{DR}(\nu,f)$ comes in characterizing doubly-spread channels which have correlation functions which are concentrated in one or more of the variables time t, Doppler spread f, delay spread τ, or delay frequency ν. We shall find in Section 2.6 that the two-frequency correlation function is useful in parameterizing a subclass of doubly-spread channels.

In this section we have defined and characterized the most general WSSUS fading channel, the doubly-spread channel. Often fading radio channels exhibit spreading predominately in either the time or frequency domains only. In still other cases, the fading effects are such that they may be modeled by a random variable instead of a random process. In such cases, it is convenient to define subclasses of doubly-spread channels having specific characteristics. In the next three sections we will develop the models for three subclasses of doubly-spread fading channels, also known as degenerate channels [Van Trees, 1971].

2.5. Time-Selective Fading Channels

In Section 2.2, we developed the general model of a fading channel by assuming that the scattering medium could be modeled as a randomly moving, layered volume of scatterers; each layer of which could be modeled as a complex Gaussian process. In this section we will assume that the scattering medium can be modeled as a single layer of randomly moving scatterers. As will be seen, such an assumption leads to the development of a class of channels known as time-selective fading channels.

To begin with, assume that a signal $s_0(t)$ given by (2.1) is transmitted through a scattering medium that can be modeled as a single layer. The received signal is

$$s(t) = \mathrm{Re}[\beta(t-t_0)u_0(t-t_0)\exp(j2\pi f_0(t-t_0))] \tag{2.51}$$

where t_0 is the propagation time between the transmitter and receiver and $\beta(t)$ is the time-varying transmission coefficient due to the scattering medium. From the comments in Section 2.1, we will assume $\beta(t)$ is a sample function from a zero-mean complex Gaussian random process. Equation (2.51) may also be written as

$$s(t) = \mathrm{Re}[u(t-t_0)\exp(j2\pi f_0(t-t_0))] \tag{2.52}$$

where

$$u(t) = \beta(t)u_0(t). \tag{2.53}$$

For the WSSUS channel model, $\beta(t)$ is a stationary random process. It is important to note that since $\beta(t)$ is a complex-valued process it influences both the amplitude and the phase of the transmitted signal $s_0(t)$.

Equations (2.51) or (2.52) and (2.53) together with the condition that $\beta(t)$ be a stationary process constitute what is known as the time-selective fading channel model [Bello and Nelin, 1963]. Other adjectives often used to describe this channel model include channels dispersive only in frequency [Kennedy, 1969], frequency-flat fading channels [Bello and Nelin, 1963], or Doppler-spread channels [Van Trees, 1971]. The basis of this terminology will become clear as the properties of time-selective fading channels are discussed.

Equation (2.51) could just as easily have been derived directly from the doubly-spread fading channel model by noting that (2.51) is identical in form to (2.11), except for the argument of β. Hence the general fading channel model (2.12) reduces to (2.11) where the range variable τ of β is no longer important. In terms of covariance functions of the channel, the channel covariance function for the time-selective fading channel is

$$\rho(\tau, t-s) = \rho(0, t-s)\delta(\tau). \tag{2.54}$$

In the following, we will use (2.54) for the channel correlation function for time-selective fading channels rather than define a new time autocorrelation function that directly characterizes $\beta(t)$ in (2.51).

Some comments on the form of (2.53) are in order. First, since $u_0(t)$, the transmitted envelope, is being multiplied by $\beta(t)$, which is independent of frequency, the received envelope $u(t)$ in (2.53) is easily seen to undergo fading that is independent of frequency; i.e., the various frequency components of $u_0(t)$ fade identically (frequency-flat fading). Nevertheless, $\beta(t)$ in (2.53) is a time-varying function and as such, acts to modulate the transmitted envelope $u_0(t)$. This leads to spreading of the Fourier transform of the transmitted envelope in the frequency-domain; hence, the origin of the term Doppler-spread fading. Finally, since $\beta(t)$ in (2.53) is independent of τ, the uncorrelated scattering condition of WSSUS channels is not really necessary in characterizing time-selective fading channels.

Using (2.54) in (2.33), the scattering function for a time-selective fading channel is

$$S_{DR}(\tau,f) = S_D(0,f)\delta(\tau) = \delta(\tau)\int_{-\infty}^{\infty} e^{-j2\pi ft}\rho(0,t)dt. \tag{2.55}$$

The term $S_D(0,f)$ in (2.55) is known as the Doppler scattering function of the channel.

From (2.55) and (2.36), we see that the mean Doppler shift for a time-selective fading channel is

$$m_D = \frac{1}{2\sigma^2}\int_{-\infty}^{\infty} fS_D(0,f)df; \tag{2.56}$$

similarly, from (2.55) and (2.37) we see that the mean-square Doppler spread is

$$B = \frac{1}{2\sigma_b^2}\int_{-\infty}^{\infty} f^2S_D(0,f)df - m_D^2 \tag{2.57}$$

where

$$2\sigma_b^2 = \int_{-\infty}^{\infty} S_D(0,f)df. \tag{2.58}$$

The mean-square Doppler spread characterizes the Doppler spread around the mean Doppler shift due to the time-selective properties of the fading channel.

Using (2.55) in (2.34) and (2.35), it is readily seen that the mean delay and mean-square delay spread for a time-selective fading channel are identically zero:

$$m_R = L = 0. \tag{2.59}$$

Thus the time-selective fading channel exhibits spreading in frequency but not in delay and is therefore often called a singly-spread channel. Another singly-spread channel will be encountered in the next section.

To clarify the relationship between correlation time, the channel correlation function, and the correlation between time samples of the received signal envelope for a time-selective fading channel, consider the following example. Note first that by using (2.54) in (2.44), the correlation between time samples of the received signal envelope for a time-selective fading channel is

$$R_{TED}(t_1,t_2) = \rho(0,t_1-t_2)u_0(t_1)u_0^*(t_2) \ . \tag{2.60}$$

For this example, let the Doppler scattering function for the channel be of the form

$$S_D(0,f) = \begin{cases} 1; & -\frac{B}{2} < f < \frac{B}{2} \\ 0; & \text{elsewhere} \ . \end{cases} \tag{2.61}$$

The corresponding channel correlation function $\rho(0,\Delta t)$ is therefore

$$\rho(0,\Delta t) = B\,\frac{\sin\pi B\Delta t}{\pi B\Delta t} \ .$$

The correlation time as defined by (2.45) is given by

$$\tau_c = \frac{1}{B} \ , \tag{2.62}$$

provided

$$u_0(t_1)u_0^*(t_1-\Delta t) \neq 0 \text{ for } 0 < \Delta t < \frac{1}{B} \ . \tag{2.63}$$

Thus time samples of the received signal separated by 1/B seconds will be uncorrelated.

Suppose, however, that we transmit a pulse of duration T through the channel where

$$T \ll \frac{1}{B} \quad . \tag{2.64}$$

In this case, it is the pulse itself that determines τ_c and the correlation time is equal to the duration of the pulse. From (2.60) and this example, we may conclude that, provided (2.64) holds, time samples of the received envelope separated by less than the pulse duration T will be correlated. In Section 2.7 we will see that (2.64) is a necessary condition for the development of the non-dispersive fading channel model.

2.6. Frequency-Selective Fading Channels

The second subclass of doubly-spread fading channels that we will look at are known as frequency-selective fading channels [Bello and Nelin, 1963]. As is the case for time-selective fading channels, frequency-selective fading channels result from doubly-spread channels by making different assumptions about characteristics of the scattering medium. For frequency-selective fading channels, we assume that the scattering medium may be modeled as a fixed (non-moving) volume consisting of differential layers. For a transmitted signal $s_0(t)$ given by (2.1), the received signal scattered from a single layer is

$$s(t,\tau) = \mathrm{Re}[\beta(\tau)u_0(t-t_0-\tau)\exp(j2\pi f_0(t-t_0-\tau))]d\tau \qquad (2.65)$$

where t_0 is the nominal propagation delay between the transmitter and receiver, τ is the additional delay due to the scattering layer and $\beta(\tau)$ is the transmission coefficient for a wave scattering off a layer whose propagation delay is τ. Note in particular that $\beta(\tau)$ is a random variable that is indexed by the additional delay τ. We will assume $\beta(\tau)$ is a zero-mean complex random variable.

The total received signal is a superposition of all the responses due to the individual layers:

$$s(t) = \mathrm{Re}\left[\int_{-\infty}^{\infty}\beta(\tau)u_0(t-t_0-\tau)\exp(j2\pi f_0(t-t_0-\tau))d\tau\right] , \qquad (2.66)$$

where $\beta(\tau)$ is assumed to be zero except for the finite region where scatters exist. Since $\beta(\tau)$ is a zero-mean complex Gaussian random variable with a Rayleigh distributed amplitude and a uniformly distributed phase, the factor $\exp(-j2\pi f_0\tau)$ may be absorbed into $\beta(\tau)$. In this case (2.66) becomes

$$s(t) = \mathrm{Re}\left[\int_{-\infty}^{\infty}\beta(\tau)u_0(t-t_0-\tau)\exp(j2\pi f_0(t-t_0))d\tau\right] , \qquad (2.67)$$

or equivalently

$$s(t) = \mathrm{Re}[u(t-t_0)\exp(j2\pi f_0(t-t_0))] \qquad (2.68)$$

where

$$u(t) = \int_{-\infty}^{\infty}\beta(\tau)u_0(t-\tau)d\tau = \int_{-\infty}^{\infty}\beta(t-\tau)u_0(\tau)d\tau \ . \qquad (2.69)$$

Equations (2.67) or (2.68) and (2.69) together with the condition that the individual scattering layers are uncorrelated constitute the frequency-selective fading channel model. Observe that we could have derived (2.67) directly from (2.12) by simply dropping the time dependence of $\beta(\tau,t)$. Thus frequency selective fading channels are properly designated a subclass of doubly-spread channels. Note that (2.69) describes the input-output characteristics for a linear time-invariant filter with complex impulse response $\beta(t)$. For reasons that will become apparent, frequency-selective fading channels are also known as time-flat fading channels [Bello and Nelin, 1963], channels dispersive only in time [Kennedy, 1969], and range or delay-spread fading channels [Van Trees,1971].

The channel covariance function for a frequency-selective fading channel is

$$g(\tau) \triangleq \rho(\tau,0) \quad . \tag{2.70}$$

The term $g(\tau)$ is also known as the range scattering function for a frequency-selective fading channel.

The channel scattering function for a frequency-selective fading channel may be found by using (2.70) in (2.33):

$$S_{DR}(\tau,f) = g(\tau)\delta(f) \quad . \tag{2.71}$$

Using (2.71), the mean delay for a frequency-selective fading channel is

$$m_R = \frac{1}{2\sigma_b^2} \int_{-\infty}^{\infty} \tau g(\tau) d\tau \tag{2.72}$$

while the mean-square delay spread is given by

$$L = \frac{1}{2\sigma_b^2} \int_{-\infty}^{\infty} \tau^2 g(\tau) d\tau - m_R^2 \tag{2.73}$$

where

$$2\sigma_b^2 = \int_{-\infty}^{\infty} g(\tau) d\tau . \tag{2.74}$$

Using (2.71) in (2.36) and (2.37), the mean Doppler shift and the mean-square Doppler spread for a frequency-selective fading channel are found to be identically zero.

We will now demonstrate, by way of example, the relationship between the two-frequency correlation function, the transmitted signal envelope, and the correlation between frequency samples of the received signal envelope. To do this we first need to compute the correlation between frequency samples of the Fourier transform of the received signal envelope when a bandlimited signal is transmitted. Using (2.70) in (2.47), the frequency correlation function $R_{FE}(f_1,f_2)$ becomes

$$R_{FE}(f_1,f_2) = \int\int\int_{-\infty}^{\infty} g(\tau) u_0(t_1-\tau) u_0^*(t_2-\tau) \exp(j2\pi(f_2t_2-f_1t_1)) d\tau dt_1 dt_2 . \tag{2.75}$$

Equation (2.75) may be rewritten as

$$R_{FE}(f_1,f_2) = U_0(f_1)U_0^*(f_2) \int_{-\infty}^{\infty} g(\tau) \exp[-j2\pi\tau(f_1-f_2)] d\tau \tag{2.76}$$

where $U_0(f)$ is the Fourier transform of $u_0(t)$ as defined in (2.2). Note that the quantity

$$R_R(f,0) \triangleq \int_{-\infty}^{\infty} g(\tau) \exp(-j2\pi\tau f) d\tau \tag{2.77}$$

appearing in (2.76) is the two-frequency correlation function $R_{DR}(f,t)$ for zero time separation as defined by (2.49). Using (2.77), (2.76) may be written as

$$R_{FE}(f_1,f_2) = U_0(f_1)U_0^*(f_2)R_R(f_1-f_2,0). \tag{2.78}$$

Now let $g(\tau)$ be of the form

$$g(\tau) = \begin{cases} 1, & -\frac{L}{2} \le \tau \le \frac{L}{2} \\ 0, & \text{elsewhere} \end{cases} . \tag{2.79}$$

Using (2.77), the two-frequency correlation function for the channel covariance function given by (2.79) is

$$R_R(f_1-f_2,0) = L\,\frac{\sin \pi L(f_1-f_2)}{\pi L(f_1-f_2)} . \tag{2.80}$$

Assume a signal is transmitted whose envelope function has a Fourier transform given by

$$U_0(f) = \begin{cases} 1, & -\frac{W}{2} \le f \le \frac{W}{2} \\ 0, & \text{elsewhere} \end{cases} . \tag{2.81}$$

Using (2.80) and (2.81) in (2.78), it is readily seen that if

$$W > \frac{1}{L} \tag{2.82}$$

then the frequency components of $U_0(f)$ separated by multiples of 1/L Hz will be uncorrelated. From (2.48), we see that the correlation bandwidth of the channel for this case is

$$W_c = \frac{1}{L} . \tag{2.83}$$

If, however, instead of condition (2.82) we have the condition

$$W \ll \frac{1}{L}, \tag{2.84}$$

then using (2.80) and (2.81) in (2.78), we see that samples of the Fourier transform of the envelope of the received signal are correlated for all frequencies in the bandwidth of the signal. In Section 2.7 we will see that (2.84) is a necessary condition for the development of the non-dispersive fading channel model.

Before leaving this section, we make mention of a concept often encountered in the literature on fading channels, which is that of time-frequency duality ([Bello, 1964], [Van Trees, Sec. 12.3, 1971]). The reader may have noticed a certain similarity between the equations characterizing a time-selective fading channel and the equations characterizing a frequency-selective fading channel. As an example of this, compare the expressions for the correlation between time samples of the received signal envelope for a time-selective fading channel given by (2.60) and the correlation between frequency samples of the Fourier transform of the received signal envelope for a frequency-selective fading channel given by (2.78). Except for the fact that time appears in the arguments of (2.60) while frequency appears in the arguments of (2.78) and that Fourier transforms of the terms of (2.60)

are used in (2.78), the two expressions are identical in form. To emphasize this "duality" concept, (2.69) may be written as

$$U(f) = H(f)U_0(f) \tag{2.85}$$

where H(f) is the Fourier transform of a sample function of $\beta(\tau)$:

$$H(f) = \int_{-\infty}^{\infty} \beta(\tau)\exp(-j2\pi f\tau)d\tau \ . \tag{2.86}$$

Comparing (2.53) with (2.85), we see that except for the fact that Fourier transforms are used in (2.85), the defining equations for the two channel models are identical in form. As was mentioned in Section 2.3, even the conditions of wide-sense stationarity for the time-selective fading channel model and uncorrelated scattering for the frequency-selective fading channel model are dual concepts. Bello (1969) has thoroughly discussed the various concepts associated with time-frequency duality; the reader is urged to consult [Bello, 1969] for more details. Using Bello's definitions, Van Trees (1971) proves that a time-selective fading channel is the dual of a frequency-selective fading channel. The principal advantages of recognizing this duality appear to be in deriving equivalent circuit models of fading channels [Bello, 1963], designing optimal receivers for the two types of channels [Van Trees, 1971], and in evaluating the performance of communication systems over time-selective and frequency-selective fading channels ([Bello and Nelin, 1962], [Bello and Nelin, 1963]).

2.7. Nondispersive Fading Channels

In the previous two sections, we have discussed two subclasses of the doubly-spread fading channel model. To derive the channel models for these subclasses we have assumed either that the scattering medium is moving but may be modeled as a single layer or that the scattering medium is fixed but consists of differential layers. In this section we assume that the scattering medium is both fixed (non-moving) and may be modeled as a single layer.

For a transmitted narrowband bandpass signal given by (2.1), the received signal, after passing through a fixed, single layer scattering medium, is given by

$$s(t) = \mathrm{Re}[\beta u_0(t-t_0)\exp(j2\pi f_0(t-t_0))] \tag{2.87}$$

where t_0 is the propagation time between the transmitter and receiver and β is assumed to be a zero-mean complex Gaussian random variable. Equation (2.87) constitutes the fading channel model for a nondispersive fading channel [Kennedy, 1969]. Note that (2.87) could have been derived directly from the channel model for a doubly-spread fading channel (2.12) by dropping the time dependency of $\beta(\tau,t)$ and by noting that scattering is due to a single layer. A more precise derivation of the nondispersive fading channel model from the doubly-spread fading channel model is given below.

The channel covariance function for a nondispersive fading channel is given by

$$\rho(\tau,\Delta t) = \rho(0,0)\delta(\tau), -\infty < \tau < \infty, -\infty < \Delta t < \infty. \tag{2.88}$$

Using (2.88) in (2.33), the scattering function for the nondispersive fading channel is given by

$$(\tau,f) = \rho(0,0)\delta(\tau)\delta(f). \tag{2.89}$$

From (2.89) and (2.34)-(2.37), the mean delay, mean-square delay spread, mean Doppler shift, and mean-square Doppler shift for a nondispersive fading channel are all identically zero. The nondispersive fading channel thus exhibits no spreading in frequency or time; hence the name nondispersive. Another term often used to describe the nondispersive fading channel is flat-flat fading channel [Bello and Nelin, 1963]. Since β in (2.87) has a Rayleigh distributed amplitude and a uniformly distributed phase, the nondispersive fading channel is also known as simply a Rayleigh fading channel. In this study, however, by a Rayleigh fading channel we will mean any doubly-spread fading channel or any of its subclasses which do not contain specular components.

As mentioned above, a nondispersive fading channel is a special case of a doubly-spread channel. More generally, it is a special case of both time-selective fading and frequency-selective fading channels (which are, in turn, special cases of the doubly-spread channel). In Section 2.5 we saw that, for a time-selective fading channel and a signal satisfying (2.64), time samples of the received envelope would be correlated for the duration of the transmitted envelope.

In Section 2.6 we saw that, for a frequency-selective fading channel and a signal satisfying (2.84), frequency samples of the received envelope would be correlated for all frequencies in the bandwidth of the transmitted signal. Since a nondispersive fading channel exhibits no spreading in either time or frequency, (2.64) and (2.84) combined must be the condition for a doubly-spread channel to exhibit nondispersive fading:

$$BL \ll \frac{1}{WT} . \tag{2.90}$$

Since the time-bandwidth product for any signal must be greater than unity (c.f. [Papoulis, Sec. 4-4, 4-5, 1962])

$$TW > 1, \tag{2.91}$$

(2.91) combined with (2.90) indicates that nondispersive fading will occur provided

$$BL \ll 1. \tag{2.92}$$

From (2.42), it is seen that nondispersive fading will occur in a doubly-spread channel provided that the channel is underspread.

Finally we mention a special case of the nondispersive fading channel known either as the "slow and flat" fading channel model [Nesenbergs, 1967] or the pure fading channel model [Wozencraft and Jacobs, 1965]. For this case, β appearing in (2.87) is assumed to be a <u>real</u> Rayleigh (or Rician, if a specular component is present) distributed random variable. This channel model will result from the nondispersive fading channel model if the phase of β may be modeled as a real, nonrandom variable.

Figure 3 summarizes the fading channel models that we have considered up to this point.

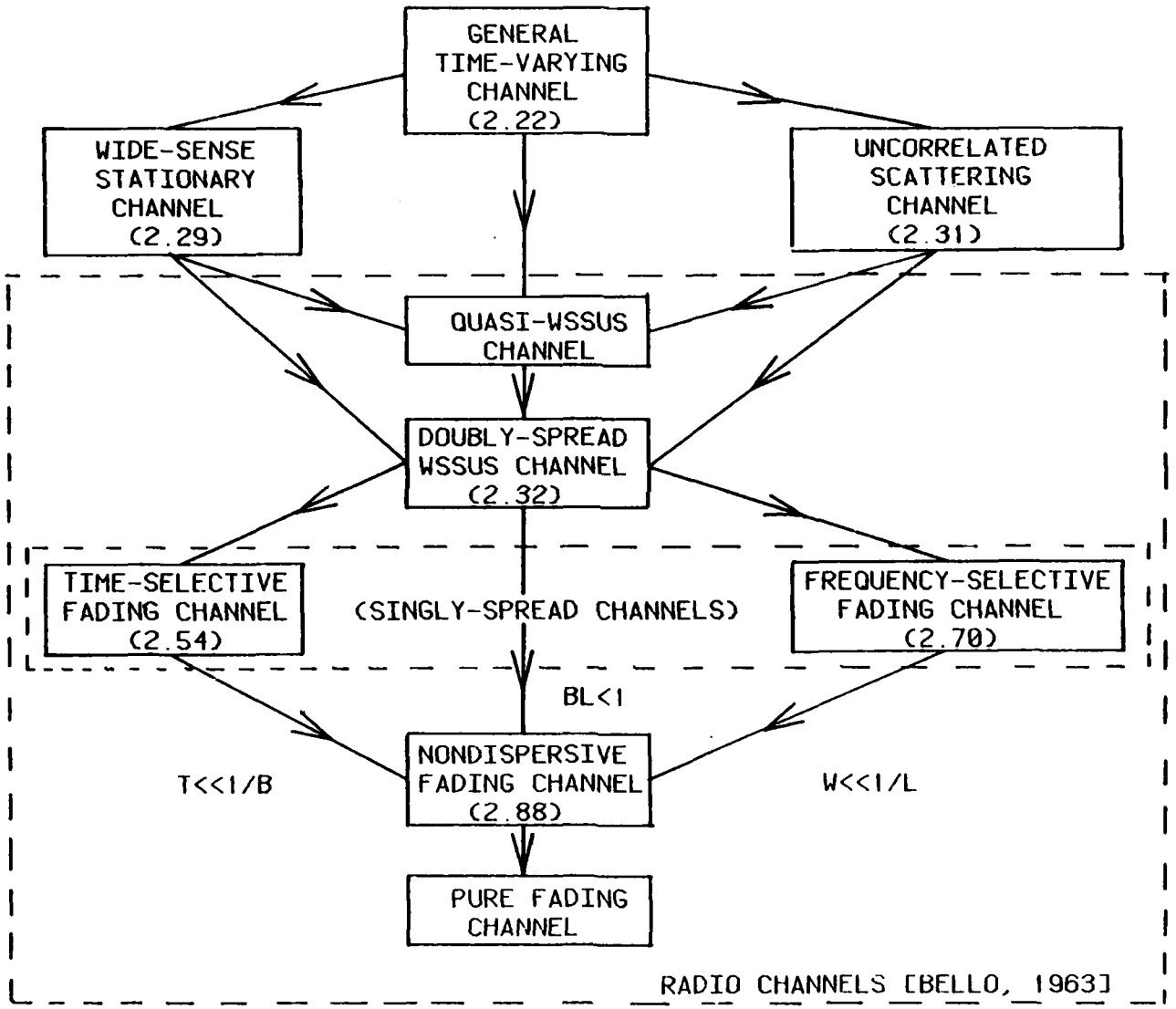

Figure 3. Summary of fading channel models. Numbers in parentheses refer to defining equations for the channel.

CHAPTER 3

AVERAGE SNR ANALYSIS OF DS/SSMA COMMUNICATIONS VIA FADING CHANNELS

One useful measure of performance of a DS/SSMA system is the average signal-to-noise ratio SNR. In this chapter, we analyze the average signal-to-noise ratio performance of DS/SSMA communications for a general class of fading channels. In making this analysis we shall use the DS/SSMA model from Chapter 1 together with the WSSUS fading channel model of Chapter 2. The results presented represent a generalization of the performance analysis of [Pursley, 1977] which considered only additive white Gaussian noise (AWGN) channels.

The type of fading considered in this chapter is Rician or specular-plus-Rayleigh fading [Stein, p. 372, 1966]. That is, for a single transmitted signal given by (2.1), the received signal (2.18) consists of a replica of the transmitted signal plus a weaker Rayleigh-faded version of this signal. This will be the situation whenever the transmission medium is such that there is a strong stable path and a number of weak paths. The component of the received signal that is produced by the strong stable path is called the specular component or the desired signal component; this component can be coherently demodulated. However, unless restrictions are imposed on the fading rate, the Rayleigh-fading signal that arises from the weak paths cannot in general be coherently demodulated [Stein, pp. 406-407, 1966], and hence we shall treat it as interference. An

example of a situation in which this type of fading occurs is the example given in Section 2.1 of communication between an aircraft and a satellite. In this example there exists a direct communication path between the aircraft and the satellite in addition to one or more communication paths due to reflection off the earth.

If the channel exhibits Rayleigh fading rather than Rician fading (i.e., if there is no strong stable component in the received signal), then the direct-sequence form of spread-spectrum communication would not generally be suitable, since it could not be coherently demodulated unless the fading is sufficiently slow. This follows from the results of Viterbi (1965) who showed that for a correlation receiver with a phase reference having a uniform probability density function, as would be the case for a nondispersive Rayleigh-fading channel, the probability of error for an antipodal signaling set is $\frac{1}{2}$. For this chapter, it is assumed that the specular component is of sufficient amplitude that the effects of fading on the performance of the DS/SSMA synchronization subsystem may be neglected. The performance of synchronization subsystems in the presence of fading communication channels has been analyzed elsewhere (e.g., see [Weber, 1976]).

3.1. DS/SSMA System Performance for Doubly-Spread Fading Channels

In this section, we shall develop the results for the average signal-to-noise ratio at the output of a correlation receiver for DS/SSMA communications via a doubly-spread channel. In Sections 3.2 and 3.3 we will specialize the results obtained to the singly-spread time-selective and frequency-selective channels, respectively.

The system model that we will consider is shown in Fig. 4 for K users. The system model as shown is assumed to be time-asynchronous, i.e. there exists no common timing reference among each of the K-users. In Fig. 4, the fading channel is assumed to be able to be modeled by a linear time-varying filter whose transfer function is, in general, nondeterministic. With this one exception, the system model of Fig. 4 is identical to the system model of Fig. 1 for the AWGN channel.

For each k ($1 \leq k \leq K$) the k-th user's data signal $b_k(t)$ is a sequence of statistically independent, unit amplitude, positive and negative, rectangular pulses of duration T. The data signal for the k-th user is therefore given by (1.1). As was the case for the AWGN channel model, each user is assigned a code waveform $a_k(t)$ which consists of a periodic sequence of unit amplitude, positive and negative, rectangular pulses of duration T_c. The code waveform for the k-th user is therefore given by (1.2). We assume that each signature sequence has period $N = T/T_c$ so that there is one code period per data symbol.

The data signal $b_k(t)$ is modulated onto the phase-coded carrier $c_k(t)$, which is given in complex envelope form by

$$c_k(t) = \sqrt{2P}\ \mathrm{Re}[a_k(t)\exp(j\omega_c t + j\theta_k)], \tag{3.1}$$

so that the transmitted signal for the k-th user is

$$s_k(t) = \sqrt{2P}\ \mathrm{Re}[a_k(t)b_k(t)\exp(j\omega_c t + j\theta_k)]. \tag{3.2}$$

In the above expressions, P is the common signal power, θ_k is the phase of the k-th carrier, and ω_c is the common carrier frequency.

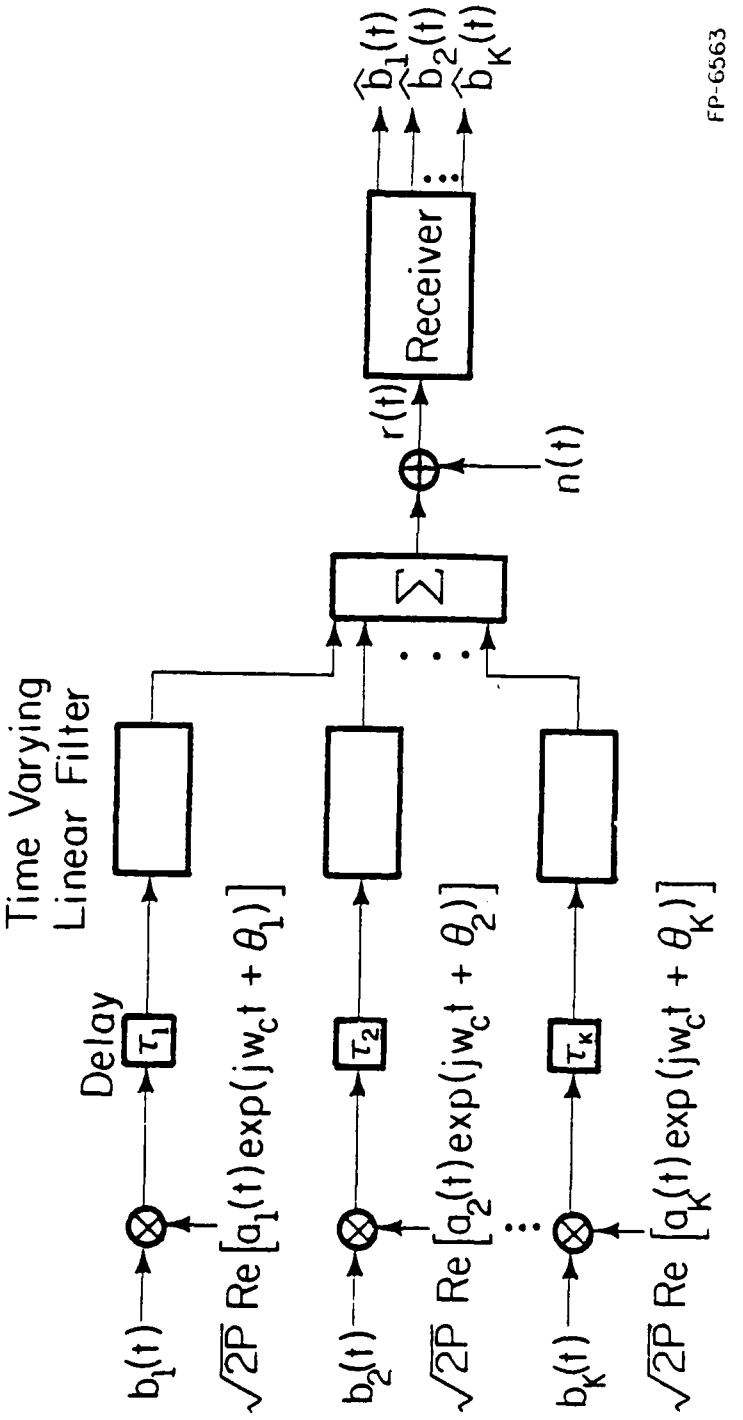

Figure 4. DS/SSMA system model with a fading channel.

In the absence of fading, the received signal at the input to a receiver is given by

$$r(t) = n(t) + \sum_{k=1}^{K} s_k(t-\tau_k), \tag{3.3}$$

where n(t) is the AWGN term and τ_k accounts for the nominal propagation time for the k-th signal as well as for the time asynchronism between the k-th transmitter and the other K-1 transmitters in the system.

In the presence of fading, however, the expression for the received signal at the input to a receiver becomes more complex. From Chapter 2, for a transmitted signal given by (2.1), the received signal at the output of a doubly-spread fading channel is given by (2.12) or (2.13) and (2.14). As noted in the introduction to this chapter, the type of fading being considered is specular-plus-Rayleigh fading. Thus (2.18) must be used to describe the fading process. Finally, in addition to the fading present in the channel, we will also assume that additive white Gaussian noise is also present. Thus if $x_k(t)\cos(\omega_c t+\theta_k)$ is the input to the channel from the k-th transmitter, then the corresponding output $y_k(t)$ is given by

$$y_k(t) = \mathrm{Re}\{u_k(t-\tau_k)\exp[j\omega_c(t-\tau_k) + j\theta_k]\} + n(t), \tag{3.4}$$

where n(t) is the AWGN term and

$$u_k(t) \triangleq \gamma_k \int_{-\infty}^{\infty} \beta_k(\tau,t)x_k(t-\tau)d\tau + x_k(t). \tag{3.5}$$

The first term of (3.5) is the faded portion of the received signal and the second term is the specular component. The non-negative real parameter γ_k is the transmission coefficient for the fading channel as

seen by the k-th signal; and $\beta_k(\tau,t)$ is a zero mean unit-energy (i.e., $\sigma_b^2 = \frac{1}{2}$ in (2.38)) complex Gaussian random process which will be referred to as the fading process. As pointed out in Section 2.2, $\beta_k(\tau,t)$, as it appears in (3.5), represents the equivalent low-pass time-varying impulse response for the faded portion of the fading channel. The covariance function for the fading process in a doubly-spread channel is given by (2.32):

$$\Lambda_k(\tau,\sigma;t,s) \triangleq \tfrac{1}{2}E\{\beta_k(\tau,t)\beta_k^*(\sigma,s)\}$$
$$= \rho_k(\tau,t-s)\delta(\tau-\sigma). \tag{3.6}$$

As will be seen below (see (3.21)), for practical WSSUS channels, $\rho_k(\tau,t-s)$ is a real-valued function.

From equations (3.2)-(3.4), it follows that for a Rician doubly-spread fading channel with AWGN, $x_k(t) = \sqrt{2P}\, a_k(t)b_k(t)$, so that the received signal at the input to a receiver is

$$r(t) = n(t) + \sum_{k=1}^{K} \mathrm{Re}[u_k(t-\tau_k)\exp\{j[\omega_c t + \varphi_k]\}] \tag{3.7}$$

where $\varphi_k \triangleq \theta_k - \omega_c\tau_k$. If the received signal r(t) is the input to a correlation receiver matched to $s_i(t)$, the corresponding output is

$$Z_i = \int_0^T r(t)\mathrm{Re}\{a_i(t-\tau_i)\exp(j\omega_c t + j\varphi_i)\}dt. \tag{3.8}$$

Since we are interested in phase angles modulo 2π and time delays modulo T, we shall (without loss of generality) assume $\tau_i = 0$ and $\theta_i = 0$ (and hence $\varphi_i = 0$). Therefore, as in [Pursley, 1977], the phase angles φ_k and θ_k and the time delay τ_k (for $k \neq i$) are all measured relative to the phase and time delay of the i-th signal. From (3.7) and (3.8), it

follows that, except for double-frequency terms,

$$Z_i = \int_0^T n(t)a_i(t)\cos \omega_c t \, dt + \sum_{k=1}^{K} \tfrac{1}{2} \int_0^T \mathrm{Re}\{u_k(t - \tau_k)a_i(t)e^{j\varphi_k}\}dt, \qquad (3.9)$$

where we have used the identity (2.10). The double frequency terms which are omitted from (3.9) may be ignored for practical implementations of SSMA.

As in [Pursley, 1977], the phase angles, time delays, and data symbols for the k-th signal ($k \neq i$) are modeled as mutually independent random variables which are uniformly distributed on $[0,2\pi]$, $[0,T]$, and $\{+1,-1\}$, respectively. The average signal-to-noise ratio SNR_i at the output of the i-th correlation receiver is then defined in terms of probabilistic averages (i.e., expected values) conditioned upon $b_i(t)$ for $0 \leq t < T$, where, without loss of generality, we may assume $b_i(t) = +1$ over this interval.

For convenience, the following notation will be introduced. Let

$$h_{k,i}(\tau;t) = a_k(t - \tau)b_k(t - \tau)a_i(t) \qquad (3.10)$$

and

$$f_{k,n,i}(\tau,\sigma;t,s) = h_{k,i}(\tau;t)h_{n,i}(\sigma;s) \qquad (3.11)$$

for $1 \leq k \leq K$, $1 \leq n \leq K$, $1 \leq i \leq K$; $0 \leq t \leq T$, $0 \leq s \leq T$; and $-\infty < \tau < \infty$, $-\infty < \sigma < \infty$. The function $h_{i,i}$ is denoted by h_i, and $f_{i,i,i}$ is denoted by f_i. In terms of this notation, the i-th specular component, the i-th (complex) faded signal component, the AWGN component, and the complex interference component are defined by

$$D_i = \sqrt{\tfrac{1}{2}P} \int_0^T b_i(t)dt \tag{3.12}$$

$$\tilde{F}_i = \sqrt{\tfrac{1}{2}P} \int_0^T \int_{-\infty}^{\infty} \gamma_i \beta_i(\tau,t) h_i(\tau;t) d\tau dt \tag{3.13}$$

$$N_i = \int_0^T n(t) a_i(t) \cos \omega_c t \, dt \tag{3.14}$$

$$\tilde{I}_i = \sqrt{\tfrac{1}{2}P} \sum_{\substack{k=1 \\ k\neq i}}^{K} (\gamma_k \tilde{I}_{k,i} + \tilde{I}'_{k,i}) \tag{3.15}$$

where

$$\tilde{I}_{k,i} \triangleq \int_0^T \int_{-\infty}^{\infty} \beta_k(\tau, t - \tau_k) h_{k,i}(\tau_k + \tau; t) \exp(j\varphi_k) d\tau dt \tag{3.16}$$

$$\tilde{I}'_{k,i} \triangleq \int_0^T h_{k,i}(\tau_k; t) \exp(j\varphi_k) dt \, . \tag{3.17}$$

If we then let $F_i = \mathrm{Re}\{\tilde{F}_i\}$ and $I_i = \mathrm{Re}\{\tilde{I}_i\}$, we see from (3.9) that

$$Z_i = N_i + D_i + F_i + I_i \, . \tag{3.18}$$

Since $EN_i = EI_i = EF_i = 0$ and $ED_i = \sqrt{\tfrac{1}{2}P} \int_0^T b_i(t)dt = T\sqrt{\tfrac{1}{2}P}$, then $EZ_i = T\sqrt{\tfrac{1}{2}P}$. Assuming that n(t) has a two-sided spectral density $\tfrac{1}{2}N_0$, the variance of the noise component Z_i is

$$\mathrm{Var}\, N_i = \tfrac{1}{2}N_0 T, \tag{3.19}$$

while the conditional variance of the i-th specular signal component, conditioned upon $b_i(t) = +1$ for $0 \leq t < T$, is zero. Since the fading process has zero mean, the variance of the faded portion of the i-th signal is given by

$$\text{Var } F_i = E[F_i]^2 = E[\text{Re } \tilde{F}_i]^2 = \tfrac{1}{2}E[\text{Re}\{\tilde{F}_i^2\}] + \tfrac{1}{2}E[\tilde{F}_i^*\tilde{F}_i], \tag{3.20}$$

which follows from an application of (2.10) with $x = y = \tilde{F}_i$, and from the fact $\tilde{F}_i^*\tilde{F}_i = |\tilde{F}_i|^2$ is real. The expressions for the two terms in (3.20) will involve the covariance function $\Lambda_i(\tau,\sigma;t,s)$ given by (3.6) and the function $\tilde{\Lambda}_i(\tau,\sigma;t,s)$ given by (2.21). In particular

$$E|\tilde{F}_i|^2 = P\gamma_i^2 \int_0^T \int_0^T \int_{-\infty}^{\infty} \int_{-\infty}^{\infty} \Lambda_i(\tau,\sigma;t,s) f_i(\tau,\sigma;t,s) d\tau d\sigma dt ds. \tag{3.21}$$

The expression for $E[\text{Re}\{\tilde{F}_i^2\}]$ is the right-hand side of (3.21) with Λ_i replaced by $\tilde{\Lambda}_i$. However as noted in Section 2.2, we will assume that the WSSUS fading process is such that (2.23) holds so that $E\{\tilde{F}_i^2\} = 0$ and thus

$$\text{Var } F_i = \tfrac{1}{2}E|\tilde{F}_i|^2 . \tag{3.22}$$

From (3.21), (3.22), and (3.6), it can be seen that

$$\text{Var } F_i = \frac{P}{2}\gamma_i^2 \int_0^T \int_0^T \int_{-\infty}^{\infty} \rho_i(\tau,t-s) f_i(\tau,\tau;t,s) d\tau dt ds . \tag{3.23}$$

By a similar analysis of the interference component $\tilde{I}_i$ defined by (3.15)-(3.17) it is clear that since the fading process has zero mean and the data signals are uncorrelated and have zero mean, then

$$\text{Var } I_i = \tfrac{1}{2}E|\tilde{I}_i|^2 = \tfrac{1}{2}P \sum_{\substack{k=1 \\ k\neq i}}^{K} (\gamma_k^2 v_{k,i} + v'_{k,i}) \tag{3.24}$$

where $v_{k,i} \triangleq E|\tilde{I}_{k,i}|^2$ and $v'_{k,i} \triangleq E|\tilde{I}'_{k,i}|^2$ are given by

$$v_{k,i} = E \int_0^T \int_0^T \int_{-\infty}^{\infty} \rho_k(\tau, t-s) f_{k,k,i}(\tau + \tau_k, \tau + \tau_k; t, s) d\tau dt ds \qquad (3.25)$$

and

$$v'_{k,i} = E \int_0^T \int_0^T f_{k,k,i}(\tau_k, \tau_k; t, s) dt ds \ . \qquad (3.26)$$

In general, the expression for $v_{k,i}$ in (3.25) cannot be reduced further without additional constraints on the covariance function $\rho_k(\tau, t-s)$ for the fading process. The expression $v'_{k,i}$ in (3.26), however, does not depend on the fading process. Since the assumptions used to derive $v_{k,i}$ are identical to those used to derive the variance of the k-th interference component for the AWGN channel of Chapter 1, (3.26) can be simplified as in [Pursley, 1977] to give

$$v'_{k,i} = \frac{T^2}{6N^3} r_{k,i}, \qquad (3.27)$$

where $r_{k,i}$ is the interference parameter given by (1.16).

The signal-to-noise ratio SNR_i at the output of the i-th correlation receiver is defined by

$$SNR_i \triangleq (ED_i)[\text{Var } F_i + \text{Var } I_i + \text{Var } N_i]^{-\frac{1}{2}}$$

$$= T\sqrt{\tfrac{1}{2}P}\,[\text{Var } F_i + \text{Var } I_i + \tfrac{1}{2}N_0 T]^{-\frac{1}{2}} \ . \qquad (3.28)$$

Notice that for SNR_i defined in this manner, the faded portion of the i-th signal is considered to be an interference component of Z_i (the correlation receiver cannot make use of this component).

Several observations about the results obtained up to this point will now be made. First, throughout the analysis presented above, nowhere has there been made any assumptions about the independence of the fading processes $\beta_k(\tau,t)$ for $1 \leq k \leq K$, apart from the implicit assumption that $\beta_k(\tau,t)$ is independent of the random variables $b_k(t)$, φ_k, and τ_k. Consequently, the above results are valid for the important cases where (1) all the fading processes are independent and (2) all the fading processes are identical, i.e., $\beta_k(\tau,t) = \beta(\tau,t)$ for all k, $1 \leq k \leq K$. Case (1) would arise, for example, in the situation where multiple mobile users are communicating via the ionosphere, using DS/SSMA communications. For this situation, it would be expected that each of the transmitted paths would involve different sets of scatterers and hence, following an argument similar to that used to develop the uncorrelated scattering channel model of Chapter 2, the K fading processes would be independent. Case (2), on the other hand, would arise if a satellite is transmitting multiple-user data to a single aircraft using DS/SSMA communications. In this case, all of the K users would undergo the same fading resulting in identical fading processes. Thus the results above are general enough to allow both of these fading situations.

Second, from the results above (viz., (3.23), (3.24), (3.25), and (3.27)), we see that SNR_i depends upon the signature sequences through the functions f_i in (3.23) and $f_{k,k,i}$ in (3.25) and through the interference parameters $r_{k,i}$ in (3.27). In addition, SNR_i depends on the channel covariance function ρ_k, $1 \leq k \leq K$, via (3.23) and (3.25).

Finally, throughout the analysis presented above we have used a correlation receiver structure for the receiver. This is not to imply that a correlation receiver is the optimum receiver for DS/SSMA communications via Rician fading channels. In fact, even for DS/SSMA communications via AWGN channels, the correlation receiver is not the optimum receiver. For while a correlation receiver is optimum for an antipodal signalling set and an AWGN channel (e.g. see [Viterbi, 1965]), a rate 1 convolutional decoder using the Viterbi algorithm is optimal for DS/SSMA communications via an AWGN channel [Schneider, 1979]. For a nondispersive Rician fading channel, it has been shown ([Viterbi, 1965], [Turin, 1958]) that a linear combination of the optimal coherent and optimal noncoherent receiver is optimum for a single user system. Other schemes have been devised to provide low bit error rates in the presence of "slowly" fading channels [Monsen, 1973]. Thus, it is evident that a correlation receiver is not optimum for DS/SSMA communications via fading channels (however, in general the optimal receiver is not known). Nonetheless, the analysis presented above is valuable in a practical sense, since existing DS/spread-spectrum receivers do use simple correlation receiver structures to simplify receiver design and construction [Cahn, 1973]. Therefore in the analysis that follows we will continue to use correlation receivers matched to the i-th ($1 \leq i \leq K$) user's code waveform.

3.2. DS/SSMA System Performance for Time-Selective Fading Channels

Analysis. In this section, consideration is given to one subclass of doubly-spread channels known as time-selective fading channels. The channel covariance function for a time-selective fading channel is given by (2.54):

$$\rho_i(\tau, t-s) = \rho_i(0, t-s)\delta(\tau). \tag{3.29}$$

For convenience, $\rho_i(0,t-s)$ is denoted by $r_i(t-s)$. It follows from (3.23) and (3.29) that the variance of the faded portion of the i-th signal is

$$\text{Var } F_i = \frac{P}{2}\gamma_i^2 \int_0^T \int_0^T r_i(t-s)b_i(t)b_i(s)dtds \ . \tag{3.30}$$

The expression for the data signal is given by (1.1). Making a change of variables, $u = t-s$, and using (1.1), (3.30) becomes

$$\begin{aligned}\text{Var } F_i &= \frac{P}{2}\gamma_i^2\left[\int_0^T \int_u^T r_i(u)dtdu + \int_{-T}^0 \int_0^{u+T} r_i(u)dtdu\right] \\ &= \frac{P}{2}\gamma_i^2\left[\int_0^T r_i(u)(T-u)du + \int_{-T}^0 r_i(u)(T+u)du\right] \\ &= P\gamma_i^2 \int_0^T r_i(u)(T-u)du \ . \end{aligned} \tag{3.31}$$

In a similar fashion, the variance of the interference component I_i may be found by using (3.29) in (3.25). Interchanging the order of integration and expectation in (3.25), we find

$$v_{k,i} = \int_0^T \int_0^T r_k(t-s)E\{f_{k,k,i}(\tau_k,\tau_k;t,s)\}dtds, \tag{3.32}$$

where the expectation is over $b_k(t)$ and τ_k. Note that given τ_k, $b_k(t-\tau_k)$ is a semi-random binary process [Papoulis, 1965] with an autocorrelation function for τ_k, t, and s in [0,T]

$$E\{b_k(t-\tau_k)b_k(s-\tau_k)|\tau_k\} = \begin{cases} 1, & \tau_k \le \min(t,s) \\ 1, & \tau_k \ge \max(t,s) \\ 0, & \text{otherwise.} \end{cases} \tag{3.33}$$

Evaluating the expectation in (3.32) using (3.33), we find that for t and s in [0,T]

$$E\{f_{k,k,i}(\tau_k,\tau_k;t,s)\} = a_i(t)a_i(s)\,\frac{1}{T}\,[\int_0^{\min(t,s)} a_k(t-\tau_k)a_k(s-\tau_k)d\tau_k$$

$$+ \int_{\max(t,s)}^{T} a_k(t-\tau_k)a_k(s-\tau_k)d\tau_k]$$

$$= a_i(t)a_i(s)\,\frac{1}{T}\int_{\max(0,v)}^{T+\min(0,v)} a_k(u)a_k(u-v)du \qquad (3.34)$$

where $u = t-\tau_k$, $v = t-s$ and we have used the fact that $a_k(t)$ is periodic with period T. For v positive we find

$$E\{f_{k,k,i}(\tau_k,\tau_k;t,s)\} = \frac{1}{T}\,\hat{R}_k(t-s)a_i(t)a_i(s);\ t-s > 0, \qquad (3.35)$$

while for v negative we find

$$E\{f_{k,k,i}(\tau_k,\tau_k;t,s)\} = \frac{1}{T}\,\hat{R}_k(|t-s|)a_i(t)a_i(s);\ t-s > 0, \qquad (3.36)$$

where $\hat{R}_k(\tau)$ is the continuous-time partial autocorrelation function defined in Chapter 1. Combining (3.35) and (3.36), the expectation in (3.32) reduces to

$$E\{f_{k,k,i}(\tau_k,\tau_k;t,s)\} = \frac{1}{T}\,\hat{R}_k(|t-s|)a_i(t)a_i(s). \qquad (3.37)$$

Using (3.37) in (3.32) together with the change of variables $u = t-s$, (3.32) reduces to

$$v_{k,i} = \frac{2}{T}\int_0^T r_k(u)\hat{R}_k(u)\hat{R}_i(u)du. \qquad (3.38)$$

From (3.24), (3.32), and (3.27), the variance of the interference component I_i is

$$\text{Var } I_i = \sum_{\substack{k=1 \\ k\neq i}}^{K} (\gamma_k^2 \frac{P}{T} \int_0^T r_k(u)\hat{R}_k(u)\hat{R}_i(u)du + \frac{PT^2}{12N^3} r_{k,i}) \ . \tag{3.39}$$

Using (3.31) and (3.39) in (3.28), the signal-to-noise ratio at the output of the i-th correlation receiver for a DS/SSMA system operating over a time-selective fading channel is

$$\text{SNR}_i = \{\frac{N_0}{2\mathcal{E}} + \frac{2\gamma_i^2}{T^2} \int_0^T r_i(u)(T-u)du + \sum_{\substack{k=1 \\ k\neq i}}^{K} [\frac{2}{T^3} \gamma_k^2 \int_0^T r_k(u)\hat{R}_k(u)\hat{R}_i(u)du + \frac{1}{6N^3} r_{k,i}]\}^{-\frac{1}{2}}, \tag{3.40}$$

where $\mathcal{E} \triangleq PT$ is the energy per data bit.

Numerical Results. The general result (3.40) is now specialized to channels having specific channel covariance functions $r_k(t)$ for $1 \leq k \leq K$. Throughout the remainder of this section it is assumed that

$$r_k(t) = 0 \text{ for } |t| > \lambda T_c \tag{3.41}$$

where $\lambda = (n+\beta)$, n is a positive integer less than N, β is in the range $0 \leq \beta < 1$, and λ is a positive number less than N. The quantity λT_c is called the correlation duration for the fading channel. Note that from (2.45) and (2.60), the correlation duration for the time-selective fading

channel is equal to the correlation time τ_c for the channel as defined in Section 2.4, provided we are using signals satisfying condition (2.63). For convenience, the following notation is introduced at this point. Let $\Delta_k(\ell) = C_k(\ell+1) - C_k(\ell)$ and $\pi_{k,i}(\ell) = \Delta_k(\ell)C_i(\ell)$. The function $\pi_{i,i}$ will be denoted by π_i.

From (1.10) and (3.41), (3.40) is seen to imply

$$SNR_i = \Big\{\frac{N_0}{2\mathcal{E}} + \frac{2\gamma_i^2}{T^2}\int_0^T r_i(u)(T-u)du + \sum_{\substack{k=1\\k\neq i}}^{K}\Big[\frac{2}{3}\gamma_k^2\sum_{\ell=0}^{n}\Big\{C_k(\ell)C_i(\ell)\int_{\ell T_c}^{(\ell+\beta_\ell)T_c} T_c^2\, r_k(u)du + [\pi_{k,i}(\ell) + \pi_{i,k}(\ell)]\int_{\ell T_c}^{(\ell+\beta_\ell)T_c} T_c(u-\ell T_c)r_k(u)du + \Delta_k(\ell)\Delta_i(\ell)\int_{\ell T_c}^{(\ell+\beta_\ell)T_c}(u-\ell T_c)^2 r_k(u)du\Big\} + \frac{1}{6N^3}\, r_{k,i}\Big]\Big\}^{-\frac{1}{2}} \qquad (3.42)$$

where $\beta_\ell = 1$ for $\ell < n$ and $\beta_n = \beta$. Observe that the evaluation of (3.42) requires only knowledge of the <u>discrete</u> aperiodic autocorrelation functions of the K signature sequences as well as knowledge of the channel covariance function $r_k(t)$. In this chapter, we shall consider two types of channel covariance functions to illustrate the general results. These are a triangular covariance function and an exponential covariance function. By a triangular covariance function, we shall mean a function of the form

$$r_k^{(1)}(t) = \begin{cases} A(T-\nu|t|), & |t| \le \lambda T_c \\ 0, & |t| > \lambda T_c \end{cases} \tag{3.43}$$

where $\nu = (\lambda T_c)^{-1} T$. A truncated exponential covariance function is defined by

$$r_k^{(2)}(t) = \begin{cases} Be^{-\alpha|t|}, & |t| \le \lambda T_c \\ 0, & |t| > \lambda T_c \ . \end{cases} \tag{3.44}$$

It should be noted that $r_k^{(2)}(t)$ is not a valid autocovariance function, but it is an approximation to the valid autocovariance $r(t) = B \exp(-\alpha|t|)$, $-\infty < t < \infty$. It is true that $r_k^{(2)}(t) = r_k^{(2)}(-t)$ which is the only property of an autocovariance function that is needed in what follows.

For the time-selective fading channel, the unit variance constraint on the covariance function of the channel fading process results in the conditions

$$r_k^{(1)}(0) = AT = 1, \ r_k^{(2)}(0) = B = 1. \tag{3.45}$$

Using (3.43) and (3.45) in (3.42), SNR_i for a DS/SSMA system over a time-selective fading channel with a triangular covariance function is found to be

$$SNR_i^{(1)} = \{\frac{2\gamma_i^2\lambda}{N}\left[1 - \tfrac{1}{2}(\nu+1)\frac{\lambda}{N} + \frac{\nu\lambda^2}{3N^2}\right]$$

$$+ \sum_{\substack{k=1\\k\neq i}}^{K}\left[\frac{2\gamma_k^2}{N^4}\sum_{\ell=0}^{n}\left\{\beta_\ell C_k(\ell)C_i(\ell)\Gamma_\ell(\tfrac{1}{2}) + \frac{\beta_\ell^2}{2}\left[\pi_{k,i}(\ell) + \pi_{i,k}(\ell)\right]\Gamma_\ell(\tfrac{2}{3})\right.\right.$$

$$\left.\left. + \frac{\beta_\ell^3}{3}\Delta_k(\ell)\Delta_i(\ell)\Gamma_\ell(\tfrac{3}{4})\right\}\right] + \sum_{\substack{k=1\\k\neq i}}^{K}\frac{1}{6N^3}r_{k,i} + \frac{N_0}{2\delta}\Big\}^{-\frac{1}{2}} \qquad (3.46)$$

where $\Gamma_\ell(C) \triangleq N-\nu(\ell+c\beta_\ell)$. In an identical fashion, it can be shown that SNR_i for a DS/SSMA system over a time-selective fading channel with covariance function $r_k^{(2)}$ is

$$SNR_i^{(2)} = \{\frac{2\gamma_i^2}{N\alpha}\left[(1-e^{-\alpha\lambda}) + \frac{1}{N\alpha}\left(e^{-\alpha\lambda}(\alpha\lambda+1)-1\right)\right]$$

$$+ \sum_{\substack{k=1\\k\neq i}}^{K}\frac{2\gamma_k^2}{N^3\alpha}\Big[\sum_{\ell=0}^{n}e^{-\alpha\ell}\Big\{C_k(\ell)C_i(\ell)(1-e^{-\alpha\beta_\ell})$$

$$+ \left[\pi_{k,i}(\ell) + \pi_{i,k}(\ell)\right]\left[\tfrac{1}{2}\left[(\alpha\ell+1) - e^{-\alpha\beta_\ell}(\alpha(\ell+\beta_\ell)+1)\right] - \ell(1-e^{-\alpha\beta_\ell})\right]$$

$$+ \Delta_k(\ell)\Delta_i(\ell)\Big[\Big[\ell^2 + \frac{2\ell}{\alpha} + \frac{2}{\alpha^2}\Big] - e^{-\alpha\beta_\ell}\Big[(\ell+\beta_\ell)^2 + \frac{2}{\alpha}(\ell+\beta_\ell) + \frac{2}{\alpha^2}\Big]$$

$$+ \frac{2\ell}{\alpha}\left[-(\alpha\ell+1) + e^{-\alpha\beta_\ell}(\alpha(\ell+\beta_\ell)+1] + \ell^2(1-e^{-\alpha\beta_\ell})\right]\Big]\Big]$$

$$+ \frac{1}{6N^3}\sum_{\substack{k=1\\k\neq i}}^{K}r_{k,i} + \frac{N_0}{2\delta}\Big\}^{-\frac{1}{2}} \quad . \qquad (3.47)$$

In Fig. 5, we have plotted SNR $\triangleq$ min$\{SNR_i\}$ for K = 6, using equations (3.46) and (3.47), as a function of the correlation duration of the channel correlation function. In evaluating (3.46) and (3.47) it has been assumed that $\gamma_k^2 = \gamma^2$ for all k, $1 \leq k \leq 6$ and $(\frac{\mathcal{E}}{N_0})$ = 10 dB. The correlation duration used in evaluating (3.46) was that value λT_c satisfying the equation $r_k^{(2)}(\lambda T_c) = e^{-5}$ (i.e., $\alpha\lambda T_c = 5$). This correlation duration was selected numerically to minimize the effect of ignoring the tail of an exponential correlation function (see (3.41) above). Thus $r_k^{(2)}$ is a good model for exponential correlation. The sequences used to evaluate (3.46) and (3.47) consisted of 6 maximal-length shift register sequences (m-sequences) of period 127 which collectively form a maximal-connected set [Gold and Kopitzke, 1965]. The shift-register loading selected for each m-sequence was the least-sidelobe energy/auto-optimal (LSE/AO) phase for that particular m-sequence [Pursley and Roefs, 1979]. Further details on the actual loadings used may be found in the first six entries of Fig. B.1 of [Pursley and Roefs, 1979]. In evaluating (3.46) and (3.47) we have used only values of correlation duration satisfying $\lambda \leq \frac{N}{2}$. The reason for considering this limited range of correlation duration is that for $\lambda > \frac{N}{2}$, the effects of adjacent bits must be taken into account in the performance analysis of time-selective fading channels (note that $r_k^{(1)}(t)$ and $r_k^{(2)}(t)$ are <u>double</u>-sided functions (see (3.43) and (3.44)).

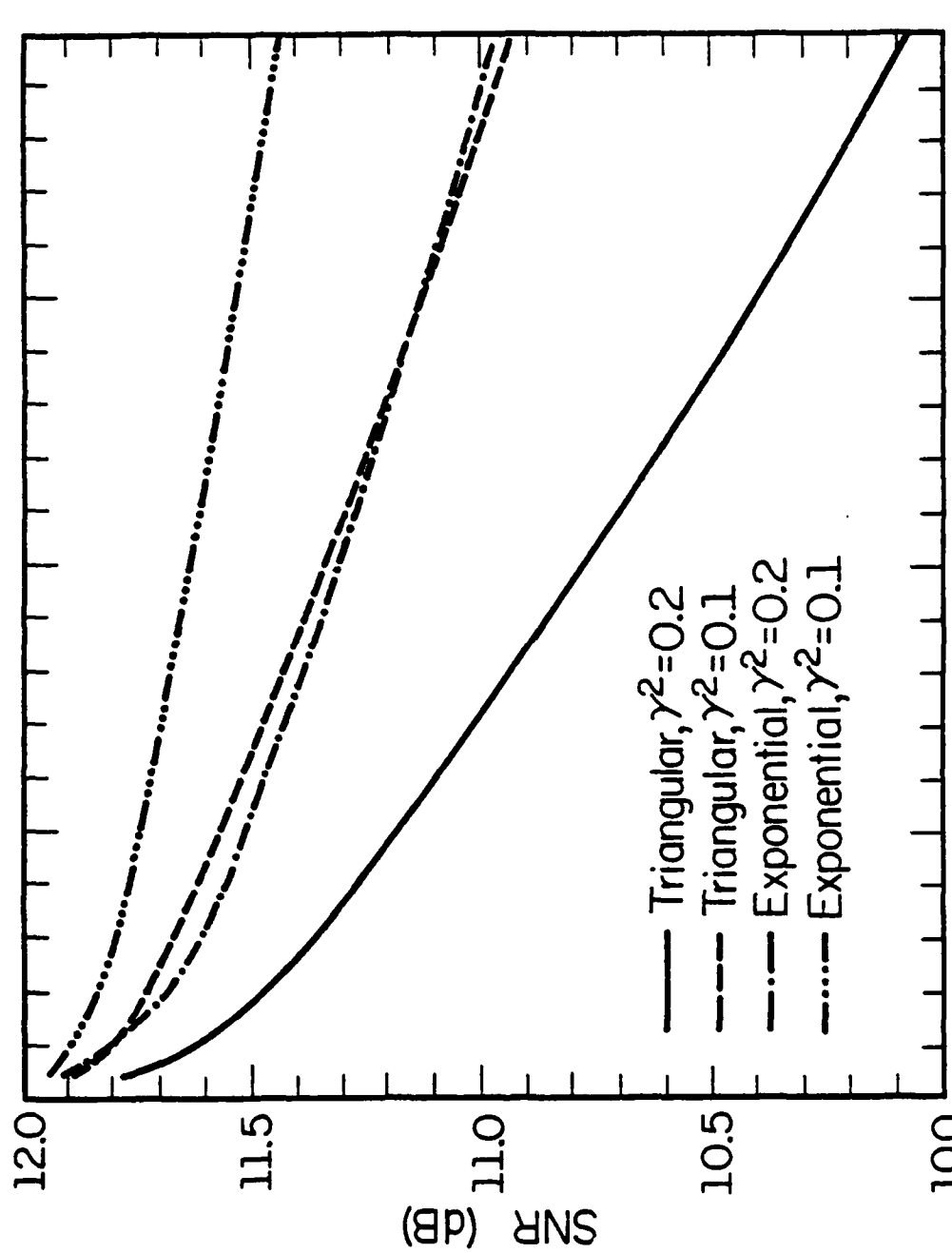

Figure 5. SNR vs. correlation duration for a time-selective fading channel with triangular and truncated-exponential covariance functions for two values of γ^2 (N = 127, K = 6, $\mathcal{E}/N_0$ = 10dB).

Note in Fig. 5 that as the correlation duration increases, the DS/SSMA system performance is degraded significantly. An explanation for this degradation is as follows: as the correlation duration of either $r_k^{(1)}(t)$ or $r_k^{(2)}(t)$ increases, the time-selective fading channel model reduces to the nondispersive fading channel model (see (2.64)) of Section 2.7, i.e., the fading portion of the transmitted signal is being multiplied by a complex random variable as opposed to being multiplied by a time-varying random process. Since the receiver structure being used is a correlation receiver, the effects of the smoothing by the integrator in the correlation receiver on the diffuse portion of the received signals is reduced as the channel correlation duration increases. Heuristically speaking, if the fading process is a zero-mean, stationary ergodic process so that time averages and probabilistic averages (expectations) may be interchanged, then for small values of correlation duration, the diffuse portion of the received signal is averaged over the bit duration by the receiver integrator so that its contribution to Z_i is essentially zero. For larger values of correlation duration, the receiver integrator is integrating over a time-independent random variable, so that the contribution to Z_i of the diffuse portion of the received signals becomes significant. As a result, there is a corresponding decrease in SNR_i. The fact that a DS/SSMA communication system performs better over a time-selective fading channel with an exponential channel correlation function than one with a triangular channel correlation function may be explained by examining (3.40). Since for a given correlation duration, the tail of an exponential channel

correlation function falls off faster than that of a triangular channel correlation function, using (3.45) we see from (3.40) that for a given value of λT_c, the contribution to Z_i of the diffuse portion of the received signal is smaller for the exponential channel correlation function.

Figure 6 illustrates the dependence of SNR on the transmission coefficient γ for a time-selective fading channel with a triangular channel correlation function. The same signature sequences as described above are used. As might be expected from (3.46), SNR is degraded in proportion to the intensity of the fading process. From Figs. 5 and 6, we may ascertain that for a given minimum SNR at the output of a correlation receiver, there exists an admissible range of γ and λT_c for which DS/SSMA communications is possible. Suppose, for example, we use the LSE/AO m-sequences described above for DS/SSMA communications over a time-selective fading channel with a triangular channel correlation function. A desired minimum SNR of 10 dB is possible provided $\gamma^2 < 0.2$ and the correlation duration of the channel is less than 20 T_c.

If a receiver SNR higher than that obtainable from the fading channel for a given $\mathcal{E}/N_0$ is required, one would expect that by increasing $\mathcal{E}/N_0$, the desired performance could be obtained. That this approach may be fruitless is illustrated by Fig. 7 in which SNR is shown as a function of $\mathcal{E}/N_0$ for a time-selective fading channel for three values of γ^2. In Fig. 7, the correlation duration is 10 T_c and the set of signature

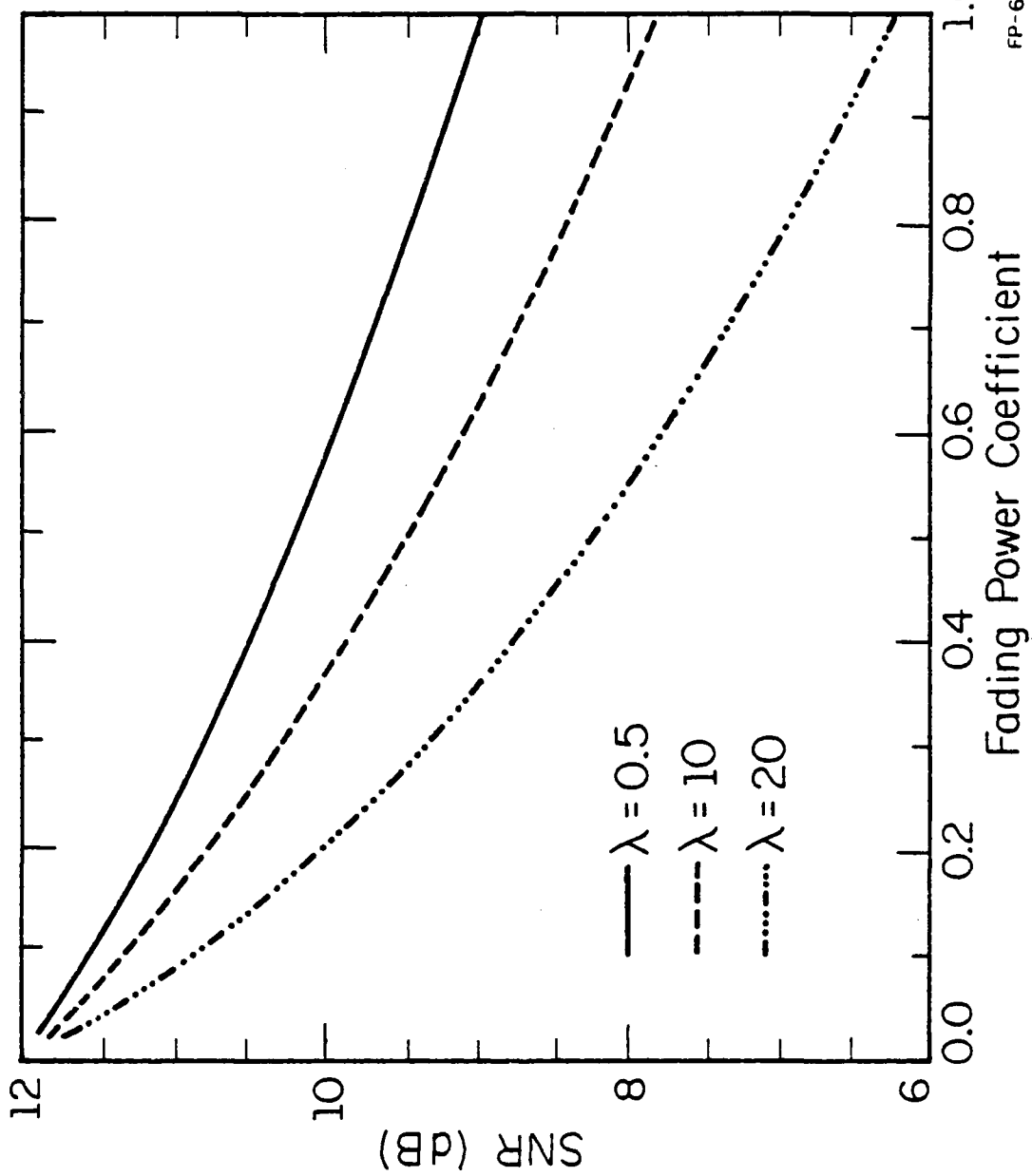

Figure 6. SNR vs. γ^2 for a time-selective fading channel with a triangular covariance function for three values of correlation duration (N = 127, K = 6, $\mathcal{E}/N_0$ = 10dB).

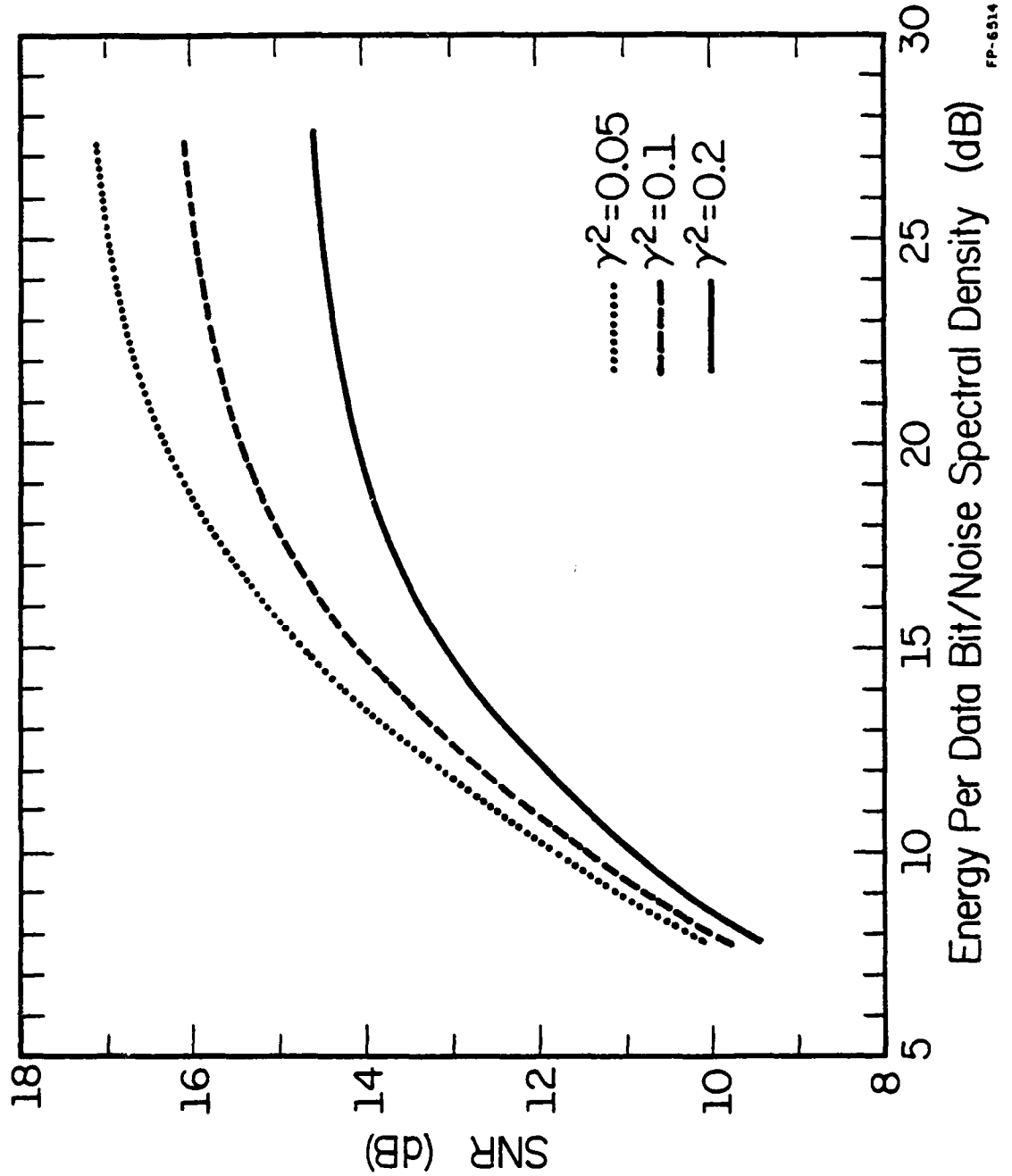

Figure 7. SNR vs. $\mathcal{E}/N_0$ for a time-selective fading channel with a triangular covariance function for three values of γ^2 (N = 127, K = 6, λ = 10).

sequences is the same as used for Fig. 1. The observed leveling-off effect of the SNR vs. $\mathcal{E}/N_0$ curve may be expected for any communication system in which the expression for Var Z_i contains a sufficiently large interference component whose power is directly proportional to the transmitted signal power (see (3.31) and (3.39)). Hence, this effect will occur for values of K and N in the range of interest; even for SSMA communication via an AWGN channel.

In the three figures immediately above we have chosen to use a maximal-connected set of m-sequences with LSE/AO phases as the signature sequences without giving any justification for this choice of signature sequences. Some justification for this choice will now be given. First, we have used a maximal-connected set of m-sequences because such a choice yields the largest possible set of m-sequences of period N for which any two sequences in the set have a preferred three-valued crosscorrelation function [Gold and Kopitzke, 1965]. Hence, by using such a set we automatically are using a set whose sequences have bounded pairwise <u>periodic</u> crosscorrelation values, a desirable feature for synchronization purposes in DS/SSMA systems and for communication in synchronous DS/SSMA systems. Second, we have used the LSE/AO phases for the individual m-sequences, primarily as a sieve over the phases of the m-sequences, but secondarily for the reason that such a choice offers promise for good performance, at least over AWGN channels [Golay, 1972]. From [Pursley and Sarwate, 1977b], we note that the interference parameter $r_{k,i}$ is bounded by

$$4N^2 - 6\{S(a^{(k)})S(a^{(i)})\}^{\frac{1}{2}} \leq r_{k,i} \leq 4N^2 + 6\{S(a^{(k)})S(a^{(i)})\}^{\frac{1}{2}} \qquad (3.48)$$

where S(u) is the sidelobe energy of sequence u defined by

$$S(u) = \sum_{\ell=1}^{N-1} C_u^2(\ell). \tag{3.49}$$

Hence by bounding the sidelobe energy of each of the signature sequences through the use of LSE/AO phases, we are bounding the value of $r_{k,i}$; thereby bounding the performance of a DS/SSMA system over an AWGN channel (see Eq. (1.19)). In fact, the choice of LSE/AO phases is not necessarily critical for fading channels. For example, if AO/LSE phases [Pursley and Roefs, 1979] were used, the results obtained for Fig. 5 would differ from the results obtained using AO/LSE phases by less than 0.004 dB. In Section 3.5 we will see that maximal-connected sets of m-sequences with LSE/AO phases perform very much like "typical" sequences. Thus it is expected that the numerical results presented above in Figs. 5-7 are typical results that would be obtained using any reasonable set of 6 signature sequences of length 127. However as will be shown later, bad choices of signature sequences will give far worse performance.

3.3. DS/SSMA System Performance for Frequency-Selective Fading Channels

Analysis. The dual of the time-selective fading channel is another special case of a WSSUS channel known as a frequency-selective fading channel. In this section the effect of frequency-selective fading on the performance of DS/SSMA systems is considered.

The channel correlation function for a frequency-selective fading channel is defined (as in (2.70)) by

$$g_i(\tau) \triangleq \rho_i(\tau,0). \tag{3.50}$$

An additional assumption about the selectivity of the channel is necessary in order to obtain useful results regarding the performance of DS/SSMA systems over frequency-selective fading channels. As can be seen from the equations that follow, a frequency-selective fading channel exhibits memory and therefore introduces intersymbol interference into the received signal. We will assume in this section that the selectivity of the channel is such that, in the detection of a given data symbol, we need only be concerned with the intersymbol interference due to the two adjacent data symbols. This condition is equivalent to assuming that

$$g_i(\tau) \approx 0 \text{ for } |\tau| > T. \tag{3.51}$$

Channels exhibiting higher degrees of selectivity will require the inclusion of the effects of more than the two adjacent bits in the analysis of the performance of the system, in which case the analysis that follows can be modified in a straightforward manner. However, as noted in [Bello and Nelin, 1963], the need to include more than two adjacent bits in the system analysis is frequently an indication that the channel is too frequency-selective for use in practical communication systems.

Using (3.50) and (3.51) in (3.23), we find that the variance of the faded portion of the i-th signal for a frequency-selective fading channel is

$$\text{Var } F_i = \frac{P}{2} \gamma_i^2 \int_{-T}^{T} g_i(\tau) \int_0^T \int_0^T f_i(\tau,\tau;t,s)\,dt\,ds\,d\tau. \tag{3.52}$$

Notice from (3.11) that the double integral with respect to t and s in (3.52) reduces to the product of two single integrals, each of which is given by

$$\int_0^T h_i(\tau;t)dt = \begin{cases} b_{i,0}\hat{R}_i(\tau) + b_{i,-1}R_i(\tau), & \tau \geq 0 \\ \\ b_{i,0}\hat{R}_i(-\tau) + b_{i,1}R_i(-\tau), & \tau < 0 \end{cases} \tag{3.53}$$

where $R_i(\tau)$ is the continuous-time partial autocorrelation function defined in Chapter 1. Upon substitution of (3.53) into (3.52), we obtain

$$\text{Var } F_i = P\gamma_i^2 \int_0^T g_i(\tau)[\hat{R}_i^2(\tau)+\{b_{i,0}b_{i,-1}+b_{i,0}b_{i,1}\}\hat{R}_i(\tau)R_i(\tau)+R_i^2(\tau)]d\tau. \tag{3.54}$$

Averaging (3.54) over all data patterns, it is easy to see that the variance of the faded portion of the i-th signal is

$$\text{Var } F_i = P\gamma_i^2 \int_0^T g_i(\tau)[\hat{R}_i^2(\tau) + R_i^2(\tau)]d\tau. \tag{3.55}$$

The variance of the interference component I_i may be evaluated for a frequency-selective fading channel by using (3.50) and (3.51) in (3.25) to obtain

$$v_{k,i} = \int_0^T \int_0^T \int_{-T}^T g_k(\tau)a_i(t)a_i(s)\, \chi(t,s,\tau)d\tau dtds \tag{3.56}$$

where

$$\chi(t,s,\tau) \triangleq \frac{1}{T}\int_0^T a_k(t-\tau_k-\tau)a_k(s-\tau_k-\tau)E\{b_k(t-\tau_k-\tau)b_k(s-\tau_k-\tau)\}d\tau_k. \tag{3.57}$$

Letting $u = t-\tau$ and $v = s-\tau$ in (3.57), we note from (3.33) that

$$a_i(t)a_i(s)\chi(t,s,\tau) = E\{f_{k,k,i}(\tau+\tau_k,\tau+\tau_k;t,s)\}, \tag{3.58}$$

and hence using (3.37), (3.57) reduces to

$$\chi(t,s,\tau) = \frac{1}{T}\hat{R}_k(|t-s|). \tag{3.59}$$

Using (3.59), (3.56) may now be rewritten as

$$v_{k,i} = \frac{1}{T}\int_{-T}^{T} g_k(\tau)d\tau \int_0^T\int_0^T a_i(t)a_i(s)\hat{R}_k(|t-s|)dtds. \tag{3.60}$$

After a change of variables $\tau = t-s$, (3.60) reduces to

$$\begin{aligned} v_{k,i} &= \frac{2}{T}\int_{-T}^{T} g_k(\tau)d\tau \int_0^T \hat{R}_i(\tau)\hat{R}_k(\tau)d\tau \\ &= \frac{1}{T}\int_{-T}^{T} g_k(\tau)d\tau \int_0^T [R^2_{k,i}(\tau) + \hat{R}^2_{k,i}(\tau)]d\tau \\ &= \frac{2T_c^3}{3T} r_{k,i}\int_0^T g_k(\tau)d\tau \end{aligned} \tag{3.61}$$

where the second step follows from [Pursley and Sarwate, Section V, 1977a] and the last step follows from [Pursley, eqs. (11)-(12), 1977]. From (3.24), (3.61), and (3.27), the variance of the interference component I_i is

$$\text{Var } I_i = P\sum_{\substack{k=1\\k\neq i}}^{K} r_{k,i}\left[\gamma_k^2\frac{T_c^3}{3T}\int_0^T g_k(\tau)d\tau + \frac{T^2}{12N^3}\right]. \tag{3.62}$$

Using (3.55) and (3.62) in (3.28), the signal-to-noise ratio at the output of the i-th correlation receiver for a DS/SSMA system operating over a frequency-selective fading channel is

$$SNR_i = \{ \frac{N_0}{2\mathcal{E}} + \frac{2\gamma_i^2}{T^2} \int_0^T g_i(\tau)[\hat{R}_i^2(\tau) + R_i^2(\tau)]d\tau$$

$$+ \frac{2}{T^2} \sum_{\substack{k=1 \\ k\neq i}}^{K} r_{k,i}[\gamma_k^2 \frac{T_c^3}{3T} \int_0^T g_k(\tau)d\tau + \frac{T^2}{12N^3}]\}^{-\frac{1}{2}} \qquad (3.63)$$

Numerical Results. In this subsection (3.63) is specialized to the case of a specific channel covariance function $g_k(\tau)$. In all that follows it is assumed that $g_k(\tau)$ satisfies (3.41); that is $g_k(\tau)$ is non-zero only over the interval $|\tau| \leq \lambda T_c$. Analogous to the time-selective fading channel case, we define λT_c to be the correlation duration of the frequency-selective fading channel. From (2.77) and (2.78) we see that, provided (2.82) is satisfied, the first zero-crossing of the Fourier transform of $g_k(\tau)$ is defined to be the correlation bandwidth of the frequency-selective fading channel. In practice, however, the correlation bandwidth of the channel is usually defined in this manner without taking into account the bandwidth of the transmitted signal ([Monsen, 1971], [Bello and Nelin, 1963]). Thus from the theory of Fourier transforms, if a frequency-selective fading channel has a correlation duration λT_c, the correlation bandwidth of the channel is proportional to $(\lambda T_c)^{-1}$ (see [Monsen, 1971]). Consequently, the correlation duration of the channel is also a measure of the correlation bandwidth of the channel.

Using (1.9), (1.10), and (3.41) in (3.63), we find that for a frequency-selective fading channel with a specified channel covariance function which satisfies (3.41), SNR_i is

$$SNR_i = \{ \frac{N_0}{2\mathcal{E}} + \frac{2\gamma_i^2}{T^2} \sum_{\ell=0}^{n} \{ [C_i^2(\ell-N) + C_i^2(\ell)] \int_{\ell T_c}^{(\ell+\beta_\ell)T_c} T_c^2 g_i(\tau)d\tau$$

$$+ 2[\pi_i(\ell-N) + \pi_i(\ell)] \int_{\ell T_c}^{(\ell+\beta_\ell)T_c} T_c(\tau-\ell T_c) g_i(\tau)d\tau$$

$$+ [\Delta_i^2(\ell-N) + \Delta_i^2(\ell)] \int_{\ell T_c}^{(\ell+\beta_\ell)T_c} (\tau-\ell T_c)^2 g_i(\tau)d\tau \}$$

$$+ \sum_{\substack{k=1 \\ k\neq i}}^{K} r_{k,i} [\frac{2\gamma_k^2}{3N^3} \int_0^T g_k(\tau)d\tau + \frac{1}{6N^3}]\}^{-\frac{1}{2}} . \qquad (3.64)$$

For the frequency-selective fading channel the unit-energy constraint on the fading process covariance function implies [Van Trees, Section 12.1, 1971]

$$\int_{-\infty}^{\infty} g_k(\tau)d\tau = 1 . \qquad (3.65)$$

Noting that $g_k(\tau) = g_k(-\tau)$ and using (3.65) in conjunction with (3.41) in (3.64), we see that the last term of (3.64) reduces to

$$\sum_{\substack{k=1 \\ k\neq i}}^{K} r_{k,i} [\frac{2\gamma_k^2}{3N^3} \int_0^T g_k(\tau)d\tau + \frac{1}{6N^3}] = \frac{1}{6N^3} \sum_{\substack{k=1 \\ k\neq i}}^{K} (1+2\gamma_k^2) r_{k,i} . \qquad (3.66)$$

Triangular and truncated exponential covariance functions for a frequency-selective fading channel are defined in a manner analogous to the definition of the corresponding channel covariance functions for a time-selective fading channel (i.e., g_k is defined as in (3.43) and (3.44)). For this channel model however, (3.65) implies that the normalization factors A and B appearing in (3.43) and (3.44) are given implicitly by

$$A\frac{T^2}{\nu} = \frac{2B}{\alpha}\left[1 - e^{-\alpha\lambda T_c}\right] = 1, \tag{3.67}$$

where λ is defined in (3.41). For a frequency-selective fading channel with a triangular channel covariance function, SNR_i is found to be

$$SNR_i^{(1)} = \{\frac{2\gamma^2}{\gamma N^3}\sum_{\ell=0}^{n}[\beta_\ell\{C_i^2(\ell-N) + C_i^2(\ell)\}\Gamma_\ell(\tfrac{1}{2}) + \beta_\ell^2\{\pi_i(\ell-N)+\pi_i(\ell)\}\Gamma_\ell(\tfrac{2}{3}) + \frac{\beta_\ell^3}{3}\{\Delta_i^2(\ell-N) + \Delta_i^2(\ell)\}\Gamma_\ell(\tfrac{3}{4})] + \frac{1}{6N^3}\sum_{\substack{k=1\\k\neq i}}^{K}(1+2\gamma_k^2)r_{k,i} + \frac{N_0}{2\mathcal{E}}\}^{-1/2}. \tag{3.68}$$

The corresponding result for a frequency-selective fading channel with a truncated-exponential channel covariance function is

$$SNR_i^{(2)} = \{\frac{N_0}{2\mathcal{E}} + \frac{\gamma_i^2}{N^2[1-e^{-\alpha\lambda}]}\sum_{\ell=0}^{n} e^{-\alpha\ell}[(C_i^2(\ell-N) + C_i^2(\ell))(1-e^{-\alpha\beta_\ell}) + 2(\pi_i(\ell-N) + \pi_i(\ell))(\frac{1}{\alpha}[\alpha\ell+1 - e^{-\alpha\beta_\ell}(\alpha(\ell+\beta_\ell)+1)] - \ell(1-e^{-\alpha\beta_\ell})) + (\Delta_i^2(\ell-N)+\Delta_i^2(\ell))([\ell^2 + \frac{2\ell}{\alpha} + \frac{2}{\alpha^2}] - e^{-\alpha\beta_\ell}[(\ell+\beta_\ell)^2 + \frac{2(\ell+\beta_\ell)}{\alpha} + \frac{2}{\alpha^2}] + \frac{2\ell}{\alpha}[e^{-\alpha\beta_\ell}(\alpha(\ell+\beta_\ell)+1) - \alpha(\ell+1)] + \ell^2(1-e^{-\alpha\beta_\ell}))] + \frac{1}{6N^3}\sum_{\substack{k=1\\k\neq i}}^{K}[1+2\gamma_k^2]r_{k,i}\}^{-1/2}. \tag{3.69}$$

Equations (3.68) and (3.69) were evaluated as a function of the correlation duration using the same code sequences as for Fig. 5, and the results are shown in Fig. 8. As in the time-selective fading case, it is assumed that $\gamma_k = \gamma$ for all k, $1 \leq k \leq 6$, and $\mathcal{E}/N_0 = 10$ dB. as before, the correlation duration for a triangular channel covariance function is defined to be λT_c. However, for a truncated exponential channel covariance function, we define the correlation duration to be the value of λT_c satisfying the equation $g_k(\lambda T_c) = 10^{-5}$ (i.e., α satisfies $\frac{1}{2}\alpha[1-e^{-\alpha\lambda T_c}]^{-1} \cdot e^{-\alpha\lambda T_c} = 10^{-5}$). Once again, this particular definition of correlation duration was selected to minimize the effect of truncating $g_k(\tau)$. From Fig. 8, we note that for small values of λT_c, SNR for a frequency-selective fading channel is degraded significantly. Because the frequency-selective fading channel is the dual of the time-selective fading channel, as was pointed out in Section 2.6, such a result could have been predicted directly from Fig. 5 using a time-frequency duality argument. Physically, what is occurring is that as the correlation duration of the channel goes to zero, the correlation bandwidth of the channel approaches infinity. From (2.84), we see that for small values of correlation duration, the frequency-selective fading channel model may therefore be replaced by the non-dispersive fading channel model of Section 2.7. Following an argument identical to that used for this limiting situation in the time-selective fading channel case, we see that small values of correlation duration lead to a reduction of the receiver integrating effect on the diffuse portion of the i-th signal. Note that the contribution to Z_i of the diffuse portion of the K-1 interfering signals is unaffected by the correlation duration of the channel, as can be seen from (3.66).

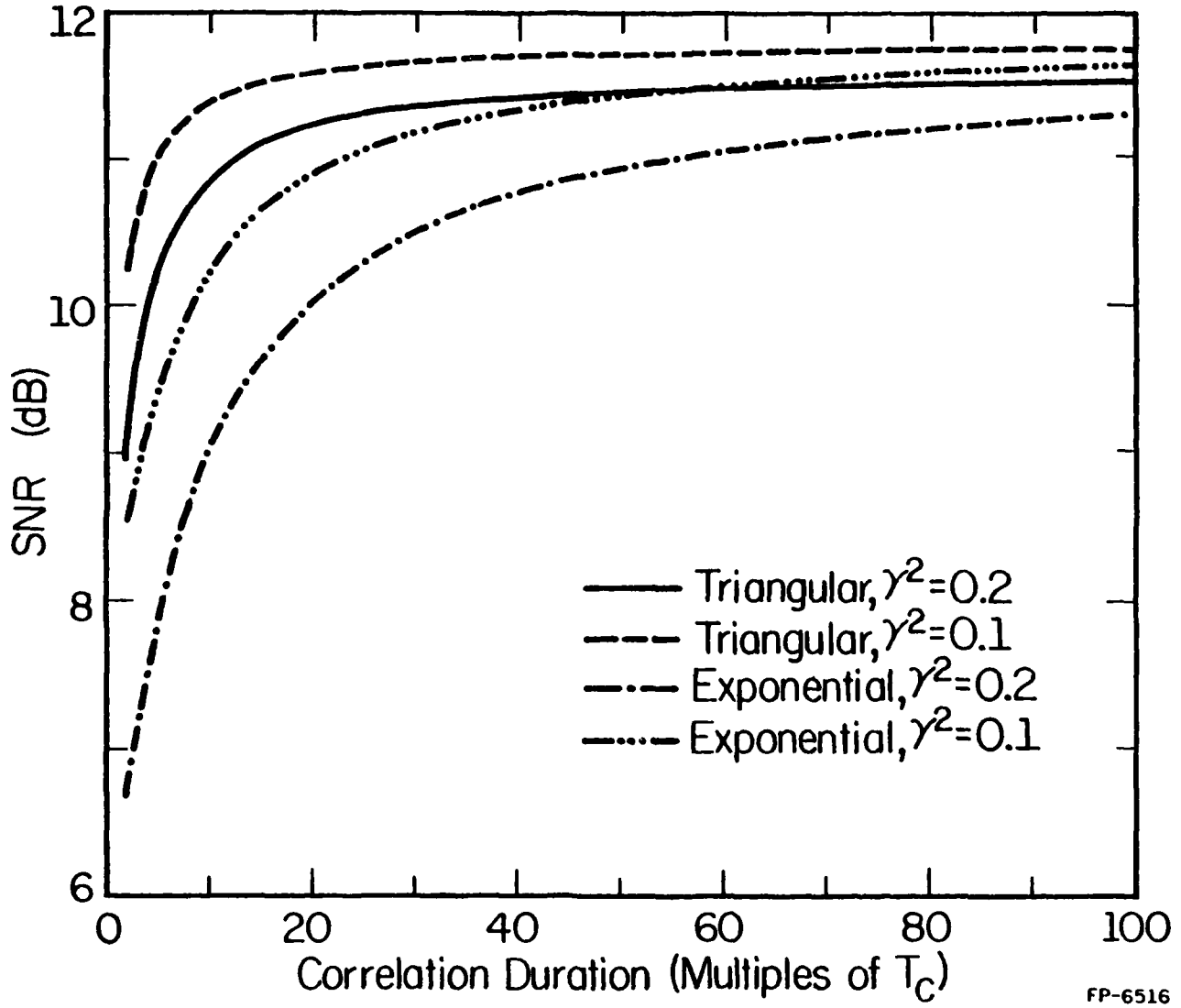

Figure 8. SNR vs. correlation duration for a frequency-selective fading channel with triangular and truncated-exponential covariance functions for two values of γ^2 (N = 127, K = 6, $\mathcal{E}/N_0$ = 10dB).

Figure 9 illustrates the dependence of the signal-to-noise ratio on the square of the transmission coefficient γ for a frequency-selective fading channel with a triangular covariance function using the same signature sequences as used for Fig. 8. As might be expected, the signal-to-noise ratio is degraded in proportion to the intensity of the fading process. From Figs. 8 and 9, we may ascertain that for a given signal-to-noise ratio to be achievable the parameters γ and λT_c must be constrained to a certain range.

The graph of SNR vs. $\mathcal{E}/N_0$ for a frequency-selective fading channel with a triangular channel covariance function is shown in Fig. 10. As in Fig. 7, the SNR curve "flattens-out" as $\mathcal{E}/N_0$ increases for the same reasons as given for the time-selective fading channel.

The comments made in the last section about the choice of signature signatures used to evaluate expressions (3.68) and (3.69) are valid for the frequency-selective fading case, also. In particular, had the AO/LSE phases of the m-sequences been used instead of the LSE/AO phases, the results obtained would differ from the results presented in Figs. 8-10 by less than 0.006 dB.

In the discussion up to this point, we have not indicated which of the two singly-spread channels is a better model for actual radio channels, especially channels over which DS/SSMA communication systems are to be used. We will now correct this omission. In practice, most fading channels exhibit some degree of frequency-selectivity; in particular, multipath channels are frequency-selective fading channels (e.g., see [Stein, pp. 351-355, 1966]). In addition, because the bandwidth

AD-A124 007 PERFORMANCE ANALYSIS OF DIRECT-SEQUENCE SPREAD-SPECTRUM 2/2
MULTIPLE-ACCESS C.. (U) ILLINOIS UNIV AT URBANA
COORDINATED SCIENCE LAB D E BORTH APR 80 R-880
UNCLASSIFIED DAAG29-78-C-0016 F/G 17/2 NL

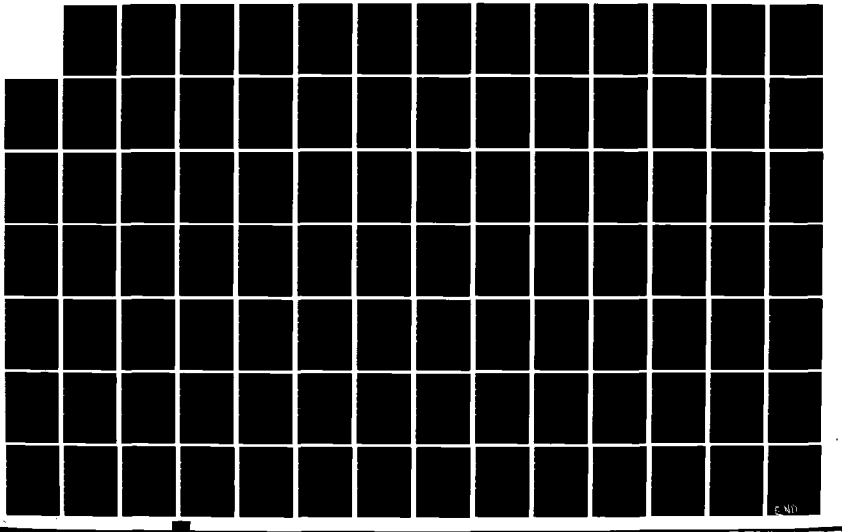

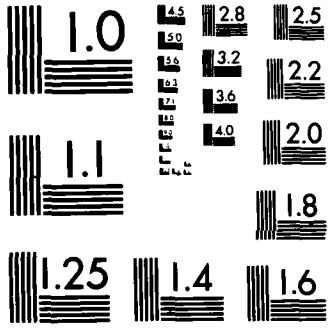

MICROCOPY RESOLUTION TEST CHART
NATIONAL BUREAU OF STANDARDS-1963-A

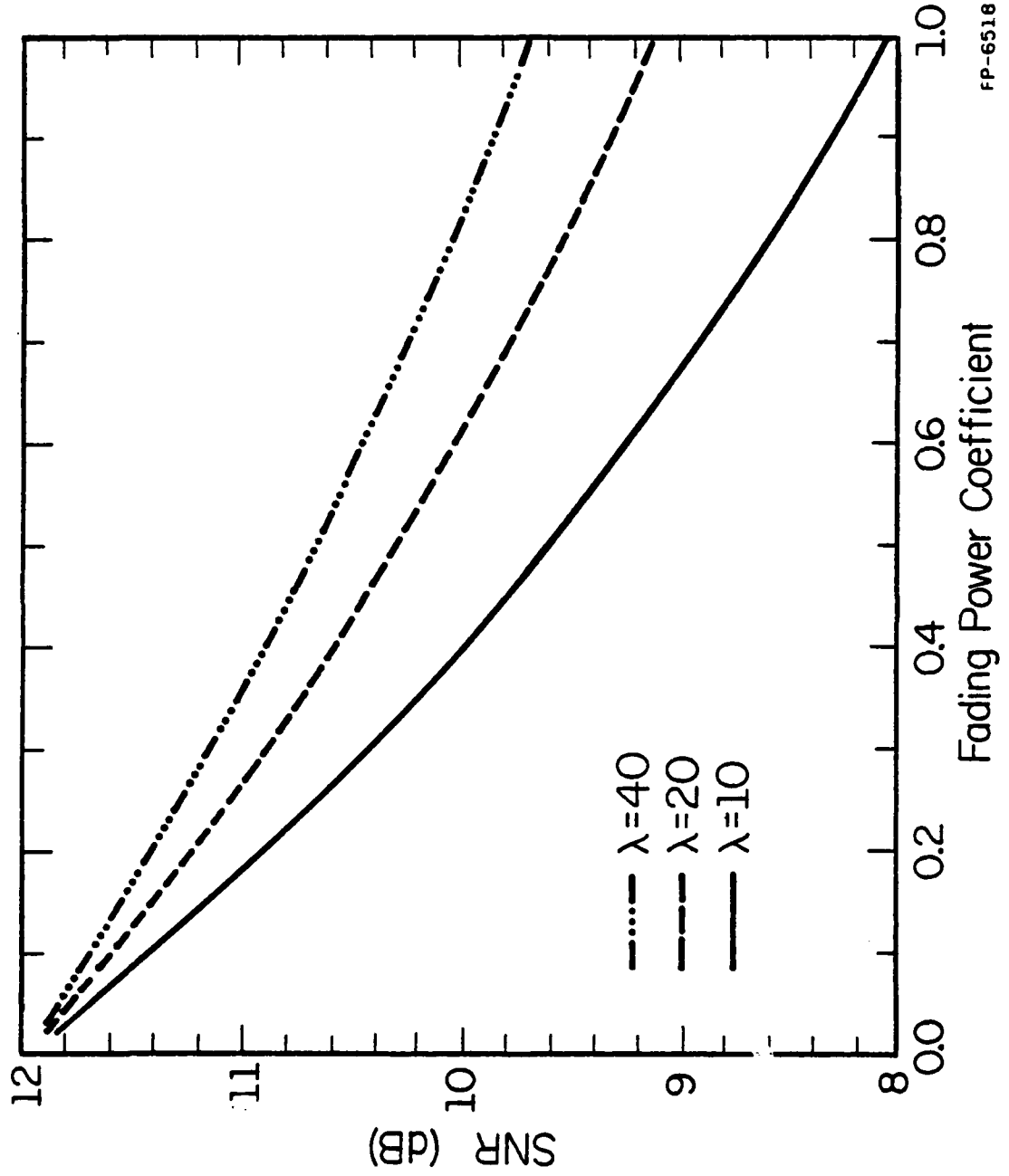

Figure 9. SNR vs. γ^2 for a frequency-selective fading channel with a triangular covariance function for three values of correlation duration (N = 127, K = 6, $\mathcal{E}/N_0$ = 10dB).

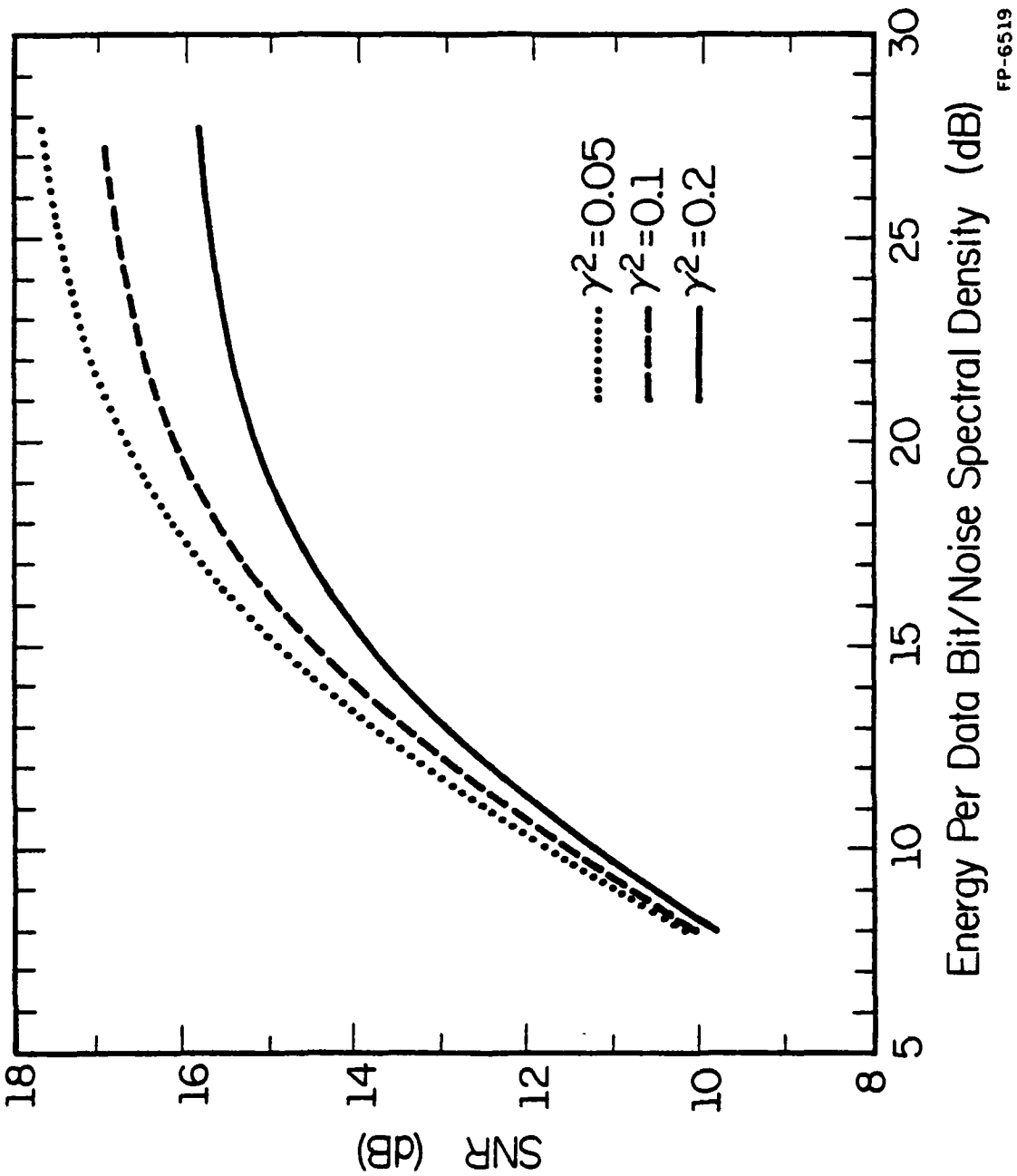

Figure 10. SNR vs. $\mathcal{E}/N_0$ for a frequency-selective fading channel with a triangular covariance function for three values of γ^2 (N = 127, K = 6, λ = 20).

occupied by spread-spectrum systems (including DS/SSMA systems) is typically quite large, the channels used by spread-spectrum systems often appear frequency-selective to the spread-spectrum signal, even though the same channel would not be frequency-selective to a non-spread-spectrum signal transmitting the same data (see (2.84)).

From the above we may conclude that while the time-selective fading channel may be a good model for some radio channels, the frequency-selective fading channel model is of more practical value when discussing the performance of direct-sequence/spread-spectrum communications via multipath channels. Hence, in the remainder of this chapter, emphasis will be placed on frequency-selective fading channels.

3.4 Comparison of Single-User PSK and DS/SS Communications via Fading Channels

In Chapter 1 it was noted that spread-spectrum techniques could, with the proper choice of modulation technique, be effective in combating the effects of fading encountered by conventional modulation systems (e.g., PSK, FSK) over communications channels. In surveying the literature, we find many references which note in particular that use of direct-sequence/spread-spectrum (DS/SS) modulation is effective in combating multipath and the associated frequency-selectivity (see Section 3.3) present on many channels (e.g., see [Cahn, 1974],

[Jacobs, 1975], [Massey and Uhran, 1975], and [Viterbi, 1979]). Although several "heuristic" proofs of this conjecture exist ([Cahn, 1974], [Jacobs, 1975]), to date no rigorous demonstration of this conjecture has been given. In the following, we will give such a demonstration. In particular, we will compare the performance of single-user PSK and DS/SS communication systems over singly-spread Rician fading channels. Throughout this comparison, average signal-to-noise ratio at the output of a correlation receiver will be used as the performance measure.

From (3.40), we see that for a single-user DS/SS system operating over a time-selective fading channel, the average signal-to-noise ratio at the output of a correlation receiver is given by

$$\text{SNR} = \{\frac{N_0}{2\mathcal{E}} + \frac{2\gamma^2}{T^2}\int_0^T r(u)(T-u)du\}^{-1} . \qquad (3.70)$$

Since the expression for average SNR given by (3.70) does not depend on the signature sequence used by the DS/SS system, we may conclude that equation (3.70) is also the expression for average SNR for a biphase PSK system operating over a time-selective fading channel. For if the signature sequence $\{a_n^{(i)}\}$ is identically one for $-\infty < n < \infty$ in (1.2), the DS/SSMA system model shown in Fig. 1 reduces to a PSK system, when $K = 1$. From the above discussion we may conclude that so far as single-user systems are concerned, the performance of PSK and DS/SS systems are identical over time-selective fading channels.

For frequency-selective fading channels however, the result of this comparison of the two systems is quite different. From (3.63), the average SNR at the output of a correlation receiver for a single-user DS/SS system operating over a frequency-selective fading channel is

$$\text{SNR} = \left\{\frac{N_0}{2\mathcal{E}} + \frac{2\gamma^2}{T^2}\int_0^T g(\tau)[\hat{R}_i^2(\tau)+R_i^2(\tau)]d\tau\right\}^{-\frac{1}{2}} . \qquad (3.71)$$

The average SNR for a PSK system operating over a frequency-selective fading channel may be found either directly from (3.52) by letting $a_i(t) = 1$ in (3.11) or by noting that for a PSK system, $R_i(\tau) = \tau$ and $\hat{R}_i(\tau) = (T-\tau)$, and using (3.71). Both of these results follow from the comments made in the previous paragraph about the reduction of the DS/SS system model to the PSK system model. Using either method, the average SNR for a PSK system is found to be

$$\text{SNR} = \left\{\frac{N_0}{2\mathcal{E}} + \frac{2\gamma^2}{T^2}\int_0^T g(\tau)[\tau^2+(T-\tau)^2]d\tau\right\}^{-\frac{1}{2}} . \qquad (3.72)$$

In Fig. 11 we have evaluated eqs. (3.71) and (3.72) as a function of the correlation duration of the channel for two values of γ^2 and for $\frac{\mathcal{E}}{N_0} = 10$ dB. In evaluating (3.71), we have used an m-sequence of length 127 with its LSE/AO phase as the signature sequence for the DS/SS system. Thus for the PSK system, the correlation duration scale is interpreted as being marked in intervals of $\frac{1}{127}$ of a bit. The relatively large advantage of DS/SS over PSK (e.g., 6.04 dB for $\lambda = 40$, $\gamma^2 = 0.2$) may be thought of as frequency diversity of spread-spectrum communication. Most of this improvement results from the multipath rejection capability of a properly designed spread-spectrum system. It should be noted that this multipath rejection is fully achieved only if the signature sequences have good aperiodic autocorrelation properties. As will be seen below, poor choices of signature sequences will result in a signal-to-noise ratio that is as much as 3 dB below the DS/SS curve of Fig. 11.

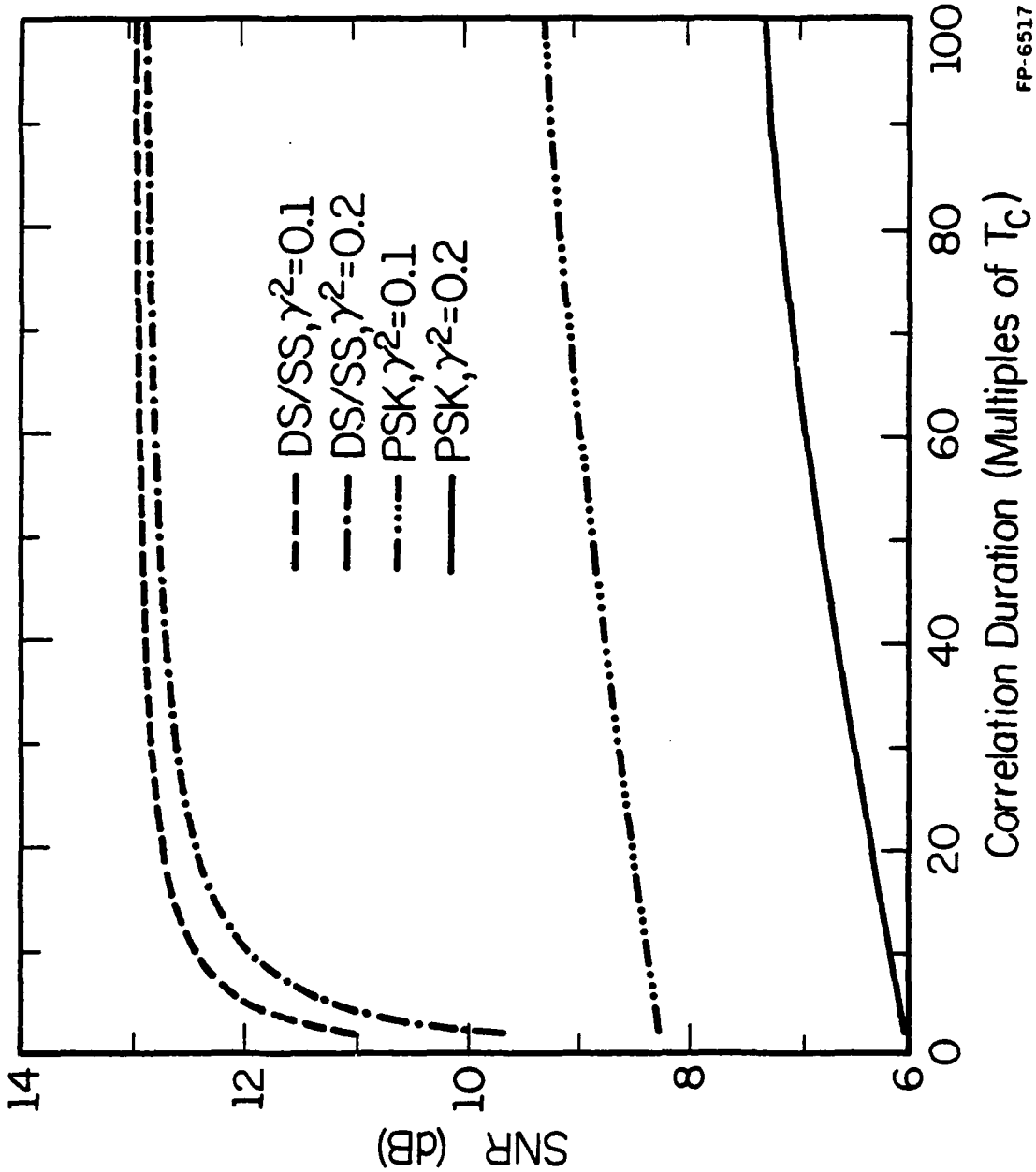

Figure 11. SNR vs. correlation duration for a frequency-selective fading channel with a triangular covariance function for single-user DS/spread-spectrum and biphase PSK systems (N = 127, $\mathcal{E}/N_0$ = 10dB).

We will now examine Fig. 11 in greater detail. First, from (3.41) and (3.65), for small values of correlation duration, $g(\tau)$ approaches a delta function of unit area. Since $R_i(0) = 0$ and $\hat{R}_i(0) = T$ from (1.7) and (1.8), we see that for a correlation duration of value zero, (3.71) and (3.72) both reduce to

$$SNR = \{\frac{N_0}{2\mathcal{E}} + \gamma^2\}^{-\frac{1}{2}} \tag{3.73}$$

i.e., the performance of the two systems is identical for $\lambda T_c = 0$. From (3.73), we see that for $\lambda T_c = 0$, SNR = 8.239 for $\gamma^2 = 0.1$ and SNR = 6.020 dB for $\gamma^2 = 0.2$ for both systems. This convergence of performance at $\lambda = 0$ as well as the performance of both types of systems at other values of λT_c can be explained physically by considering the autocorrelation function of the signature sequence together with the concept of multipath. To see this, note that the continuous-time <u>periodic</u> autocorrelation function $\theta_i(\tau)$ of a code waveform $a_i(t)$ is defined as

$$\theta_i(\tau) \triangleq \int_0^T a_i(t-\tau)\, a_i(t)\, dt \tag{3.74}$$

$$= R_i(\tau) + \hat{R}_i(\tau), \tag{3.75}$$

where the last line follows from (1.7) and (1.8). Using (3.75) in (3.71), we see that SNR for a DS/SS system operating over a frequency-selective fading channel becomes

$$SNR = \{\frac{N_0}{2\mathcal{E}} + \frac{2\gamma^2}{T^2}\int_0^T g(\tau)[\theta_i^2(\tau) - 2R_i(\tau)\hat{R}_i(\tau)]d\tau\}^{-\frac{1}{2}} \tag{3.76}$$

which is a function of both the aperiodic and periodic autocorrelation functions of the code waveform. From the discussion in Section 2.6, $g(\tau)$ appearing in (3.76) may be considered to be a weighted "window-function" on the allowable range of delay-spread of the multipath of the fading channel. Thus for a given value of correlation duration, $g(\tau)$ "passes" only multipath having range delays less than λT_c. Consequently, multipath present on the channel will degrade the performance of a DS/SS system, the extent of degradation being determined by the exact form of the continuous-time autocorrelation functions of the code waveform.

To give a concrete example of how the shape of the autocorrelation functions of the code waveform affect the performance of the DS/SS system, assume that the DS/SS system employs the N = 120 sequence given by $\{a^{(i)}\} = \{1,1,1,0,0,0,\ldots\}$. The magnitude of the continuous-time periodic autocorrelation function of $a_i(t)$ is shown in Fig. 12. From Fig. 12 and (3.76) we note that multipath signals having delays which are odd multiples of $3T_c/2$ will be rejected by the DS/SS receiver. On the other hand, multipath signals having delays which are even multiples of $3T_c/2$ will not be rejected by the receiver, thus causing degradation of the DS/SS system performance. Multipath signals having delays of other values will also tend to degrade the system performance, the extent of degradation being determined by the value of $|\theta(\tau)|$ for a particular value of delay τ. Now consider the performance of the DS/SS system when an m-sequence of period 127

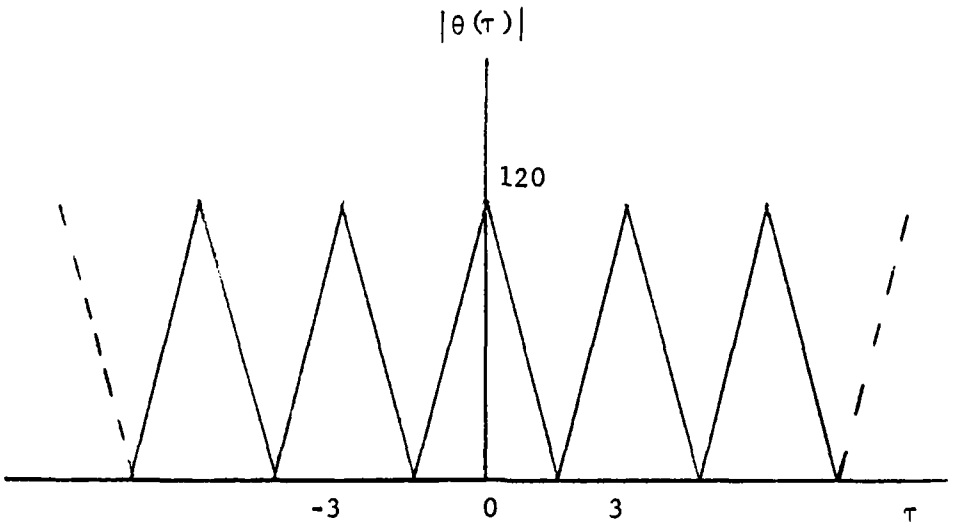

Figure 12. Magnitude of the autocorrelation function of the sequence {1,1,1,0,0,0...} (N = 120).

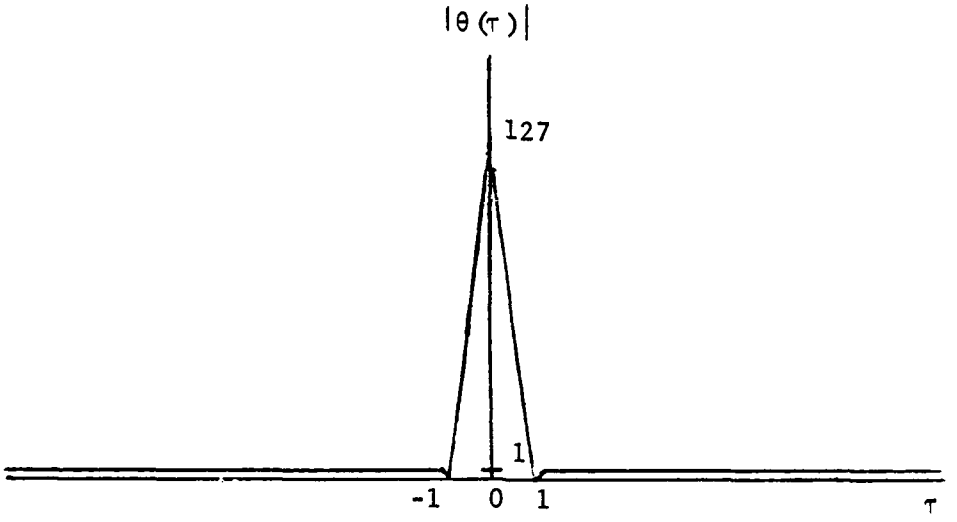

Figure 13. Magnitude of the autocorrelation function of an m-sequence (N = 127).

is used for the signature sequence. The magnitude of the continuous-time periodic autocorrelation function of this signature sequence is shown in Fig. 13 [Stiffler, 1971]. In this case, because of the "noise-like" periodic autocorrelation function of the m-sequence, all multipath signals arriving with delays greater than one chip duration will tend to be rejected by the receiver, as can be seen from (3.76). Because of its good periodic autocorrelation function an m-sequence is expected to be a better candidate for a signature sequence than the "periodic" signature sequence discussed above, when system performance is being evaluated for a frequency-selective fading channel. In Fig. 14 we have evaluated (3.76) for three "periodic" signature sequences of length 120 having periods of 2, 6, and 12, respectively, and for one m-sequence of period 127 for a triangular channel covariance function and for $\frac{\mathcal{E}}{N_0}$ = 10 dB, γ^2 = 0.2. From this figure we see that our conjectures about the performance of the two types of signature sequences are valid. For values of λ greater than two, the m-sequence outperforms all other signature sequences, primarily due to the periodicity of the periodic autocorrelation functions of the other signature sequences. Note that for λ = 20, the difference in performance of the two types of signature sequences is 2.87 dB. The reason that all of the SNR curves exhibit a

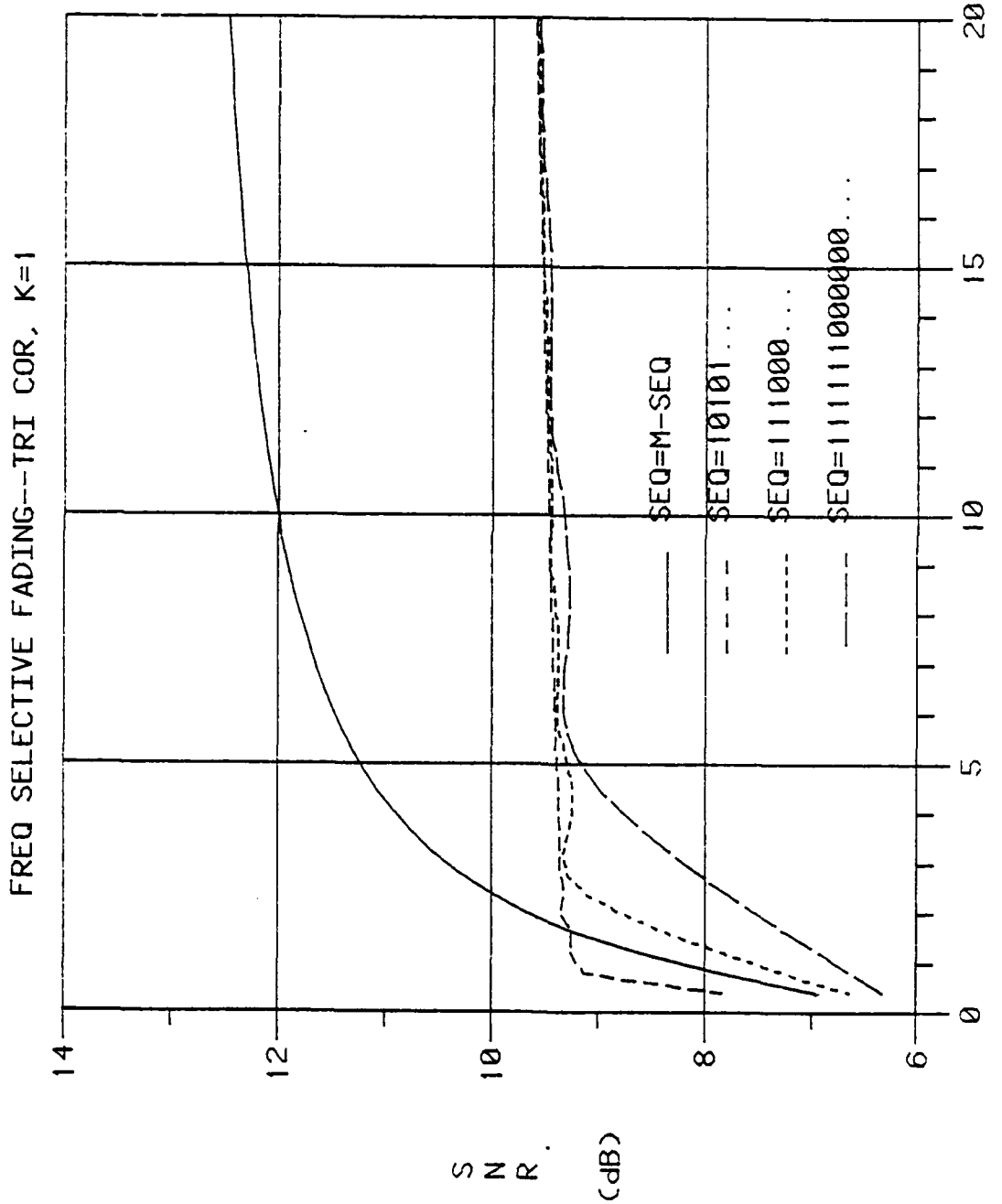

Figure 14. Comparison of SNR vs. correlation duration for a frequency-selectiv fading channel with a triangular covariance function for a single-user DS/spread-spectrum system for four choices of signature sequences ($\gamma^2 = 0.2$, $\mathcal{E}/N_0 = 10$dB)

general upward trend is due to the unit variance constraint (3.65) on the channel covariance function $g_i(\tau)$. For large values of correlation duration, $g_i(\tau)$ is "spread-out" over the range $0 \leq \tau \leq \lambda T_c$ and since the area under $g_i(\tau)$ is constant, the magnitude of $g_i(\tau)$ decreases for increasing values of λT_c, resulting in a smaller contribution of the integral term appearing in (3.76).

The above explanation has centered upon the periodic autocorrelation function of the code waveform as the basis for DS/SS system performance, without taking into account the aperiodic autocorrelation terms which also appear in (3.76). In addition, we have neglected the "smoothing" effects of the integral appearing in (3.76). Thus the explanation given above should be treated as a "first-order" model of what is physically occurring in the DS/SS system. Nevertheless, this first-order model is accurate enough to predict the performance of a PSK system over a frequency-selective fading channel. Treating the PSK system as simply a DS/SS system with a constant-code waveform, the periodic autocorrelation function of the PSK code waveform is a constant function. Thus the PSK system does not reject any multipath signals, resulting in its inferior performance compared to a DS/SS system using an m-sequence for its signature sequence.

3.5. Performance Evaluation for Random Signature Sequences

In this section approximate expressions are obtained for SNR_i for both time-selective and frequency-selective fading channels with a specific channel correlation function. These approximations are the expected values of SNR_i when the signature sequences are random binary

sequences. By random binary sequences we mean a set of K statistically independent binary sequences $\{a_n^{(k)}\}$, $1 \le k \le K$. Each sequence $\{a_n^{(k)}\}$ is a sequence of independent random variables $a_n^{(k)}$ for which $\Pr\{a_n^{(k)} = +1\} = \Pr\{a_n^{(k)} = -1\} = \frac{1}{2}$. The expected value of SNR_i is just the average signal-to-noise ratio $\overline{SNR}$, where the averaging is over all possible sets of K binary sequences of period N. One reason for computing $\overline{SNR}$ is that, in some sense, $\overline{SNR}$ is a measure of the asymptotic performance of a DS/SSMA system for which the signature sequence length N is very large [Roefs, 1977]. A second reason for computing $\overline{SNR}$ is that, as we will show below, $\overline{SNR}$ is a close approximation (for a reasonable set of signature sequence) to SNR_i, yet evaluation of $\overline{SNR}$ does not require computation of the aperiodic correlation functions of any specific sets of signature sequences.

First we note that for random binary sequences the moments of the aperiodic autocorrelation functions are given by

$$E\{C_k(\ell)\} = \begin{cases} 0, & \ell \neq 0 \\ N, & \ell = 0 \end{cases} \tag{3.77a}$$

$$E\{C_k^2(\ell)\} = \begin{cases} N-|\ell|, & \ell \neq 0 \\ N^2, & \ell = 0 \end{cases} \tag{3.77b}$$

$$E\{C_k(\ell)C_i(\ell)\} = \begin{cases} 0, & \ell \neq 0,\ k \neq i \\ N^2, & \ell = 0 \end{cases} \tag{3.77c}$$

$$E\{C_k(\ell)C_i(\ell+1)\} = 0 \qquad \forall k,i\ . \tag{3.77d}$$

Equations (3.77a)-(3.77d) were previously derived by Roefs (1977) except for the case $\ell = 0$ in (3.77a) through (3.77c). From the definitions of $C_k(\ell)$ and random binary sequences, for $\ell = 0$ we obtain

$$E\{C_k(0)\} = E\{\sum_{j=0}^{N-1} [a_j^{(k)}]^2 = E\{\sum_{j=0}^{N-1} 1\} = N. \tag{3.78}$$

Similarly we find that

$$E\{C_{k,i}^2(0)\} = E\{\sum_{j=0}^{N-1} [a_j^{(k)}]^2 \sum_{h=0}^{N-1} [a_h^{(i)}]^2\} = N^2 \qquad \forall k,i\ . \tag{3.79}$$

Using (3.77), we may evaluate the expected values of the code-dependent terms in (3.46) and (3.47). Let $\overline{SNR} \triangleq T\sqrt{\frac{1}{2}P}\,[E\{\text{Var } F_i + \text{Var } I_i\} + \frac{1}{2}N_0T]^{-\frac{1}{2}}$, where Var F_i and Var I_i are now random variables because the signature sequences $\{a_n^{(k)}\}$ are random. Using the above results, we find that for a time-selective fading channel with a triangular channel covariance function, $\overline{SNR}$ is

$$\overline{SNR} = \{\frac{\gamma^2\beta}{N}\,[1 - \frac{1}{3}\frac{\beta}{N}\,] + \frac{\gamma^2(K-1)\beta}{6N}\,\{\beta^2-4\beta+6\} + \frac{(K-1)}{3N} + \frac{N_0}{2\delta}\,\}^{-\frac{1}{2}} \tag{3.80a}$$

for $\lambda < 1$ and

$$\overline{SNR} = \{\frac{\gamma^2}{N}\,[1 - \frac{1}{3}\frac{\lambda}{N}] + \frac{2\gamma^2}{3N}\,(K-1)[1 - \frac{1}{4\lambda}] + \frac{(K-1)}{3N} + \frac{N_0}{2\delta}\,\}^{-\frac{1}{2}}\ , \tag{3.80b}$$

for $\lambda \geq 1$. The corresponding result for a time-selective fading channel with a truncated-exponential channel covariance function is

$$\overline{SNR} = \{ \frac{2\gamma^2}{N\alpha} [(1 - e^{-\alpha\lambda}) + \frac{1}{N\alpha} (e^{-\alpha\lambda}(\alpha\lambda + 1)-1)]$$

$$+ \frac{2\gamma^2(K-1)}{N\alpha} [(1 - e^{-\alpha\beta}) -2(\frac{1}{\alpha} (1-e^{-\alpha\beta}(\alpha\beta + 1)))$$

$$+ (\frac{2}{\alpha^2} - e^{-\alpha\beta}(\beta^2 + \frac{2\beta}{\alpha} + \frac{2}{\alpha^2}))] + (\frac{(K-1)}{3N} + \frac{N_0}{2\delta} \}^{-\frac{1}{2}} \qquad (3.81a)$$

for $\lambda < 1$ and

$$\overline{SNR} = \{ \frac{2\gamma^2}{N\alpha} [(1-e^{-\alpha\lambda}) + \frac{1}{N\alpha} (e^{-\alpha\lambda}(\alpha\lambda + 1)-1)]$$

$$+ \frac{2\gamma^2(K-1)}{N\alpha} [1 + \frac{2}{\alpha} (\frac{1}{\alpha}(1-e^{-\alpha})-1)] + \frac{(K-1)}{3N} + \frac{N_0}{2\delta} \}^{-\frac{1}{2}} \qquad (3.81b)$$

for $\lambda \geq 1$, where as before, $\gamma_k^2 = \gamma^2$ for all k.

Similarly, $\overline{SNR}$ for a frequency-selective fading channel with a triangular channel covariance function is given by

$$\overline{SNR} = \{\frac{2\gamma^2}{\lambda N} [\frac{1}{2} \beta N - \frac{1}{3} \beta^2 N + \frac{1}{12} \beta^3(N+1)] + \frac{(K-1)}{3N}(1+2\gamma^2) + \frac{N_0}{2\delta} \}^{-\frac{1}{2}}, \qquad (3.82a)$$

for $\lambda < 1$,

$$\overline{SNR} = \{\frac{2\gamma^2}{\lambda N} [\frac{2N}{3\lambda} - \frac{N}{2\lambda} + \frac{1}{3}(N+1)(1 - \frac{3}{4\lambda}) + \beta(1 - \frac{1}{\lambda}(1 + \frac{1}{2} \beta))$$

$$- \beta^2(1 - \frac{1}{\lambda}(1+ \frac{2}{3} \beta))+ \frac{2}{3} \beta^3(1 - \frac{1}{\lambda}(1+ \frac{3}{4} \beta))]+ \frac{(K-1)}{3N}(1+2\gamma^2)+ \frac{N_0}{2\delta} \}^{-\frac{1}{2}} \qquad (3.82b)$$

for $1 \leq \lambda < 2$, and

$$\overline{SNR} = \{ \frac{2\gamma^2}{\lambda N} [\frac{1}{3} N + \frac{1}{12} (4 - \frac{N}{\lambda}) - \frac{1}{4\lambda} + (n-1)(\frac{2}{3} - \frac{1}{3\lambda}) - \frac{n(n-1)}{3\lambda}$$

$$+ \beta(1 - \frac{1}{\lambda}(n + \frac{1}{2}\beta)) - \beta^2(1 - \frac{1}{\lambda}(n + \frac{2}{3}\beta)) + \frac{2}{3}\beta^2(1 - \frac{1}{\lambda}(n + \frac{3}{4}\beta))]$$

$$+ \frac{(K-1)}{3N}(1 + 2\gamma^2) + \frac{N_0}{2\delta} \}^{-\frac{1}{2}} \qquad (3.82c)$$

for $2 \leq \lambda < N-1$. The corresponding result for a frequency-selective fading channel with a truncated-exponential channel covariance function is

$$\overline{SNR} = \{\frac{\gamma^2}{(1-e^{-\alpha\lambda})} [(1-e^{-\alpha\beta}) - \frac{2}{\alpha}(1-e^{-\alpha\beta}(\alpha\beta + 1))$$

$$+ (1 + \frac{1}{N})(\frac{2}{\alpha^2} - e^{-\alpha\beta}(\beta^2 + \frac{2\beta}{\alpha} + \frac{2}{\alpha^2}))] + \frac{(K-1)}{3N}(1+2\gamma^2) + \frac{N_0}{2\delta} \}^{-\frac{1}{2}}, \qquad (3.83a)$$

for $\lambda < 1$,

$$\overline{SNR} = \{\frac{\gamma^2}{(1-e^{-\alpha\lambda})} [(1-e^{-\alpha} - \frac{2}{\alpha} + \frac{2}{\alpha} e^{-\alpha}(\alpha+1))$$

$$+ (1 + \frac{1}{N})(\frac{2}{\alpha^2} - e^{-\alpha}(\alpha(1 + \beta)+1)) + e^{-\alpha}\{\frac{1}{N}(1-e^{-\alpha\beta})$$

$$- \frac{2}{N}[\frac{1}{\alpha}((\alpha + 1) - e^{-\alpha\beta}(\alpha(1 + \beta)+1)) - (1-e^{-\alpha\beta})]$$

$$+ \frac{2}{N}[(1 + \frac{2}{\alpha} + \frac{2}{\alpha^2}) - e^{-\alpha\beta}((1 + \beta^2) + \frac{2(1 + \beta)}{\alpha} + \frac{2}{\alpha^2})$$

$$+ \frac{2}{\alpha}((e^{-\alpha\beta}(\alpha(1 + \beta)+1) - (\alpha + 1)) + (1-e^{-\alpha\beta})]\}]$$

$$+ \frac{K-1}{3N}(1 + 2\gamma^2) + \frac{N_0}{2\delta} \}^{-\frac{1}{2}}, \qquad (3.83b)$$

for $1 \leq \lambda < 2$, and

$$\overline{SNR} = \{\frac{\gamma^2}{(1-e^{-\alpha\lambda})N^2}\,[N^2(1-e^{-\alpha} - \frac{2}{\alpha} + \frac{2}{\alpha}\,e^{-\alpha}(\alpha + 1))$$

$$+ (N^2 + N)(\frac{2}{\alpha^2} - e^{-\alpha}(1 + \frac{2}{\alpha} + \frac{2}{\alpha^2})) + \sum_{\ell=1}^{n-1} e^{-\alpha\ell}[N(1-e^{-\alpha})$$

$$- 2N[\frac{1}{\alpha}((\alpha\ell + 1)-e^{-\alpha}(\alpha(\ell + 1) +1)) - \ell(1-e^{-\alpha})]$$

$$+ 2N[(\ell^2 + \frac{2\ell}{\alpha} + \frac{2}{\alpha^2}) - e^{-\alpha}((\ell + 1)^2 + \frac{2}{\alpha}(\ell + 1) + \frac{2}{\alpha^2})$$

$$+ \frac{2\ell}{\alpha}(e^{-\alpha}(\alpha(\ell + 1) +1) - \alpha\ell - 1) + \ell^2(1-e^{-\alpha})]]$$

$$+ e^{-\alpha n}[N(1-e^{-\alpha\beta}) - 2N(\frac{1}{\alpha}(\alpha n + 1 - e^{-\alpha\beta}(\alpha(n + \beta) + 1))$$

$$- n(1-e^{-\alpha\beta})) + 2N(n^2 + \frac{2n}{\alpha} + \frac{2}{\alpha^2} - e^{-\alpha\beta}((n + \beta)^2 + \frac{2}{\alpha}(n + \beta) + \frac{2}{\alpha^2})$$

$$+ \frac{2n}{\alpha}(e^{-\alpha\beta}(\alpha(n + \beta) + 1) - \alpha n - 1) + n^2(1-e^{-\alpha\beta}))]]$$

$$+ \frac{K-1}{3N}(1 + 2\gamma^2) + \frac{N_0}{2\mathcal{E}}\}^{-\frac{1}{2}} \qquad (3.83c)$$

for $2 \leq \lambda < N-1$. Note that expressions (3.80) through (3.83) for $\overline{SNR}$ are functions only of the channel covariance function, the parameter γ^2, the number of users K, the length of the signature sequence, and the bit energy to noise spectral density.

In order to ascertain the accuracy of the above results as an approximation to (3.46), (3.47), (3.68), and (3.69), $\overline{SNR}$ was evaluated for various values of γ^2 and λT_c for N = 127, K = 6, and these results were compared with those obtained in Sections 3.2 and 3.3 for the corresponding channel type and channel correlation function. For the ranges of γ^2, λT_c, and $\mathcal{E}/N_0$ used in Figs. 5 and 8, the expression for $\overline{SNR}$ differed from the exact expression for SNR_i by less than 0.05 dB, for the specific signature sequences used to obtain Figs. 5 and 8. As a further check on the accuracy of the above results, (3.46) was evaluated for a maximal-connected set of m-sequences using LSE/AO phases [Pursley and Roefs, 1979] for N = 31 and N = 63 and the results were compared with the corresponding results obtained from (3.80). Once again, for γ^2 in the range $0.05 \leq 0.2$ and $\lambda \leq 0.1N$ the difference between $\overline{SNR}$ and SNR_i was found to be less than 0.05 dB. Thus, based on this comparison of numerical results, we conclude that $\overline{SNR}$ is a very good approximation to SNR_i for the sets of signature sequences used above. Furthermore, from the comments in Section 3.2, it follows that $\overline{SNR}$ is also a good approximation to SNR_i for maximal-connected sets of m-sequences of length 127 with AO/LSE phases. Since the expressions for $\overline{SNR}$ are considerably easier to evaluate than the corresponding exact expressions, the quantity $\overline{SNR}$ is a useful approximation for the preliminary design of a DS/SS system operating over a Rician fading channel. Examples of this application of $\overline{SNR}$ for the AWGN channel may be found in [Pursley and Roefs, 1979]. It should be noted that in the absence of fading, expressions (3.80) through (3.83) all reduce to the expression obtained by Roefs and Pursley (1977) for $\overline{SNR}$ for the AWGN channel by setting $\gamma^2 = 0$ in (3.80)-(3.83).

The accuracy of the expressions for $\overline{SNR}$ as approximations to SNR_i for the sets of signature sequences studied above (i.e., maximal-connected sets of m-sequences with LSE/AO or AO/LSE loadings) does not imply that any arbitrary collection of m-sequences will provide the same performance. As an example of this, (3.68) was evaluated for N = 31, K = 3, using two different collections of m-sequences. One set maximizes the parameters $r_{k,i}$ and the other minimizes $r_{k,i}$. These two sets were found by an exhaustive search of sets of 3 m-sequences of length 31 having every possible phase [Garber, 1978]. The comparison of (3.82) with (3.68) for these two sets is shown in Fig. 15 for $\gamma^2 = 0.05$. Note that there is a significant difference (> 0.7 dB) in performance between the best set (curve 1) and the worst set (curve 3) of signature sequences. This difference is larger for larger values of $\mathcal{E}/N_0$ or smaller values of γ^2. For very large $\mathcal{E}/N_0$ and very small γ^2, this difference is given by

$$\Delta SNR(dB) = 10 \log_{10}\left\{ \frac{\sum_{\substack{k=1 \\ k\neq i}}^{K} r_{k,i} \text{ (worst case)}}{\sum_{\substack{k=1 \\ k\neq i}}^{K} r_{k,i} \text{ (best case)}} \right\} \tag{3.84}$$

which, for these two sets of signature sequences, is 2.353 dB.

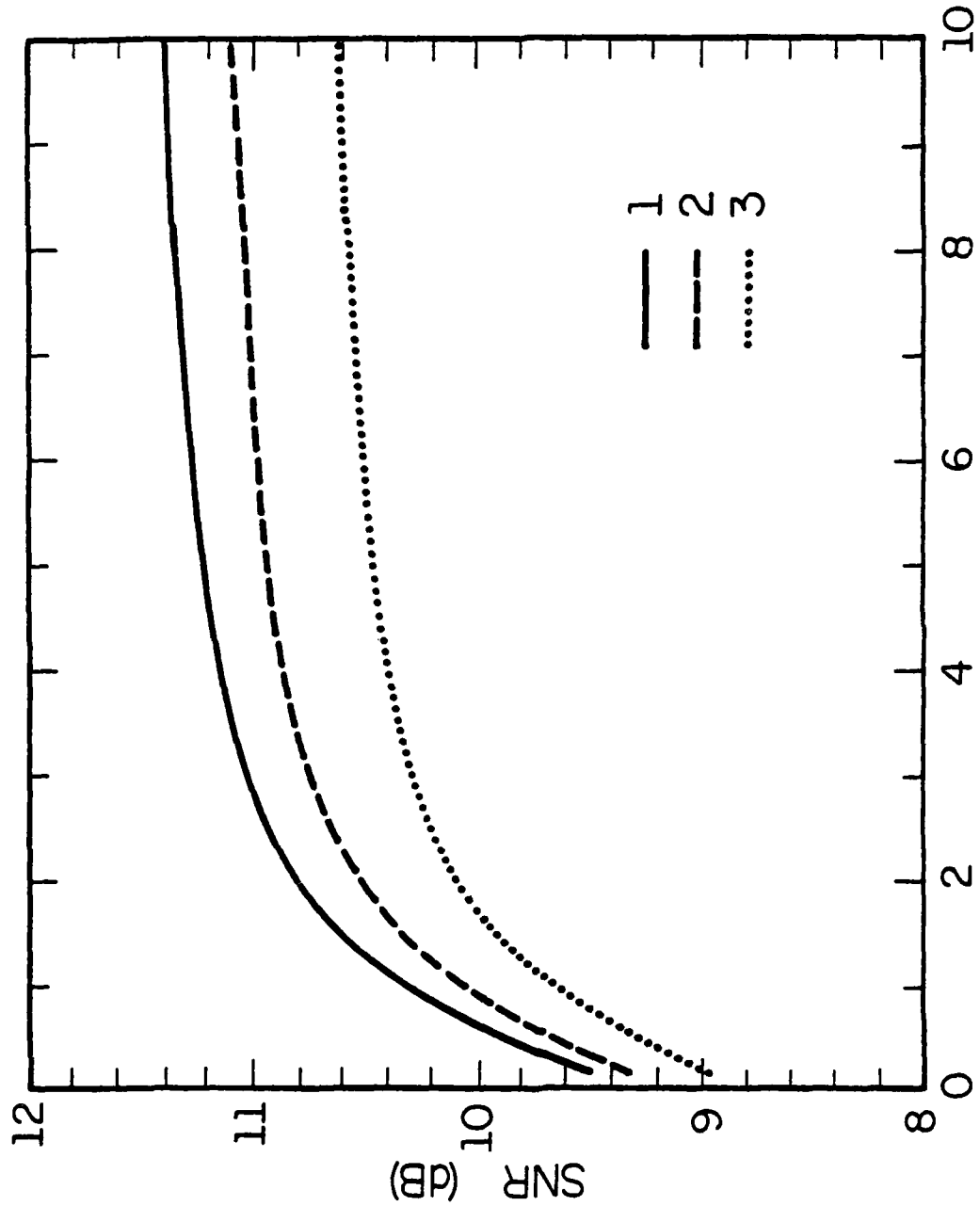

Figure 15. SNR vs. correlation duration for a frequency-selective fading channel with a triangular covariance function (N = 31, K = 3, γ^2 = 0.05, $\mathcal{E}/N_0$ = 10dB), 1-m-sequences for minimum $r_{k,i}$, 2-random binary sequences, 3-m-sequences for maximum $r_{k,i}$.

CHAPTER 4

PROBABILITY OF ERROR BOUNDS FOR DS/SSMA COMMUNICATIONS VIA FADING CHANNELS

In Chapter 1 we noted that for DS/SSMA communications via an AWGN channel, three measures of system performance are available: average signal-to-noise ratio (SNR), worst case performance, and probability of error (P_e). In the previous chapter we have analyzed the performance of DS/SSMA communications via fading channels using SNR as the system performance measure. In this chapter we analyze the performance of DS/SSMA communications via fading channels using probability of error at the output of a correlation receiver as the system performance measure. The results obtained here represent a generalization of the performance analysis of [Yao, 1977] which considered only AWGN channels.

Although we shall use probability of error as the system performance measure, as noted in Section 4.1, exact evaluation of the probability of error at the output of a correlation receiver for a DS/SSMA system operating over a fading channel is very difficult. Hence we shall concentrate our effort on obtaining bounds on P_e. Specifically we shall bound P_e through the use of an isomorphism theorem from the theory of moment spaces which provides relationships among arbitrary moments of a random variable.

Throughout this chapter we shall concentrate on the two singly-spread channels considered in Chapter 3: time-selective fading channels and frequency-selective fading channels. With appropriate changes in the equations that follow, the results presented below may be generalized to other classes of WSSUS fading channels.

4.1. Moment Space Bounds on Probability of Error

In this section we shall present the general problem of obtaining moment space bounds on the probability of error at the output of a correlation receiver for the DS/SSMA system model considered in Chapter 3. In Sections 4.2 and 4.3 we shall consider specific examples of the moment space bounding technique applied to time-selective and frequency-selective fading channels for second and N-th moment bounds, respectively.

From Chapter 3, we found that for a DS/SSMA system operating over a doubly-spread fading channel, the output of the correlation receiver matched to the i-th user's phase-coded waveform is given by (see 3.18)

$$Z_i = N_i + D_i + F_i + I_i \tag{4.1}$$

where N_i and D_i are given by (3.14) and (3.12), respectively and F_i and I_i are the real parts of the complex quantities $\tilde{F}_i$ and $\tilde{I}_i$ defined by (3.13) and (3.15), respectively. Assuming that the data bit $b_{i,0}$ takes on the values $\{+1,-1\}$ with equal probability, the probability of error at the output of the i-th correlation at the decision instant $t = T$ is given by

$$\begin{aligned} P_e &= \tfrac{1}{2} \Pr\{\text{error} | b_{i,0} = -1\} + \tfrac{1}{2} \Pr\{\text{error} | b_{i,0} = +1\} \\ &= \tfrac{1}{2} \Pr\{Z_i > 0 | b_{i,0} = -1\} + \tfrac{1}{2} \Pr\{Z_i < 0 | b_{i,0} = +1\} \\ &= \tfrac{1}{2} E\{\Pr[Z_i > 0 | b_i(t), b_{i,0} = -1]\} + \tfrac{1}{2} E\{\Pr[Z_i < 0 | b_i(t), b_{i,0} = +1]\} \end{aligned} \tag{4.2}$$

Note that in (4.2) we are simply evaluating P_e conditioned upon $b_i(t)$ and then averaging over $b_i(t)$ to obtain an expression for P_e.

For convenience, define $h \triangleq \sqrt{P/2}\,T$ and $z \triangleq F_i + I_i$. Then the first term inside the curly brackets of (4.2) may be rewritten as

$$\Pr\{Z_i > 0 | b_i(t), b_{i,0} = -1\} = E\{Q(\frac{h-z}{\sigma}) | b_i(t), b_{i,0} = -1\} \tag{4.3}$$

where $Q(x) = 1 - \Phi(x)$ and $\sigma = \sqrt{\frac{1}{4}N_0 T}$ is the standard deviation of N_i (see 3.19). In (4.3), the expectation over z conditioned upon $b_i(t)$ and $b_{i,0} = -1$ denotes expectation over all the random variables $b_k(t)(k \neq i)$, τ_k, ϕ_k, and $\beta_k(\tau, t)$ appearing in z. Since given $b_i(t)$, z is symmetric about zero, (4.3) may also be written as

$$\Pr\{Z_i > 0 | b_i(t), b_{i,0} = -1\} = E\{\tfrac{1}{2}Q(\frac{h+z}{\sigma}) + \tfrac{1}{2}Q(\frac{h-z}{\sigma}) | b_i(t), b_{i,0} = -1\} \tag{4.4}$$

In a similar fashion, the second term inside the curly brackets of (4.2) may be expressed by

$$\Pr\{Z_i < 0 | b_i(t), b_{i,0} = +1\} = E\{\tfrac{1}{2}Q(\frac{h+z}{\sigma}) + \tfrac{1}{2}Q(\frac{h-z}{\sigma}) | b_i(t), b_{i,0} = +1\} \tag{4.5}$$

From (4.2), (4.4), and (4.5) we find that

$$\Pr\{\text{error} | b_{i,0} = -1\} = \tfrac{1}{2}E[E\{Q(\frac{h+z}{\sigma}) + Q(\frac{h-z}{\sigma}) | b_i(t), b_{i,0} = -1\} | b_{i,0} = -1] \tag{4.6}$$

and

$$\Pr\{\text{error} | b_{i,0} = +1\} = \tfrac{1}{2}E[E\{Q(\frac{h+z}{\sigma}) + Q(\frac{h-z}{\sigma}) | b_i(t), b_{i,0} = +1\} | b_{i,0} = +1]\,. \tag{4.7}$$

Hence, if the expectations in (4.6) and (4.7) can be evaluated, the probability of error at the output of the i-th correlation receiver may be obtained.

Several approaches are available for evaluating (4.2). The first is the direct approach, in which the expectations in (4.6) and (4.7) are directly evaluated. In general, because of the complicated form of z, however, P_e is very difficult to evaluate either analytically or numerically. To give an indication of the amount of difficulty required to evaluate (4.2) numerically, a recent attempt to evaluate the expectations in (4.6) over only τ_k and b_k required 1.4 minutes of CPU time on a Digital Equipment Corporation DEC-10 computer system for a two-user DS/SSMA system employing a code sequence of length 127 for a single value of $\mathcal{E}/N_0$. Clearly the analytical or numerical approach to evaluating (4.2) becomes unwieldy for larger numbers of users, longer code sequences, or a large number of $\mathcal{E}/N_0$ values.

A second approach to evaluation of (4.2) is by simulation and use of the Monte Carlo method. Such an approach was taken by Orr (1977) in evaluating the probability of error of a DS/SSMA system using a slowly-fading (nondispersive) fading channel. The major drawbacks of the simulation method of evaluating P_e are that the technique requires a considerable amount of computation time and that it provides very little insight into the design aspect of the problem.

A third technique to evaluating (4.2) and the one employed in the remainder of this chapter is the moment-space bounding method. In order to understand the theoretical background for the moment-space bounding method, we will now state, without proof, an isomorphism theorem [Yao, 1977] originally developed in the theory of games ([Dresher, et. al., 1950], [Dresher, 1953]) which provides relationships among arbitrary moments of a random variable.

Isomorphism Theorem: Let Y be a random variable with a probability distribution function $G_Y(y)$ defined over a finite closed interval $I = [a,b]$. Let $k_1(y), k_2(y), \ldots, k_N(y)$ be a set of N continuous functions defined on I. The generalized moment of the random variable Y induced by the function $k_i(y)$ is

$$m_i = \int_I k_i(y)\, dG_Y(y) = E_Y\{k_i(y)\}, \qquad i = 1, \ldots, N. \tag{4.8}$$

We denote the N-th moment space $\mathcal{M}$ by

$$\mathcal{M} = \{\underline{m} = (m_1, \ldots, m_N) \in R^N \mid m_i = \int_a^b k_i(y) dG_Y(y), 1 \leq i \leq N, G_Y \in \mathcal{P}(I)\} \tag{4.9}$$

where $\mathcal{P}(I)$ is the set of probability distributions defined on $I = [a,b]$ and R^N denotes N-dimensional Euclidean space. Then $\mathcal{M}$ is a closed, bounded, and convex set. Now let $\mathcal{C}$ be the curve $\underline{r} = (r_1, \ldots, r_N)$ traced out in R^N by $r_i = k_i(y)$ for y in I. Let $\mathcal{K}$ be the convex hull of $\mathcal{C}$. Then

$$\mathcal{K} = \mathcal{M}. \tag{4.10}$$

A brief proof of the above theorem may be found in [Yao and Tobin, 1976]; a detailed discussion of the proof is given in [Dresher, et. al., 1950].

To demonstrate how the isomorphism theorem can be used to solve the problem at hand, let N = 2 and let $k_2(z)$ be equal to the expression inside the curly brackets of (4.6). Let $k_1(z)$ be some continuous function of z whose generalized moment m_1 given by (4.8) may be readily evaluated. Now consider a plot of $k_2(z)$ versus $k_1(z)$ and denote the convex hull of the resulting figure by $\mathcal{K}$. From the isomorphism theorem, $\mathcal{K} = \mathcal{M}$ so that knowledge of $m_1 = E\{k_1(z) \mid b_i(t), b_{i,0} = -1\}$ enables us to obtain bounds on $m_2 = E\{k_2(z) \mid b_i(t), b_{i,0} = -1\}$. But by our choice of $k_2(z)$,

$$\Pr\{\text{error}|b_i(t), b_{i,0} = -1\} = m_2 \qquad (4.11)$$

so that we have, in fact obtained bounds on the conditional probability of error, conditioned upon $b_i(t)$ and $b_{i,0} = -1$. Repeating this process for $\Pr\{\text{error}|b_i(t), b_{i,0} = +1\}$ and averaging the sum of these two bounds over $b_i(t)$, from (4.2) we see that we have bounded the probability of error (P_e) through use of the isomorphism theorem.

In practice, we would like to choose $k_1(z)$ so that the convex hull of the plot of $k_2(z)$ versus $k_1(z)$ is "thin" and hence the P_e bounds obtained are tight. Ideally we would like to choose $k_1(z) = k_2(z)$, in which case the convex hull $\mathcal{K}$ is infinitely thin and the upper bound P_e^U equals the lower bound P_e^L. However, this would require knowledge of $m_2 = E\{k_2(z)\}$ which we assumed could not be directly evaluated. Thus in choosing $k_1(z)$ we must, in general, trade-off the thickness of $\mathcal{K}$ with the ease of evaluating m_1. Based on previous results in the published literature ([Yan, 1975],[Yao and Tobin, 1976],[Yao, 1977]) a promising choice for $k_1(z)$ is $k_1(z) = z^N$, where N is even. The error bounds resulting from such a choice are known as N-th moment bounds.

For a given choice of $k_1(z)$ and $k_2(z)$, three methods are available for evaluating Pe^U and Pe^L through the use of the isomorphism theorem: graphical techniques, numerical techniques, and analytical techniques. The graphical technique is attractive from the viewpoint that in order to employ it, we need only plot $k_2(z)$ versus $k_1(z)$ over the range of z and complete the convex hull $\mathcal{K}$ by means of a straightedge. Assuming that m_1 is known, the conditional upper and lower error bounds, conditioned

upon $b_i(t)$, may be read directly off the graph. Repeating this process for all data bit patterns $b_i(t)$ of interest and averaging the conditional error bounds over $b_i(t)$, we obtain bounds on Pe^U and Pe^L. However as pointed out in [Yan, 1975], for sufficiently complex plots of $k_2(z)$ versus $k_1(z)$, determination of $\mathcal{K}$ by eye becomes quite difficult. In these cases, it becomes necessary to find $\mathcal{K}$ by numerical or analytical means. As might be expected, the numerical technique involves finding the convex $\cup$ and convex $\cap$ regions of $\mathcal{C}$ through numerical evaluation of the second derivation of $k_2(z)$ with respect to $k_1(z)$ over the range of z. The convex hull of $\mathcal{C}$ is then found directly using numerical techniques. The analytical approach to finding $\mathcal{K}$ is by writing equations for $\mathcal{K}$ based on knowledge of the convex regions of $\mathcal{C}$. From a design viewpoint, the analytical technique of finding $\mathcal{K}$ is the preferred method since the resulting equations describing $\mathcal{K}$ are explicit functions of the DS/SSMA system parameters and the fading channel characteristics. Because bounds on P_e^U and P_e^L are determined by $\mathcal{K}$ and m_1, DS/SSMA system performance can therefore be optimized for specific fading channels. In practice, as noted in Sections 4.2 and 4.3, the actual method used in evaluating $\mathcal{K}$ is a combination of both numerical and analytical techniques.

The above techniques of bounding P_e through the use of the isomorphism theorem have already been used successfully in the evaluation of the performance of several other types of communication systems including binary pulse-amplitude modulation (PAM) systems with intersymbol interference ([Yao and Tobin, 1975],[Yan, 1975],[Yao and Tobin, 1976]),

coherent phase shift keyed (CPSK) systems with cochannel interference [Tobin and Yao, 1977], DS/SSMA systems over AWGN channels ([Yao, 1976a], [Yao, 1976b],[Yao, 1977]), and PSK systems employing bandpass limiters [Yao and Milstein, 1978]. In all of these studies, either Nth moment (i.e., $k_1(z) = z^N$) or exponential moment (i.e., $k_1(z) = \exp(c(h+z))$ where c is a constant chosen to optimize the bounds) bounds were used to bound the probability of error. In the next two sections we shall apply Nth moment space bounds to bound the probability of error of DS/SSMA systems operating over specific classes of fading channels.

4.2. Second Moment Bounds

In this section we shall evaluate the second moment space bound on the probability of error for a DS/SSMA system operating over either a time-selective or a frequency-selective fading channel. In the following section we shall generalize the results obtained to Nth moment bounds. In order to clearly present our results we shall first consider the time-selective fading channel and later, the frequency-selective fading channel. At the end of this section we will present various criteria that are useful in selecting the range of z denoted by I in the isomorphism theorem of the previous section.

4.2.1. Second Moment Error Bounds for Time-Selective Fading Channels

To simplify the derivation of moment space bounds for the probability of error of a DS/SSMA system with a time-selective fading channel, instead of deriving results directly from the doubly-spread fading channel model as was done in Section 3.2, we shall use the simpler (but equivalent)

model of a time-selective fading channel developed in Section 2.5. Hence, from (2.52) and (2.53), the output of the i-th correlation receiver for a DS/SSMA system with a time-selective fading channel is given by (4.1), where D_i and N_i are given by (3.12) and (3.14), respectively and $F_i = \mathrm{Re}\{\tilde{F}_i\}$ and $I_i \triangleq \hat{I}_i + \hat{I}_i'$ where

$$\tilde{F}_i = \sqrt{\tfrac{1}{2}P} \int_0^T \gamma_i \beta_i(t) b_i(t) dt \tag{4.12}$$

$$\hat{I}_i \triangleq \mathrm{Re}\{\tilde{\hat{I}}_i\} = \mathrm{Re}\{\sqrt{\tfrac{1}{2}P} \sum_{\substack{k=1 \\ k\neq i}}^{K} \gamma_k \tilde{I}_{k,i}\} \tag{4.13}$$

$$\hat{I}_i' \triangleq \mathrm{Re}\{\tilde{\hat{I}}_i'\} = \mathrm{Re}\{\sqrt{\tfrac{1}{2}P} \sum_{\substack{k=1 \\ k\neq i}}^{K} \tilde{I}_{k,i}'\} \tag{4.14}$$

and

$$\tilde{I}_{k,i} \triangleq \int_0^T \beta_k(t-\tau_k) h_{k,i}(\tau_k;t) \exp(j\varphi_k) dt \tag{4.15}$$

$$\tilde{I}_{k,i}' \triangleq \int_0^T h_{k,i}(\tau_k;t) \exp(j\varphi_k) dt. \tag{4.16}$$

In (4.12) and (4.16) $\beta_k(t)$ is a zero-mean, unit variance complex Gaussian random process with covariance functions

$$E\{\tfrac{1}{2}\beta_k(t)\beta_k^*(s)\} = r_k(t-s) \tag{4.17a}$$

$$E\{\tfrac{1}{2}\beta_k(t)\beta_k(s)\} = 0 \ . \tag{4.17b}$$

From Section 4.1 we note that in order to determine second moment bounds on P_e, we must first evaluate the moments

$$m_1 = E\{z^2 | b_i(t)\} \tag{4.18}$$

where z is defined as in Section 4.1 and the expectation is over all $b_k(t)$ for $k \neq i$, φ_k and $\beta_k(t)$ in z conditioned upon all values of $b_i(t)$ of interest. As in Chapter 3, we shall model the phase angles, time delays, and data symbols for the k-th signal as mutually independent random variables which are uniformly distributed on $[0,2\pi]$, $[0,T]$, and $\{+1,-1\}$, respectively. From (4.12) through (4.16) we find that

$$\begin{aligned} E\{z^2 | b_i(t)\} &= E\{F_i^2 | b_i(t)\} + E\{I_i^2 | b_i(t)\} \\ &= E\{F_i^2 | b_i(t)\} + E\{I_i^2\} \end{aligned} \tag{4.19}$$

where we have used fact that I_i is independent of $b_i(t)$ and that the φ_k are independent random variables. Because F_i and I_i are identical to the terms F_i and I_i appearing in Section 3.2, noting that I_i is a zero mean random variable, the term $E\{I_i^2\}$ appearing in (4.19) is identical to Var I_i, previously evaluated in (3.39). Furthermore, using (1.1) in (4.12), we find that

$$\tilde{F}_i = \sqrt{\tfrac{1}{2}P}\, b_{i,0} \int_0^T \beta_i(t)dt \ . \tag{4.20}$$

Hence using (2.10) and (4.17), we find, as in (3.31), that

$$\begin{aligned} E\{F_i^2 | b_i(t)\} &= \frac{P}{2} \gamma_i^2 \int_0^T \int_0^T r_i(t-s)dtds \\ &= P\gamma_i^2 \int_0^T r_i(u)(T-u)du, \end{aligned} \tag{4.21}$$

which is independent of $b_i(t)$. Thus from (4.18), (3.39), and (4.21),

$$E\{z^2|b_i(t)\} = E\{F_i^2\} + E\{I_i^2\}$$

$$= E\{z^2\} = m_1 , \tag{4.22}$$

a result independent of the choice of $b_i(t)$.

Once the finite closed interval I of z is known, as required by the isomorphism theorem, we may evaluate second moment error bounds for a DS/SSMA system with a time-selective fading channel. Let the distortion D be defined as the maximum value of the random variable z, i.e.

$$D = \max_z |z| . \tag{4.23a}$$

By the symmetry of z about zero, the interval I defined in the isomorphism theorem may therefore be taken to be I = [-D,D]. However by the choice of $k_2(z)$ made in Section 4.1 (see (4.6)), we may reduce the actual range I to the interval I = [0,D] because of the symmetry of $k_2(z)$ about zero. In Section 4.2.3 we will present various criteria for the actual selection of D.

In Appendix B, a presentation of the methods used to evaluate the convex hull of the plot of $k_2(z)$ versus $k_1(z)$ over I is given along with development of the conditional upper and lower error bounds, conditioned upon $b_i(t)$, through the use of the isomorphism theorem. Once the conditional error bounds are known, from (4.4), (4.6), and (4.7) we may obtain bounds on P_e^U and P_e^L.

In Figure 16 we have plotted upper and lower second moment space bounds on the probability of error for a DS/SSMA system with a time-selective fading channel with a triangular channel covariance function as a function of the bit energy to noise spectral density. In plotting Figure 16 we have used a value of normalized distortion of 0.5, where the normalized distortion D' is defined by

$$D' = \frac{D}{h} . \tag{4.23b}$$

In addition to the upper and lower error bounds, we have also plotted the Gaussian approximation to the probability of error

$$P_e^{G} = 1 - \Phi(SNR_i) \tag{4.24}$$

where SNR_i is given by (3.40) for a time-selective fading channel. The Gaussian approximation is exact when F_i and I_i are Gaussian random variables [see the definition of SNR_i, eq. (3.28)]. Note that for small values of $\mathcal{E}/N_0$, the bounds on P_e are quite tight. However for larger values of $\mathcal{E}/N_0$, the upper bound on P_e becomes practically useless. Furthermore for larger values of D', larger numbers of users, and shorter signature sequences, even the bounds for smaller values of $\mathcal{E}/N_0$ become loose. This phenomenon of second order bounds was also noted by Yao (1977) for DS/SSMA systems with AWGN channels. To improve the probability of error bounds, in Section 4.3 we will consider Nth moment bounds for $n \geq 4$.

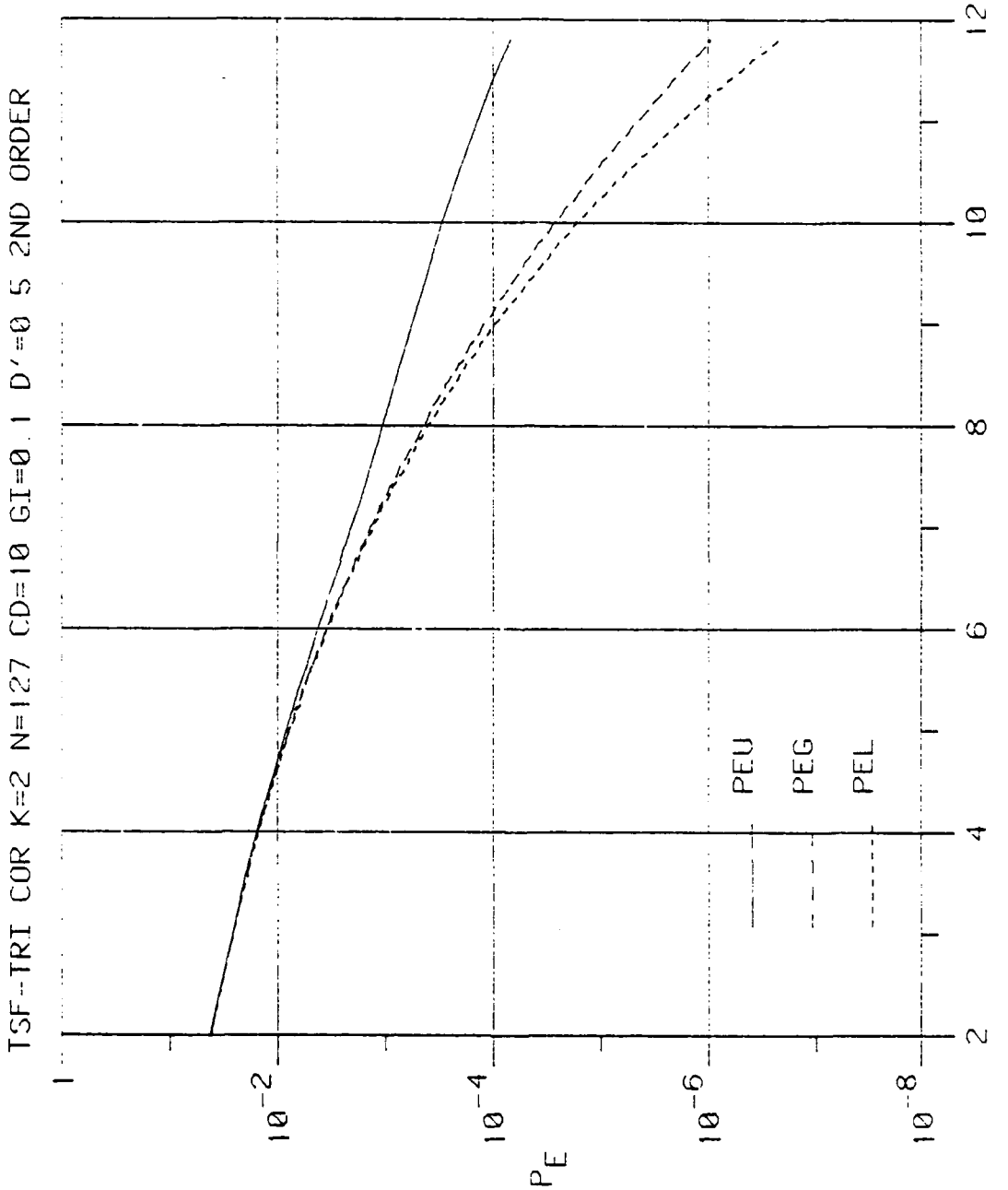

Figure 16. Probability of error bounds vs. $\mathcal{E}/N_0$ for a time-selective fading channel with a triangular covariance function -- second moment bounds ($N = 127$, $K = 2$, $\gamma^2 = 0.1$, $\lambda = 10$, $D' = 0.5$, LSE/AO sequences).

4.2.2. Second Moment Error Bounds for Frequency-Selective Fading Channels

Following the evaluation of second moment bounds for the time-selective fading channel as presented in the previous subsection, we shall now evaluate the second moment error bounds for a DS/SSMA system employing a frequency-selective fading channel. Once again we shall use the singly-spread channel characterization of the frequency-selective fading channel developed in Section 2.6 rather than employ the equivalent method of developing the frequency-selective fading channel model from the doubly-spread channel model, as was done in Section 3.3. For a DS/SSMA system with a frequency-selective fading channel, the output of the i-th correlation receiver is once again given by (4.1), where N_i and D_i are given by (3.14) and (3.12), respectively. In this case, however F_i and I_i are given by $F_i = \mathrm{Re}\{\tilde{F}_i\}$ and $I_i \triangleq \hat{I}_i + \hat{I}_i'$ where

$$\tilde{F}_i = \sqrt{\tfrac{1}{2}P}\,\gamma_i \int_{-\infty}^{\infty} \beta_i(\tau) \int_0^T h_i(\tau;t)\,dt\,d\tau \tag{4.25}$$

$$\hat{I}_i \triangleq \mathrm{Re}\{\tilde{\hat{I}}_i\} = \mathrm{Re}\Big\{\sqrt{\tfrac{1}{2}P} \sum_{\substack{k=1 \\ k\neq i}}^{K} \gamma_k \tilde{I}_{k,i}\Big\} \tag{4.26}$$

$$\hat{I}_i' \triangleq \mathrm{Re}\{\tilde{\hat{I}}_i'\} = \mathrm{Re}\Big\{\sqrt{\tfrac{1}{2}P} \sum_{\substack{k=1 \\ k\neq i}}^{K} \tilde{I}_{k,i}'\Big\} \tag{4.27}$$

and

$$\tilde{I}_{k,i} \triangleq \int_{-\infty}^{\infty} \beta_k(\tau) \int_0^T h_{k,i}(\tau_k + \tau;t)\exp(j\varphi_k)\,dt\,d\tau \tag{4.28}$$

$$\tilde{I}'_{k,i} \triangleq \int_0^T h_{k,i}(\tau_k;t)\exp(j\varphi_k)dt \ . \tag{4.29}$$

In (4.24) and (4.27) $\beta_k(\tau)$ is a zero mean, unit energy (i.e., $\sigma_b^2 = \frac{1}{2}$ in (2.74)) complex Gaussian random process with covariance functions

$$E\{\tfrac{1}{2}\beta_k(\tau)\beta_k^*(\sigma)\} = g_k(\tau)\delta(\tau - \sigma) \tag{4.30a}$$

and

$$E\{\tfrac{1}{2}\beta_k(\tau)\beta_k(\sigma)\} = 0 \ . \tag{4.30b}$$

In order to obtain moment space error bounds for the frequency-selective fading channel case, we must again obtain bounds on the innermost conditional expectation of (4.6) and (4.7) through the evaluation of $m_1 \triangleq E\{z^2|b_i(t)\}$. For the time-selective fading channel case, it was found (see (4.20) above) that F_i was dependent upon the data bit $b_{i,0}$ only. Hence conditional error bounds were needed for only two data bit values: $b_{i,0} = +1$ and $b_{i,0} = -1$. From the form of (4.25), however, for the frequency-selective fading channel case, conditional error bounds are needed for an <u>infinite</u> number of data bit patterns because the frequency-selective fading channel exhibits memory. To display this dependence of F_i on <u>all</u> preceeding and successive values of data bits, using (1.1) and (3.10) in (4.25), we find that

$$\tilde{F}_i = \sqrt{\tfrac{1}{2}P}\,\gamma_i \int_{-\infty}^{\infty} \beta_i(\tau) \int_0^T \sum_{\ell=-\infty}^{\infty} b_{i,j}P_T(t-\tau-\ell T)a_i(t-\tau)a_i(t)dtd\tau$$

$$= \sqrt{\tfrac{1}{2}P}\,\gamma_i \sum_{j=-\infty}^{\infty} \int_{jT}^{(j+1)T} \beta_i(\tau)[b_{i,-j-1}R_i(\tau-jT) + b_{i-j}\hat{R}_i(\tau-jT)]d\tau, \tag{4.31}$$

where $R_i(\tau)$ and $\hat{R}_i(\tau)$ are defined by (1.7) and (1.8), respectively. Clearly, we cannot evaluate an infinite number of moment space bounds as required by (4.6), (4.7), and (4.31). Hence we must truncate the number of preceeding and successive data bits required to evaluate (4.6) and (4.7) in some sensible manner. Note that this corresponds to the problem of evaluation of the probability of error of a baseband PAM system with intersymbol interference (e.g., see [Lucky, et. al., 1968]). In Section 3.3 we assumed the selectivity of the channel is such that only the two adjacent symbols need be taken into account in evaluating the performance of a DS/SSMA system with a frequency-selective fading channel. If we also apply this constraint to (4.31), (4.31) reduces to

$$\tilde{F}_i = \sqrt{\tfrac{1}{2}P}\,\gamma_i \int_{-T}^{T} \beta_i(\tau) \int_0^T h_i(\tau;t)\,dt\,d\tau \ . \tag{4.32}$$

Note that the constraint on $\beta_i(\tau)$ implied by (4.32) is a <u>stronger</u> constraint than that made in (3.51), since the former is actually a constraint on the range spread of the channel [Van Trees, 1971], while the latter is a constraint on the selectivity of the channel. In a similar manner, (4.28) becomes

$$\tilde{I}_{k,i} \triangleq \int_{-T}^{T} \beta_k(\tau) \int_0^T h_{k,i}(\tau_k+\tau\,;t)\exp(j\varphi_k)\,dt\,d\tau \ . \tag{4.33}$$

Thus for the frequency-selective fading channel case, we need to evaluate the conditional bounds on the probability of error for 8 different sets of the bit pattern $\{b_{i,-1}, b_{i,0}, b_{i,+1}\}$. Each evaluation of the conditional error bounds requires evaluation of $m_1 = E\{z^2 | b_i(t)\}$

for one of the eight bit patterns. Following the same reasoning given for (4.18), $E\{z^2|b_i(t)\}$ is given by (4.18), where for the frequency-selective fading case, $E\{I_i^2\}$ is given by Var I_i in (3.62). Using (2.10) and (4.30) we find that $E\{F_i^2|b_i(t)\}$ is given by (3.54). Thus we can evaluate m_1 for each of the eight sets of bit patterns.

Using the methods of Appendix B, we have evaluated the second moment space bounds for the probability of error of a DS/SSMA system with a frequency-selective fading channel having a triangular channel covariance function and have plotted the results as a function of $\mathcal{E}/N_0$ in Figure 17. In plotting these results we have used K = 2 users employing signature sequences of length 127 and have assumed a normalized distortion of D' = 0.5. In Figure 17 we have also plotted the Gaussian approximation (4.24) to the probability of error, where SNR_i for the frequency-selective fading channel is given by (3.63). The comments made in the previous section on the looseness of the second order moment space bounds apply here also. In Section 4.3 we will consider higher order moment space bounds in an effort to tighten the bounds on the probability of error.

4.2.3. Selection of the Normalized Distortion

Up to this point we have not given any consideration toward selecting the value of the normalized distortion D' to be used in evaluating the moment space bounds for a DS/SSMA system operating over a given fading

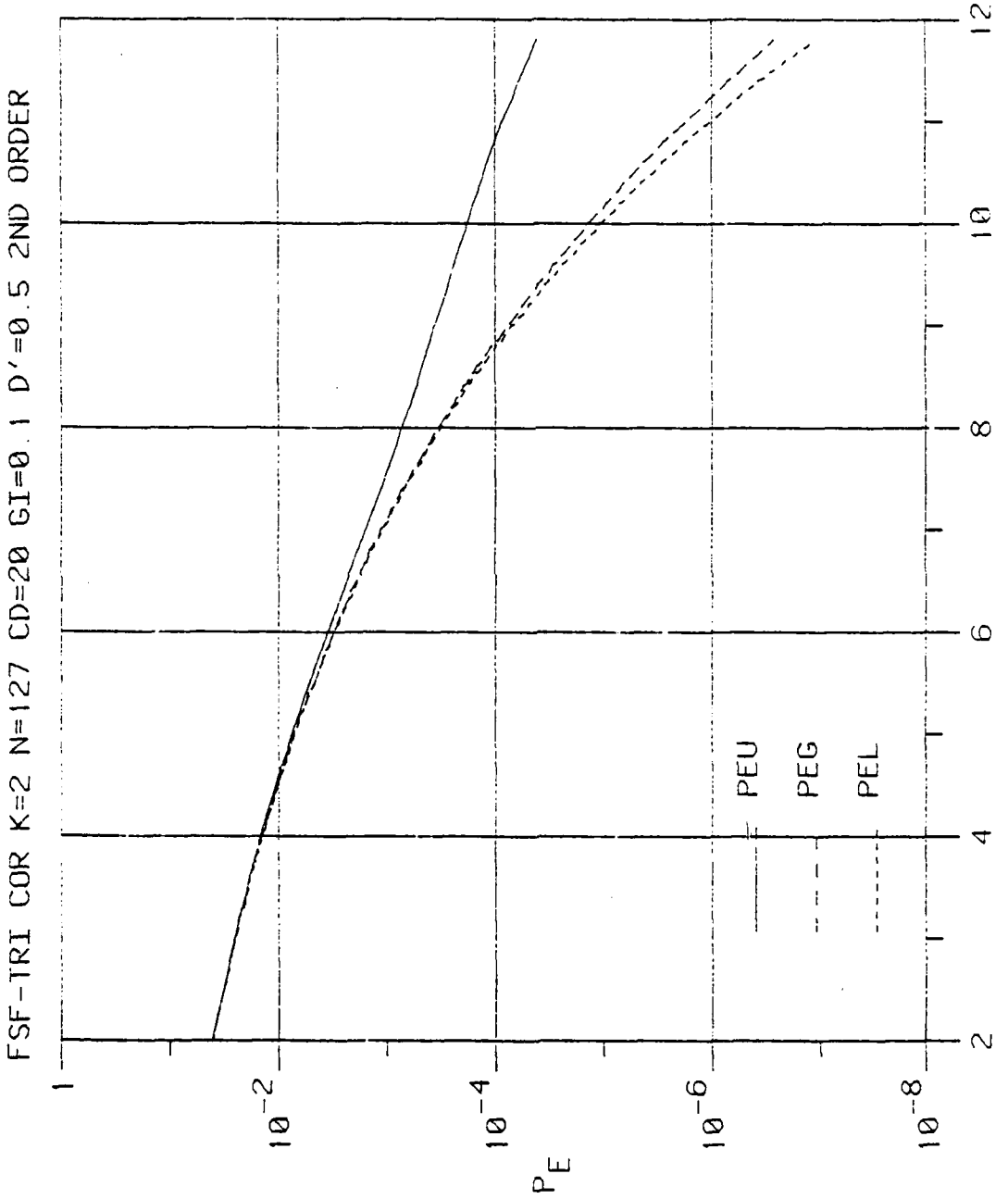

Figure 17. Probability of error bounds vs. $\mathcal{E}/N_0$ for a frequency-selective fading channel with a triangular covariance function -- second moment bounds (N = 127, K = 2, γ^2 = 0.1, λ = 20, D' = 0.5, LSE/AO sequences).

channel. From the isomorphism theorem of Section 4.1 and the determination of moment space bounds given in Appendix B, such a selection of a particular value of D' is required before moment space bounds can be obtained. In this subsection three possible criteria are given for selection of D'.

At first examination, it may appear that determination of D' is straightforward from the definition of D' given by (4.23). Further examination of z however reveals that because we have assumed $\beta_k(\tau;t)$ to be a complex Gaussian random process, the "tails" of $\mathrm{Re}\{\beta_k(\tau;t)\}$ are infinite and hence $D' = \infty$. The isomorphism theorem requires, however, that D' be finite. Our goal then is to sensibly choose a finite D' in such a manner that truncation of D' will only marginally affect the actual bounds.

The first approach will be termed the distribution function method. Basically this method assume a <u>priori</u> knowledge of the distribution function of z in order to sensibly truncate the "tails" of z. One method of truncation is to simply assume that the tails of z may be neglected if

$$\Pr\{z > D\} \leq \frac{1}{10} P_e \tag{4.34}$$

where P_e is the probability of error. For example, if z is assumed to be a zero mean Gaussian random variable with variance σ^2, for P_e on the order of 10^{-5}, D should be selected so as to satisfy

$$D \geq 4.753423\,\sigma \tag{4.35a}$$

or

$$D' \geq 4.753423\,\frac{\sigma}{h}\,. \tag{4.35b}$$

Of course the major drawback of this method is that we have also assumed P_e could not be evaluated directly, which would be the implication if the distribution function of z were known (see (4.1)). Still, this method merits consideration for cases in which the moment space bounds are exceptionally tight and an approximating distribution function for z yields results for P_e which lie between the upper and lower bounds.

A second approach utilizes Chebyshev's inequality to obtain a finite value for D'. By Chebychev's inequality we have that

$$\Pr\{|z| > D\} \leq \frac{E\{z^n\}}{D^n} \quad . \tag{4.36}$$

Since we have assumed that the moments $E\{z^n\}$ can be evaluated, (4.36) may be used in a manner identical to (4.34) to bound D'. As an example of this, for the second moment case for values of P_e on the order of 10^{-5}, we choose D to satisfy

$$10^{-6} \geq \frac{\sigma^2}{D^2} \tag{4.37}$$

or $D' \geq 10^3 \frac{\sigma}{h}$, where $\sigma^2 = E\{z^2\}$. Assuming that higher order moments of z can be evaluated, we may then use (4.36) to further reduce this initial choice of D'

A third approach to choosing D' is based on the actual DS/SSMA system dynamic range. Because any physical system must have a finite dynamic range, D is automatically limited to the dynamic range of the DS/SSMA system. If we use this approach to limit the range of D', we must have prior knowledge of the actual system dynamic range.

Ideally we would, of course, like to choose D' as large as possible so that the effects on the probability of error bounds of truncating D' can be minimized. Fortunately, as will be seen in the next section, for Nth moment space bounds, the probability of error bounds are relatively insensitive to the choice of D', for values of D' greater than a certain minimum value. For the remainder of this chapter we will compute moment space error bounds with the assumption that D' has been computed using one of the three methods outlined above.

4.3. Nth Moment Bounds

In this section we shall consider Nth moment bounds for $n \geq 2$. Our goal here is to obtain tighter moment space bounds on the probability of error of a DS/SSMA system with a fading channel than could be obtained using the second moment bounds of the previous section.

4.3.1. Fourth Moment Bounds

As noted in Section 4.1, in order to evaluate the Nth moment space bounds on the probability of error of a DS/SSMA system with a fading channel, we first need to evaluate the moment

$$\begin{aligned} m_1 &= E\{z^n | b_i(t)\} \\ &= E\{[F_i + I_i]^n | b_i(t)\} \end{aligned} \tag{4.38}$$

for all data bit patterns $b_i(t)$ of interest. For the fourth moment space bound, we therefore need to evaluate

$$E\{[F_i+I_i]^4 | b_i(t)\} = E\{F_i^4+4F_i^3I_i+6F_i^2I_i^2+4F_iI_i^3+I_i^4 | b_i(t)\}. \tag{4.39}$$

In the following we shall assume that the fading processes $\beta_j(\tau;t)$ and $\beta_k(\tau;t)$ are independent for $j \neq k$. Then from (3.13), (3.15), and (3.16), (4.39) reduces to

$$E\{[F_i+I_i]^4|b_i(t)\} = E\{F_i^4+6F_i^2I_i^2+I_i^4|b_i(t)\}$$

$$= E\{F_i^4|b_i(t)\}+6E\{F_i^2|b_i(t)\}E\{I_i^2\}+E\{I_i^4\} \qquad (4.40)$$

where we have used the fact that I_i is independent of $b_i(t)$ and that $\beta_k(\tau;t)$ is a zero mean process. The middle term of (4.40) has been previously evaluated in Sections 4.2.1 and 4.2.2 for time-selective fading channels and frequency-selective fading channels, respectively. Hence in this section we shall concentrate on evaluating the first and last terms of (4.40). Recognizing that $F_i = Re\{\tilde{F}_i\}$ and $I_i = Re\{\tilde{I}_i\}$, in order to evaluate the fourth moments of these quantities, we shall need the following identity which may be derived directly from (2.10):

$$8Re(w)Re(x)Re(y)Re(z) = Re(wxyz)+Re(w^*x^*yz)+Re(wxy^*z)$$
$$+ Re(w^*x^*y^*z)+Re(w^*xyz)+Re(wx^*yz)+Re(w^*xy^*z)$$
$$+ Re(wx^*y^*z), \qquad (4.41)$$

for complex numbers w, x, y, z.

From (4.40), (4.41), (3.15), and (3.16), we note that the fourth moments of F_i and I_i will be a function of the fourth moments of $\beta_k(\tau;t)$, for $1 \leq k \leq K$. To evaluate the fourth moment of $\beta_k(\tau;t)$ we shall make use of the following theorem due to Reed (1962) and Miller (1968).

Theorem: Let $x(t)$ be a zero-mean, complex Gaussian random process with covariance functions

$$E\{x^*(t)x(s)\} = R(t,s) \tag{4.42}$$

$$E\{x(t)x(s)\} = 0 \tag{4.43}$$

Suppose $x_n \equiv x(t_n)$ for $n \in \{1,2,\ldots,N\}$ are samples from $x(t)$.

a.) If $s \neq t$, then

$$E\{x^*_{m_1} x^*_{m_2} \ldots x^*_{m_s} x_{n_i} x_{n_2} \ldots x_{n_t}\} = 0 \tag{4.44}$$

where m_k and n_j are integers from the set $\{1,2,3,\ldots,N\}$.

b.) If $s = t$, then

$$E\{x^*_{m_1} x^*_{m_2} \ldots x^*_{m_t} x_{n_1} x_{n_2} \ldots x_{n_t}\} =$$

$$\sum_{\pi} E\{x^*_{m_{\pi(1)}} x_{n_1}\} E\{x^*_{m_{\pi(2)}} x_{n_2}\} \ldots E\{x^*_{m_{\pi(t)}} x_{n_t}\} \tag{4.45}$$

where π is a permutation of the set of integers $\{1,2,3,\ldots,t\}$.

A proof of this theorem for stationary random processes was originally given in [Reed, 1962]; Miller (1968) subsequently generalized the theorem to nonstationary, non-zero mean random processes. A discussion of both of these results may be found in [McGee, 1971].

Hence from (4.44) and (4.45), the fourth moments of a zero-mean complex Gaussian process $\beta(t)$ satisfying (4.42) and (4.43) are

$$E\{\beta^*(t)\beta^*(s)\beta(t')\beta(s')\} = R(t,s)R(t',s) + R(t,s')R(t',s) \tag{4.46}$$

$$E\{\beta(t)\beta(s)\beta(t')\beta(s') = E\{\beta^*(t)\beta(s)\beta(t')\beta(s')\}$$

$$= E\{\beta^*(t)\beta^*(s)\beta^*(t')\beta(s')\} = 0 \,. \tag{4.47}$$

For the time-selective fading case, from (4.41), (4.46), (4.47), and (4.20) the conditional fourth moment of F_i conditioned upon $b_i(t)$ is given by

$$E\{F_i^4|b_i(t)\} = \frac{3}{4}P^2\gamma_i^4 \mathrm{Re}\{\int_0^T\int_0^T\int_0^T\int_0^T r_i(t-s)r_i(u-v)dtdsdudv\}$$

$$= 3[\mathrm{Var}\ F_i]^2 \tag{4.48}$$

where Var F_i is given by (3.31) and we have used (4.17).

In a similar fashion, for the frequency-selective fading case $E\{F_i^4|b_i(t)\}$ is given by

$$E\{F_i^4|b_i(t)\} = \frac{3}{4}P^2\gamma_i^4 \mathrm{Re}\{\int_{-T}^T\int_{-T}^T g_i(\tau)g_i(\tau')\int_0^T\int_0^T\int_0^T\int_0^T$$

$$f_i(\tau,\tau;t,s)f_i(\tau',\tau';t',s')dtdsdt'ds'd\tau d\tau'\}$$

$$= 3[\mathrm{Var}\ F_i]^2 \tag{4.49}$$

where Var F_i is given by (3.54). In deriving (4.49) from (4.32), we have used (4.41), (4.46), (4.47), and (4.30).

In order to evaluate $E\{I^4\}$ appearing in (4.40), assume, without loss of generality, that user 1 is the i-th user (i.e., i = 1). Letting

$$I_i \triangleq \hat{I}_i + \hat{I}_i' \tag{4.50}$$

where $\hat{I}_i$ and $\hat{I}_i'$ are given by (4.13) and (4.14), respectively, for the time-selective fading channel and by (4.26) and (4.27), respectively, for the frequency-selective fading channel, we find that

$$E\{\hat{I}_i^4\} = E\{\hat{I}_i^4 + 4\hat{I}_i^3\hat{I}_i' + 6\hat{I}_i^2(\hat{I}_i')^2 + 4\hat{I}_i(\hat{I}_i')^3 + (\hat{I}_i')^4\}$$

$$= E\{\hat{I}_i^4 + 6\hat{I}_i^2(\hat{I}_i')^2 + (\hat{I}_i')^4\} \tag{4.51}$$

where we have used the zero-mean condition on $\beta_k(\tau;t)$ for the second step. Noting that the last term of (4.51) has been previously evaluated in [Yao, eq. (14)-(18), 1977], we shall concentrate on evaluating the first two terms of (4.51). Let

$$I_{k,i} \triangleq \sqrt{\tfrac{1}{2}P}\,\gamma_k \mathrm{Re}\{\tilde{I}_{k,i}\} \tag{4.52}$$

where $\tilde{I}_{k,i}$ is defined by (3.16). Then

$$\hat{I}_i = \sum_{k=2}^{K} I_{k,i}\ , \tag{4.53}$$

which follows from (3.15). Using (4.53) in (4.51), we see that

$$E\{\hat{I}_i^4\} = E\{[\sum_{k=2}^{K} I_{k,i}]^4\}$$

$$= E\{\sum_{h=2}^{K}\sum_{j=2}^{K}\sum_{k=2}^{K}\sum_{\ell=2}^{K} I_{h,i}I_{j,i}I_{k,i}I_{\ell,i}\}$$

$$= E\{\sum_{k=2}^{K} I_{k,i}^4\} + 6\sum_{k=2}^{K-1}\sum_{j=k+1}^{K} E\{I_{k,i}^2 I_{j,i}^2\}$$

$$= \sum_{k=2}^{K} E\{I_{k,i}^4\} + 6\sum_{k=2}^{K-1}\sum_{j=k+1}^{K} E\{I_{k,i}^2\}E\{I_{j,i}^2\} \tag{4.54}$$

where we have used the independence of $\beta_k(\tau;t)$ for $2 \le k \le K$ and the fourth moment properties of $\beta_k(\tau;t)$.

For the time-selective fading case, from (4.52), (4.15), (4.17), (4.41), (4.46), and (4.47), $E\{I_{k,i}^4\}$ is given by

$$E\{I_{k,i}^4\} = \frac{3}{4} P^2 \gamma_k^4 \int_0^T \int_0^T \int_0^T \int_0^T r_k(t-s) r_k(u-v) E\{f_{k,k,i}(\tau_k,\tau_k;t,s) \cdot f_{k,k,i}(\tau_k,\tau_k;u,v)\} dt\,ds\,du\,dv, \tag{4.55}$$

where the expectation is over $b_k(t)$ and τ_k. From (3.10) we see that in order to evaluate this expectation, we need to evaluate

$$\frac{1}{T} \int_0^T a_k(t-\tau_k) a_k(s-\tau_k) a_k(u-\tau_k) a_k(v-\tau_k) E\{b_k(t-\tau_k) b_k(s-\tau_k) b_k(u-\tau_k) b_k(v-\tau_k)\} d\tau_k. \tag{4.56}$$

Note that (4.56) is a function of t, s, u, and v and consequently may only be evaluated numerically for given values of the four parameters. Furthermore, unlike previous "moments" of $a_k(t)$ that we have encountered up to this point, evaluation of (4.56) requires knowledge of the actual sequence $a_k(t)$ rather than just its aperiodic correlation functions. Consequently, the objective of applying higher order moment space bounds to bound P_e becomes questionable unless (4.56) can be evaluated in some manner. One such approach is to simply bound the expectation appearing in (4.55) so that bounds on $E\{I_{k,i}^4\}$ may be obtained. Noting that a "worst case" bounding approach is to assume that the expectation appearing in (4.55) is upper bounded by 1 and lower bounded by 0, (4.55) becomes, using (3.30) and (3.31),

$$E\{I_{k,i}^4\} = \begin{cases} 0, \text{ best case} \\ \\ 3[\text{Var } F_i]^2, \text{ worst case} \end{cases} \tag{4.57}$$

where Var F_i is given by (3.31). In a similar manner, the second term of (4.51) may also be bounded, and hence, from (4.40), (4.48), (4.51), (4.54), and (4.57), upper and lower bounds on m_1 appearing in (4.38) may be obtained. If we use these upper and lower bounds on m_1 to evaluate upper and lower moment space bounds on P_e through use of the methods described in Appendix B, however, we find that the results obtained are actually slightly looser than those obtained using the second moment space bounds described in the previous section. This looseness of the higher order bound may be attributed to the crude bounds on the expectation appearing in (4.55).

For the frequency-selective fading case, from (4.52), (4.30), (4.33), (4.41), (4.46), and (4.47), $E\{I_{k,i}^4\}$ is given by

$$E\{I_{k,i}^4\} = \frac{3}{4} P^2 \gamma_k^4 \int_{-T}^{T}\int_{-T}^{T} g_k(\tau) g_k(\sigma) \int_0^T\int_0^T\int_0^T\int_0^T E\{F_{k,k,i}(\tau_k+\tau,\tau_k+\tau_j t,s)$$

$$\cdot F_{k,k,i}(\tau_k+\sigma,\tau_k+\sigma_j u,v)\}dtdsdudvd\tau d\sigma. \qquad (4.58)$$

As was the case for the time-selective fading channel, the expectation appearing in (4.58) may not be easily evaluated analytically. Consequently, once again a simple bound on this expectation may be made in an effort to bound $E\{I_{k,i}^4\}$ and subsequently m_1. However, it was found that the resulting bounds on P_e obtained through the use of the bounds on m_1 are actually looser than the second order bounds obtained in Section 4.2.

4.3.2. Higher Moment Bounds for DS/SS Communications via Fading Channels

In the previous subsection we noted that for the cases in which multiple users are present, fourth moment space bounds on the probability of error of DS/SSMA communications via a fading channel cannot be readily evaluated. This observation may, in fact, be generalized to Nth order bounds for $n > 2$, since evaluation of higher order bounds will require evaluation of higher order "moments" of the signature sequences. For a single user system, however, the above comments do not apply, since, as noted in the previous subsection, we are able to evaluate the fourth moments of F_i for both time-selective and frequency-selective fading channels. In this subsection we shall consider moment space bounds for single user DS/SS systems with fading channels.

To begin with, note from (4.20), (4.31), and (4.32) that $F_i = \mathrm{Re}\{\tilde{F}_i\}$ is conditionally Gaussian, conditioned upon $b_i(t)$. This follows from the observation that the real part of a complex Gaussian random variable is Gaussian. Furthermore, throughout all of our analysis presented to this point, we have assumed that the fading process $\beta(\tau;t)$ is independent of the additive noise process $n(t)$. Hence for a single user DS/SS system with either a time-selective or a frequency-selective fading channel, we may write an exact expression for the probability of error. For a single user DS/SS system, the output of the i-th user's correlation receiver is given by

$$Z_i = N_i + D_i + F_i . \tag{4.59}$$

The probability of error at the decision instant t = T is then given by (4.2). Letting h be defined as above, we find that

$$\Pr\{Z_i > 0 | b_i(t), b_{i,0} = -1\} = Q(\frac{h}{\sigma_1}) \tag{4.60}$$

while

$$\Pr\{Z_i < 0 | b_i(t), b_{i,0} = +1\} = Q(\frac{h}{\sigma_2}) \tag{4.61}$$

where σ_1 and σ_2 are the square root of the sum of the noise variance plus the conditional fading variance, i.e.,

$$\sigma_1 = [\tfrac{1}{4} N_0 T + E\{F_i^2 | b_i(t), b_{i,0} = -1\}]^{\frac{1}{2}} \tag{4.62}$$

and

$$\sigma_2 = [\tfrac{1}{4} N_0 T + E\{F_i^2 | b_i(t) b_{i,0} = +1\}]^{\frac{1}{2}} . \tag{4.63}$$

For the time-selective fading channel, from (4.21), (4.2) and (4.59)-(4.63), the probability of error at the output of the i-th correlation receiver is given by

$$P_e = Q([\frac{N_0}{2\mathcal{E}} + \frac{2\gamma_i^2}{T^2} \int_0^T r_i(u)(T-u)du]^{-\frac{1}{2}}) \tag{4.64}$$

where $r_i(u)$ is the covariance function of the i-th user's fading channel process. The corresponding expression for probability of error for the frequency-selective fading channel is

$$\begin{aligned} P_e = {} & \tfrac{1}{2} Q([\frac{N_0}{2\mathcal{E}} + \frac{2\gamma_i^2}{T^2} \int_0^T g_i(\tau)[\hat{R}_i^2(\tau) + R_i^2(\tau)]d\tau]^{-\frac{1}{2}}) \\ & + \tfrac{1}{2} Q([\frac{N_0}{2\mathcal{E}} + \frac{2\gamma_i^2}{T^2} \int_0^T g_i(\tau)[\hat{R}_i(\tau) + R_i(\tau)]^2 d\tau]^{-\frac{1}{2}}) \\ & + \tfrac{1}{2} Q([\frac{N_0}{2\mathcal{E}} + \frac{2\gamma_i^2}{T^2} \int_0^T g_i(\tau)[\hat{R}_i(\tau) - R_i(\tau)]^2 d\tau]^{-\frac{1}{2}}), \end{aligned} \tag{4.65}$$

where we have used (3.54), (4.2), (4.59)-(4.63), and where $g_i(\tau)$ is the covariance function of the i-th user's fading process.

Because we can evaluate the probability of error exactly for the single user DS/SS case, there appears to be no need to evaluate moment space bounds on the probability of error. Nevertheless, it is of interest to evaluate moment space error bounds in this instance since the results are useful in evaluating the performance of the bounds themselves for related DS/SSMA system problems. Two such examples of related problems are DS/SSMA systems with faded multiple-access interference and with non-faded multiple-access interference. In the following we will evaluate Nth order moment space bounds for a DS/SS system in the presence of a fading channel.

In the previous subsection we presented methods for obtaining fourth moment error bounds for a DS/SSMA system with faded multiple-access interference. For a single user system, these same methods apply except that the interference term I_i is neglected in all of the calculations. From (4.38), it follows that in order to evaluate Nth moment bounds on P_e, we need to evaluate

$$m_1 = E\{[F_i]^n | b_i(t)\} \ . \tag{4.66}$$

Two approaches are available for evaluating (4.66). The first requires derivation of an expression for the product of real parts of complex numbers in terms of sums of real parts of products of complex numbers and then applying (4.44) and (4.45) to this result. This is the approach taken in the previous subsection. The second approach makes use of the

fact that F_i is conditionally Gaussian, as noted above. To use this second approach, we will need the following result from [Wang and Uhlenbeck, 1945] regarding moments of real multivariate Gaussian distributions:

Theorem: Let $X_n = \{x_1, x_2, \ldots, x_n\}$ have a zero-mean multivariate Gaussian distribution with covariance $E\{x_i x_j\} = R_{ij}$.

(i) Then for m odd:

$$E\{x_{i_1} x_{i_2} x_{i_3} \ldots x_{i_m}\} = 0. \tag{4.67}$$

(ii) For m even:

$$E\{x_{i_2} x_{i_2} x_{i_3} \ldots x_{i_m}\} = \Sigma R_{j_1 j_2} R_{j_3 j_4} \ldots R_{j_{m-1} j_m} \tag{4.68}$$

where the sum is taken over all possible ways of dividing the m points into m/2 combinations of pairs. The number of terms in the sum is equal to

$$1 \cdot 3 \cdot 5 \cdots (m-3)(m-1) \ . \tag{4.69}$$

From (4.66), (4.68), (4.69), and the observation that F_i is conditionally Gaussian, we have the following result: for n even

$$m_1 = E\{[F_i]^n | b_i(t)\} = 1 \cdot 3 \cdot 5 \cdots (n-3)(n-1)[E\{F_i^2 | b_i(t)\}]^{n/2} \ . \tag{4.70}$$

Hence using (4.70), (4.2), and the procedures given in Appendix B, we may evaluate the Nth moment space bounds on the probability of error of a single user DS/SS system with a fading channel.

In Figure 18 we have plotted upper and lower sixth moment space bounds on the probability of error as a function of $\mathcal{E}/N_0$ for a single user DS/SS system with a time-selective fading channel. In plotting Figure 18 we have assumed that the fading channel has a triangular covariance function with correlation duration $10T_c$ and $\gamma_i^2 = 0.05$. Also shown in Figure 18 is the exact probability of error for this system which was evaluated using (4.64). For the purposes of this plot we have assumed a normalized distortion of $D' = 1.0$ in evaluating the moment space bounds. Note that the moment space bounds on the probability of error are quite tight for this particular set of channel specifications. From the form of (4.64) we see that P_e for the time-selective fading channel is independent of the choice of signature sequences used. Following a line of reasoning identical to that given in Section 3.4 in discussing the time-selective fading channel, we may conclude that our results are valid also for a PSK system using a Rician fading channel.

In our discussion in Section 3.3 we noted the relative importance of frequency-selective fading channels as compared to time-selective fading channels for SSMA systems. For the remainder of this subsection we will present results only for a single user DS/SS system with a frequency-selective fading channel. In Figures 19 and 20 we have plotted eighth moment bounds on P_e versus $\mathcal{E}/N_0$ for a DS/SS system with a frequency-selective fading channel having a triangular channel covariance function for two values of γ_i^2. In plotting these figures

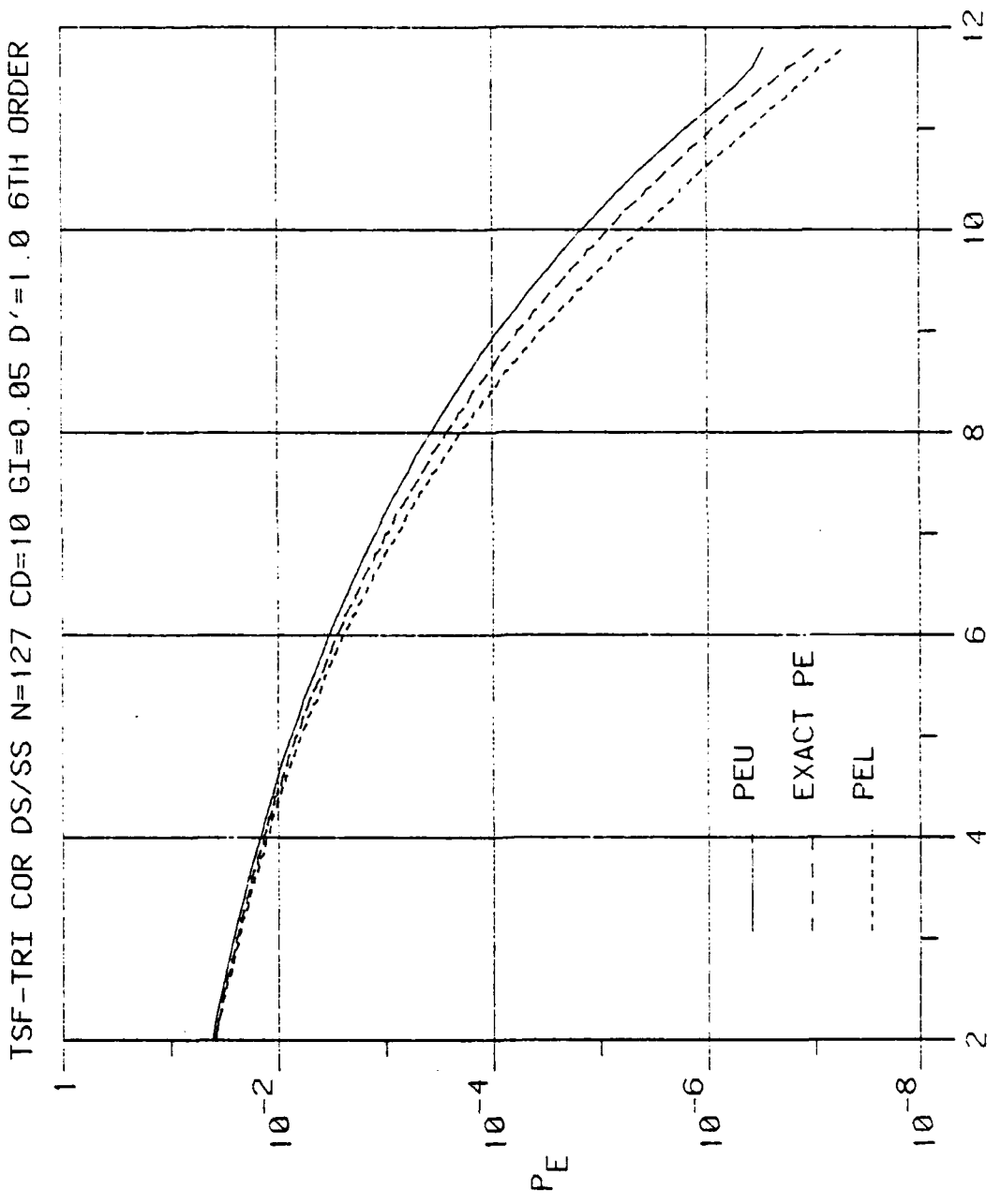

Figure 18. Probability of error bounds vs. $\mathcal{E}/N_0$ for a single-user DS/spread-spectrum system with a time-selective fading channel with a triangular covariance function -- sixth moment bounds (N = 127, γ^2 = 0.05, λ = 10, D' = 1.0).

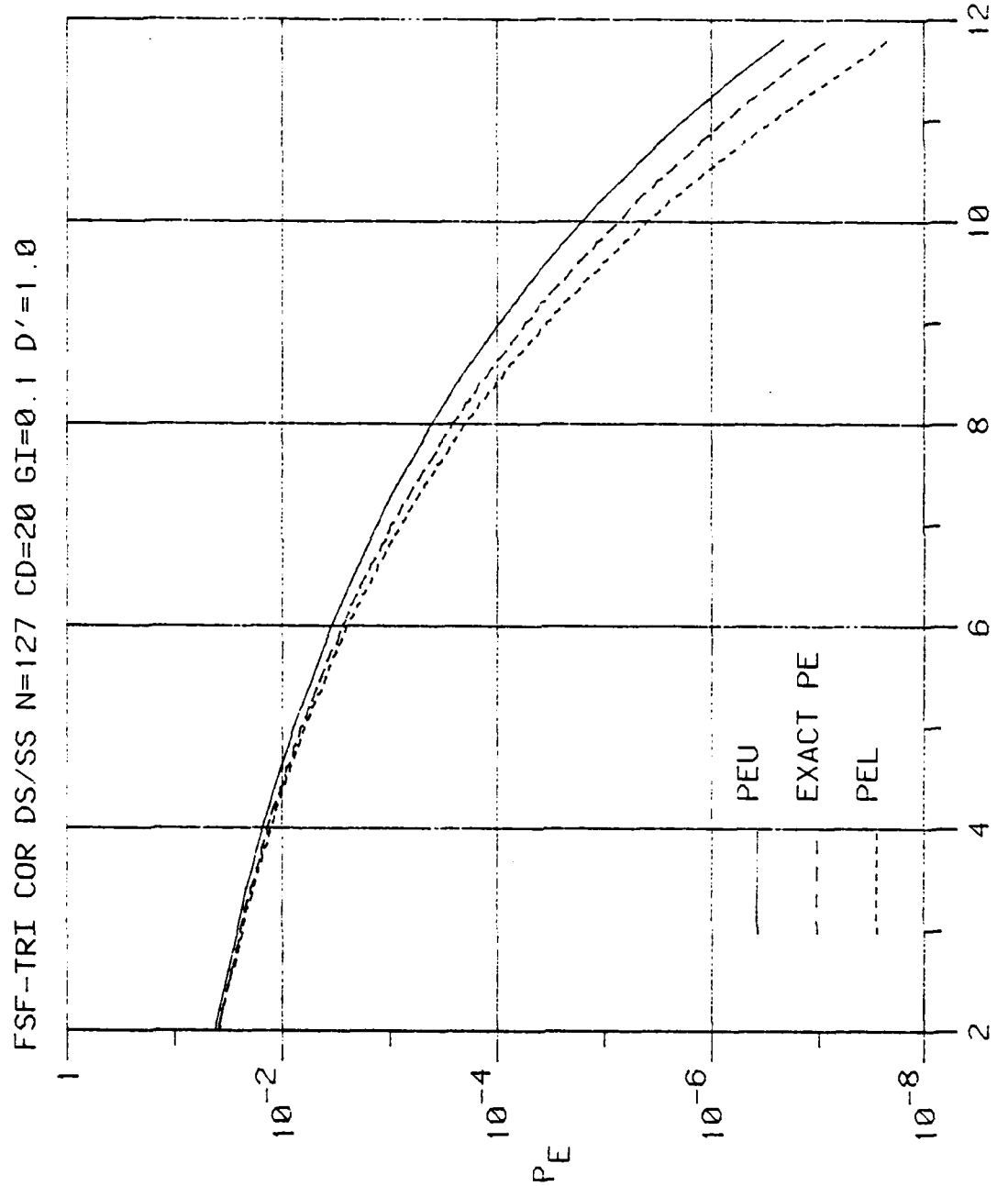

Figure 19. Probability of error bounds vs. $\mathcal{E}/N_0$ for a single-user DS/spread-spectrum system with a frequency-selective fading channel with a triangular covariance function -- eighth moment bounds (N = 127, γ^2 = 0.1, λ = 20, D' = 1.0, LSE/AO sequences).

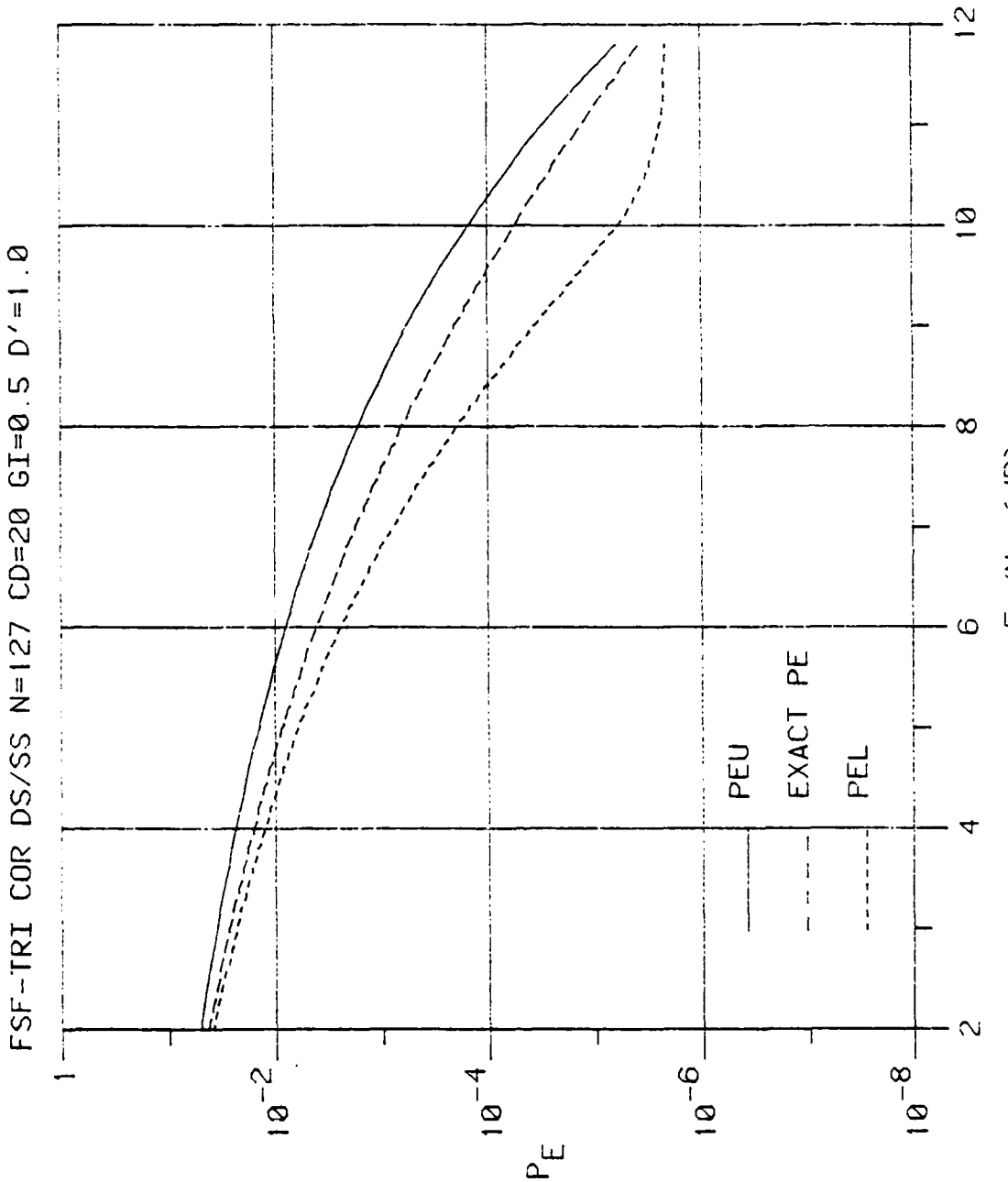

Figure 20. Probability of error bounds vs. $\mathcal{E}/N_0$ for a single-user DS/spread-spectrum system with a frequency-selective fading channel with a triangular covariance function -- eighth moment bounds (N = 127, γ^2 = 0.5, λ = 20, D' = 1.0, LSE/AO sequence).

we have assumed a correlation duration of $20T_c$ and a normalized distortion of $D' = 1.0$ and have used an m-sequence of length 127 with its LSE/AO shift register loading. Note that as γ_i^2 is increased from 0.1 to 0.5 the moment space bounds become less tight. This looseness in the bounds is to be expected for large values of γ_i^2 because of the strong dependence of m_1 on Var F_i (see (4.69)) and consequently on the parameter γ_i^2 (see (3.31) and (3.54)).

In order to compare the tightness of various orders of bounds, in Figure 21 we have plotted fourth moment, sixth moment, and eighth moment space bounds on the probability of error as a function of $\mathcal{E}/N_0$ for the same DS/SS system parameters and channel characteristics used in plotting Figure 19. Generally speaking, for values of $\mathcal{E}/N_0$ less than 10 dB, fourth moment bounds are tighter than the higher order bounds. For larger values of $\mathcal{E}/N_0$, though, only the eighth order bounds do not "level off." This phenomenon, first observed by Yan (1975), may be simply explained using the results of Appendix B. In Appendix B we note that for values of $\mathcal{E}/N_0$ less than a certain critical value SNR_C, the plot of $k_2(z)$ versus $k_1(z)$ is convex $\cap$ for any value of D'. To evaluate P_e^U and P_e^L for $SNR < SNR_C$, we need to evaluate $m_1 = E\{F_i^n | b_i(t)\}$, take the nth root of m_1, and then use this result to find the upper and lower bounds on P_e by the equations

$$P_e^U = E\{k_2(m_1^{1/n})\} \tag{4.71}$$

$$P_e^L = E\left\{\frac{k_2(D') - k_2(0)}{k_1(D') - k_2(0)}\,(m_1) + k_2(0)\right\} \tag{4.72}$$

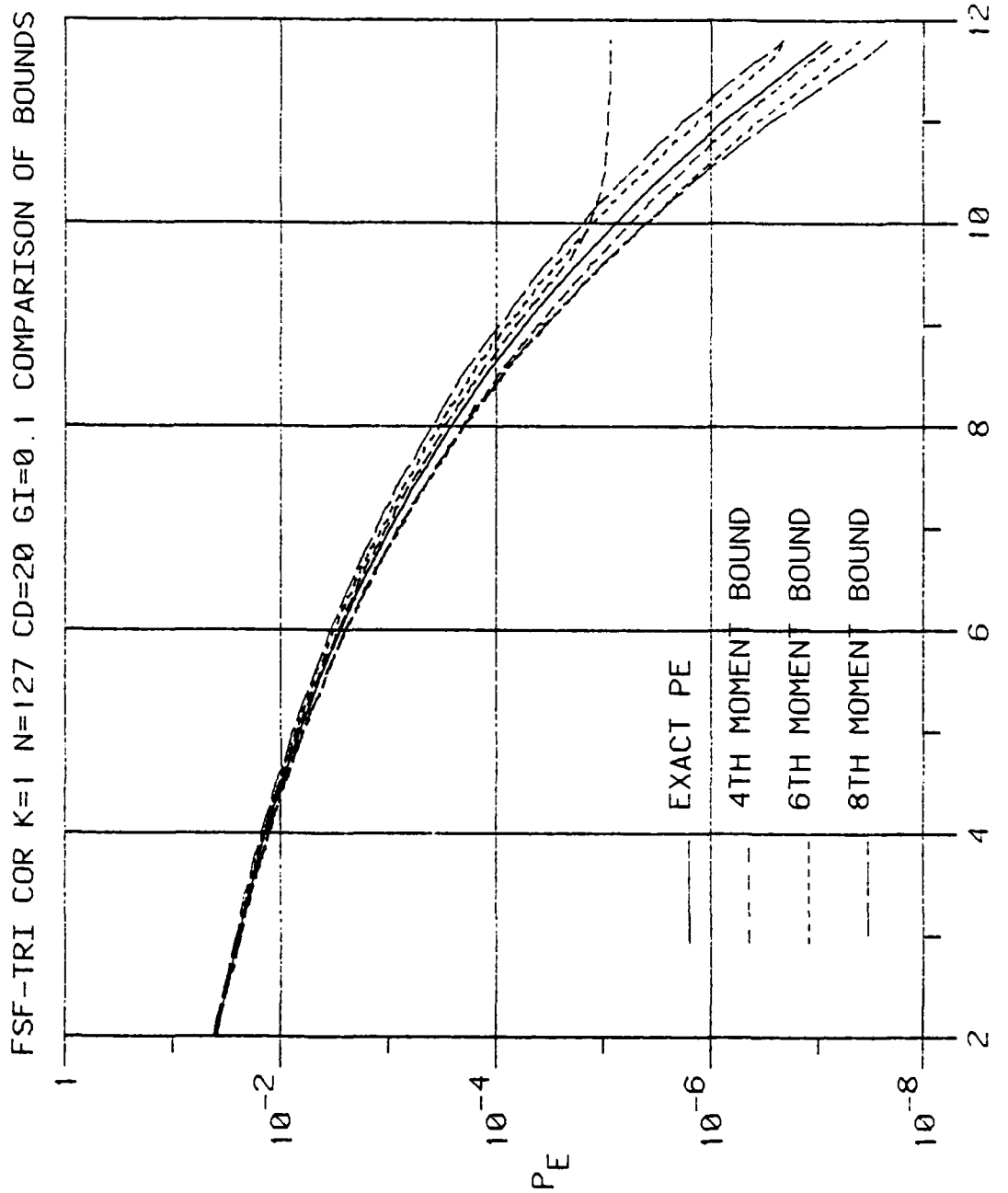

Figure 21. Probability of error bounds vs. $\mathcal{E}/N_0$ for a single-user DS/spread-spectrum system with a frequency-selective fading channel with a triangular covariance function -- comparison of fourth, sixth, and eighth moment bounds ($N = 127$, $\gamma^2 = 0.1$, $\lambda = 20$, $D' = 1.0$, LSE/AO sequence).

where the expectation is over $b_i(t)$. From (4.69), however we note that

$$1 < \sqrt[4]{3} < \sqrt[6]{15} < \sqrt[8]{105} \tag{4.73}$$

and consequently that

$$m_{l_2} < m_{l_4} < m_{l_6} < m_{l_8} \tag{4.74}$$

where

$$m_{l_n} = [E\{F_i^n | b_i(t)\}]^{1/n} . \tag{4.75}$$

Using (4.74) in (4.71) and (4.72), we see that for SNR < SNR_C, the lower order bounds on P_e are actually tighter. We may conclude that unless a "leveling-off" effect is observed, n-2 order bounds are tighter than n order bounds.

In the previous section we commented that for fading channels, Nth moment space bounds are somewhat insensitive to the exact value of the normalized distortion being used to evaluate the bounds. To illustrate this insensitivity of the bounds on D', eighth order moment space bounds were evaluated for a DS/SS system with a frequency-selective fading channel for a correlation duration of $20T_C$, $\gamma^2 = 0.05$, and for three values of D'. As D' was varied from 0.5 to 10.0, the error bounds varied by less than 5×10^{-5} %, for the case considered. Thus in most cases of interest, we may apply any of the methods suggested in the previous section to bound D' and still obtain approximately equivalent error bounds.

CHAPTER 5

SUMMARY AND CONCLUSIONS

This study has investigated the problem of analyzing the performance of a biphase DS/SSMA system operating over a fading channel. The receiver model used throughout this analysis has been a correlation receiver; a receiver structure which is not optimal for signaling in the presence of multi-user interference and fading but one that is typically used in implementing DS/SSMA systems. Two measures of system performance were considered: average signal-to-noise ratio and average probability of error. A third system performance measure considered for DS/SSMA systems operating over AWGN channels -- worst case performance -- was not treated here since it is easily shown that for a channel undergoing any degree of fading, the worst case probability of error is always $\frac{1}{2}$ for equal a priori probabilities of the transmitted data bits.

The study began with a review of various models of fading channels. From physical and phenomenological considerations we have shown how fading may be modeled as a complex Gaussian random process. With this assumption, a general fading channel model was developed which could be modeled as a time-varying linear filter whose time-varying impulse response is the fading process. Statistical phenomena observed for actual radio channels led us to consider a specialization of the general fading channel model known as the WSSUS channel. This channel model was characterized by the fact that it is the simplest channel model of physical interest exhibiting both time- and frequency-selective

behavior. A review of various techniques for characterizing the WSSUS channel in terms of observable effects was presented next. We then noted that by making certain additional assumptions about the covariance functions of the WSSUS doubly-spread channel, the WSSUS channel further simplified to two types of singly-spread channels -- time-selective fading channels and frequency-selective fading channels -- and to a channel known as a nondispersive-fading channel. In discussing these various channel models we noted the importance of assuming a specular-plus-diffuse fading channel model as a typical fading channel model over which DS/SSMA communications could be conducted. As was noted in Chapter 3, a channel exhibiting only diffuse fast fading renders a DS/SSMA system useless due to the lack of phase-reference needed for coherent communications.

After a review of fading channel models we then considered analysis of the average signal-to-noise ratio of a DS/SSMA system communicating over a WSSUS Rician fading channel. It was shown that with such a channel, the output of the correlation receiver matched to the i-th user's code waveform consisted of four components: the i-th user's direct (non-faded) signal, a faded version of the i-th user's transmitted signal, a multiple-user interference term consisting of direct and faded signal components, and an AWGN term. Treating the data symbols, phase shifts, and time delays of the other K-1 users as random variables with given distribution functions, we then defined the average signal-to-noise ratio in terms of expectations of the four components at the output of the correlation receiver. In general it was found that the resulting

expectations could not be evaluated directly in terms of the correlation functions of the fading channel unless certain additional assumptions about the covariance function of the channel were made. Hence, we considered the two singly-spread channels -- time-selective fading channels and frequency-selective fading channels. For both of these subclasses of WSSUS channels we were able to evaluate expressions for the average signal-to-noise ratio in terms of the covariance function of the fading channel, the continuous-time partial crosscorrelation functions of the K users' code waveforms, and the AWGN spectral density. For specific channel covariance functions, the resulting expressions become functions of the discrete aperiodic autocorrelation functions of the code signature sequences. A parameter of the channel covariance function known as the correlation duration was defined and was then used as the independent variable in plotting SNR_i for both time- and frequency-selective fading channels. It was found that the general trends of the plots could be explained by exploiting the duality existing between the two singly-spread channels as well as by noting the effect of the integrator in the correlation receiver on the performance of these two channels. We noted that most fading channels occurring in practice exhibit some degree of frequency-selectivity and that this phenomenon, together with the observation that SSMA systems occupy very large bandwidths, led us to conclude that a frequency-selective fading channel is a more realistic fading channel model for DS/SSMA systems than a time-selective fading channel model.

We then examined the performance of single user DS/SS systems over both classes of singly-spread channels and compared this performance to that of a PSK system operating over the channel. We found the DS/SS system performance identical to that for a PSK system for a time-selective fading channel, but the DS/SS system outperformed the PSK system for a frequency-selective fading channel. This performance difference in the latter channel may be attributed to the frequency-diversity achieved by the DS/SS system through the use of a signalling set with an improved autocorrelation function.

By randomizing the code signature sequences in the DS/SSMA system we were able to obtain approximate expressions for the average SNR which were independent of the actual choice of signature sequences used. These expressions are therefore useful in the preliminary design of a DS/SSMA system using a fading channel. It was found that for maximal connected sets of m-sequences employing either LSE/AO or AO/LSE shift register loadings, the difference between the actual SNR and the approximate value of SNR was negligible.

After considering SNR as a performance measure we next considered average probability of error as a measure of system performance. At the outset, it was noted that due to the complicated form of the resulting expression for the average probability of error, it would be desirable to obtain bounds on the probability of error. Because of the success of its use in bounding error probability in other types of digital communication systems, the moment space bounding technique was used to obtain

bounds for DS/SSMA communication via fading channels. Based on results in the published literature, we chose to use Nth moment space bounds, bounds which require evaluation of the Nth moment of the sum of the faded version of the i-th user's transmitted signal plus the multiple-access interference. For the second moment bound, we were able to evaluate the probability of error bounds using results from the analysis of the signal-to-noise ratio at the output of the i-th user's correlation receiver. It was noted that, in general, the second moment error bounds were too loose for practical application. Hence, we then considered higher order moment bounds in an effort to obtain tighter error bounds. For $n > 2$, however, we were unable to directly evaluate the nth moment of the sum of the faded version of the i-th user's transmitted signal plus the multiple-access interference and consequently we were unable to obtain tighter error bounds. It should be noted that much of the difficulty in applying the moment space bounding technique to DS/SSMA communications via fading channels is due to the relative complexity of the singly-spread fading channel model being used throughout this study. We conjecture that for simpler channel models, such as the recently developed three path fading channel model mentioned in Chapter 2, it would be possible to evaluate moment space bounds on the probability of error. Of course, such a channel model is less general than the singly-spread channel model.

In contrast to the results obtained for the multiple-user case, we were able to directly evaluate the probability of error for a single-user DS/spread-spectrum system for either a time-selective or a frequency-

selective fading channel. To investigate the performance of Nth moment space error bounds for fading channels, we considered the single-user DS/spread-spectrum system and evaluated the fourth, sixth, and eighth moment error bounds. We found that for small values of SNR, the lower moment error bounds yield the tightest bounds, but for larger values of SNR and D', only the higher moment bounds yield good results.

REFERENCES

Anderson, D. R. and Wintz, P. A., "Analysis of a spread-spectrum multiple-access system with a hard limiter," IEEE Transactions on Communication Technology, vol. COM-17, pp. 285-290, April 1969.

Aoki, M., Introduction to Optimization Techniques. New York: MacMillan, 1971.

Bello, P. A., "On the approach of a filtered-pulse train to a stationary Gaussian process," IRE Transactions on Information Theory, vol. IT-7, pp. 144-149, July 1961.

Bello, P. A., "Characterization of randomly time-variant linear channels," IEEE Transactions on Communications Systems, vol. CS-11, pp. 360-393, December 1963.

Bello, P. A., "Time-frequency duality," IEEE Transactions on Information Theory, vol. IT-10, pp. 18-33, January 1964.

Bello, P. A., "Channel-probing techniques and their effectiveness," in Aspects of Network and System Theory, (R. E. Kalman and N. DeClaris, editors). New York: Holt, Rinehart, and Winston, 1971.

Bello, P. A. and Nelin, B. D., "The influence of fading spectrum on the binary error probabilities of incoherent and differentially coherent matched filter receivers," IRE Transactions on Communications Systems, vol. CS-10, pp. 160-168, June 1962.

Bello, P. A. and Nelin, B. D., "The effect of frequency selective fading on the binary error probabilities of incoherent and differentially coherent matched filter receivers," IEEE Transactions on Communications Systems, vol. CS-11, pp. 170-186, June 1963.

Bond, F. E. and Meyer, H. F., "Fading and multipath considerations in aircraft/satellite communication systems," in Communication Satellite Systems Technology, (R. B. Marsten, editor). New York: Academic Press, 1966.

Borth, D. E. and Pursley, M. B., "Direct-sequence spread-spectrum multiple-access communication for a class of Rician fading channels," Proceedings of the National Telecommunications Conference, vol. 3, pp. 35.2.1-35.2.6, December 1978.

Borth, D. E. and Pursley, M. B., "Analysis of direct-sequence spread-spectrum multiple-access communication over Rician fading channels," IEEE Transactions on Communications, vol. COM-27, October 1979.

Borth, D. E., Pursley, M. B., Sarwate, D. V., and Stark, W. E., "Bounds on error probability for direct-sequence spread-spectrum multiple-access communications," 1979 MIDCON Conference Proceedings, Chicago, Illinois 1979.

Brown, W. M. and Crane, R. B., "Conjugate linear filtering," IEEE Transactions on Information Theory, vol. IT-15, pp. 462-465, July 1969.

Cahn, C. R., "Spread spectrum applications and equipments," in Spread Spectrum Communications (L. A. Gerhardt, editor), AGARD Lecture Series No. 58, NATO, July 1973.

Chang, J., "The effect of multipath interference on the performance of a digital matched filter," IEEE Transactions on Communications, vol. COM-27, pp. 737-745, April 1979.

Chen, C. C. and Burnett, J. W., "TDRS multiple access channel design," Proceedings of the National Telecommunications Conference, vol. II, pp. 19:2-1-19:2-7, December 1977.

Dresher, "Moment spaces and inequalities," Duke Mathematical Journal, vol. 20, pp. 261-271, June 1953.

Dresher, M., Karlin, S., and Shapley, L. S., "Polynomial games," in Contributions to the Theory of Games, vol. I., (H. W. Kuhn and A. W. Tucker, editors), Annals of Mathematics Study, no. 24, pp. 161-180, 1950.

Drouilhet, P. R. and Bernstein, S. L., "TATS--a bandspread modulation-demodulation system for multiple access tactical satellite communication," EASCON Convention Record, pp. 126-132, October 1969.

Garber, F. D., "Signal-to-noise ratio analysis of two implementations of quadriphase direct-sequence spread-spectrum multiple-access," M.S. Thesis, Department of Electrical Engineering, University of Illinois, (also Coordinated Science Laboratory Report R-815), May 1978a.

Garber, F. D., private communication, 1978b.

Gardner, C. S. and Orr, J. A., "Fading effects on the performance of a spread spectrum multiple access communication system," IEEE Transactions on Communications, vol. COM-27, pp. 143-149, January 1979.

Grettenberg, T. L., "A representation theorem for complex normal processes," IEEE Transactions on Information Theory, vol. IT-11, pp. 305-306, April 1965.

Grisdale, G. L., Morris, J. G., and Palmer, D. S., "Fading of long-distance radio signals and a comparison of space- and polarization-diversity reception in the 6-18 Mcs range," Proceedings of the IEE, vol. 104, pp. 39-51, January 1957.

Golay, M. J. E., "A class of finite binary sequences with alternate autocorrelation values equal to zero," IEEE Transactions on Information Theory, vol. IT-18, pp. 449-450, May 1972.

Gold, R. and Kopitzke, E., "Study of correlation properties of binary sequences," Interim Technical Report Number 1, vol. 1, (AD 470696), Magnavox Research Laboratories, Torrance, California, August 1965.

Jacobs, I. M., "Practical applications of coding," IEEE Transactions on Information Theory, vol. IT-20, pp. 305-310, May 1974.

Jakes, W. C., "An approximate method to estimate an upper bound on the effect of multipath delay distortion on digital transmission," IEEE International Conference on Communications, Conference Record, vol. 3, pp. 47.1.1-47.1.5, June 1978.

Kadar, I. and Schreiber, H. H., "Performance of spread-spectrum systems in a multipath environment," in Communication Satellites for the 70's: Systems 1971, (N. E. Feldman and C. M. Kelly, editors). Cambridge, Massachusetts: MIT Press, 1971.

Kailath, T., "Channel characterization: time-variant dispersive channels," in Lectures in Communication Theory, (E. Baghdady, editor). New York: McGraw-Hill, 1961.

Kennedy, R. S., Fading Dispersive Communication Channels. New York: Wiley, 1969.

Kochevar, H. J., "Spread spectrum multiple access communications experiment through a satellite," IEEE Transactions on Communications, vol. COM-25, pp. 853-856, August 1977.

Lebow, I. L., Drouilhet, P. R., Dagget, N. L., Harris, J. N., Nagy, F., Jr., "The West Ford Belt as a communications medium," Proceedings of the IEEE, vol. 52, pp. 543-563, May 1964.

Lebow, I. L., Jordan, K. L., and Drouilhet, P. R., "Satellite communications to mobile platforms," Proceedings of the IEEE, vol. 59, pp. 139-159, February 1971.

Lerner, R. M., "Means for counting "effective" numbers of objects or durations of signals," Proceedings of the IRE, vol. 47, p. 1653, September 1959.

Lucky, R. W., Salz, J., and Weldon, E. J., Principles of Data Communication. New York: McGray-Hill, 1968.

Malm, R. and Schreder, K., "Fast frequency hopping techniques," in Proceedings of the 1973 Symposium on Spread Spectrum Communications, vol. 1, (AD-915 852), pp. 37-42, March 1973.

Massey, J. L. and Uhran, J. J., "Final report for multipath study," (Contract No. NAS5-10786), University of Notre Dame, Notre Dame, Indiana, 1969.

Massey, J. L. and Uhran, J. J., "Sub-baud coding," Proceedings of the Thirteenth Annual Allerton Conference on Circuit and System Theory, pp. 539-547, October 1975.

McGee, W. F., "Complex Gaussian noise moments," IEEE Transactions on Information Theory, vol. IT-17, pp. 149-157, March 1971.

McNicol, R. W. E., "The fading of radio waves of medium and high frequencies," Proceedings of the IEE, vol. 96, pp. 517-524, November 1949.

Miller, K. S., "Moments of complex Gaussian processes," Proceedings of the IEEE, vol. 56, pp. 83-84, January 1968.

Miller, K. S., Complex Stochastic Processes. Reading, Massachusetts: Addison-Wesley, 1974.

Monsen, P., "Feedback equalization for fading dispersive channels," IEEE Transactions on Information Theory, vol. IT-17, pp. 56-64, January 1971.

Monsen, P., "Digital transmission performance on fading dispersive diversity channels," IEEE Transactions on Communications, vol. COM-21, pp. 33-39, January 1973.

Nesenbergs, M., "Error probability for multipath fading--the "slow and flat" idealization," IEEE Transactions on Communications Technology, vol. COM-15, pp. 797-805, December 1967.

Orr, J. A., "Effects of fading on a multi-user spread spectrum system using direct sequence modulation," Ph.D. Thesis, Department of Electrical Engineering, University of Illinois, April 1977.

Papoulis, A., The Fourier Integral and its Applications. New York: McGraw-Hill, 1962.

Papoulis, A., Probability, Random Variables, and Stochastic Processes. New York: McGraw-Hill, 1965.

Price, R., and Green, P. E., "A communication technique for multipath channels," Proceedings of the IRE, vol. 46, pp. 555-570, March 1958.

Pritchard, W. L., "Satellite communication--an overview of the problems and programs," Proceedings of the IEEE, vol. 65, pp. 294-307, March 1977.

Pritchard, W. L., "Communications in orbit," Electronics, vol. 51, pp. 120-123, October 12, 1978.

Pursley, M. B., "Evaluating performance of codes for spread spectrum multiple access communications," Proceedings of the Twelfth Annual Allerton Conference on Circuit and System Theory, pp. 765-774, October 1974.

Pursley, M. B., "Performance evaluation for phase-coded spread-spectrum multiple-access communication--part I: system analysis," IEEE Transactions on Communications, vol. COM-25, pp. 795-799, August 1977.

Pursley, M. B., and Garber, F. D., "Quadriphase spread-spectrum multiple-access communications," IEEE International Conference on Communications, Conference Record, vol. 1, pp. 7.3.1-7.3.5, 1978.

Pursley, M. B., and Roefs, H. F. A., "Numerical evaluation of correlation parameters for optimal phases of binary shift-register sequences," IEEE Transactions on Communications, vol. COM-27, October 1979.

Pursley, M. B., and Sarwate, D. V., "Evaluation of correlation parameters for periodic sequences," IEEE Transactions on Information Theory, vol. IT-23, pp. 508-513, July 1977a.

Pursley, M. B., and Sarwate, D. V., "Performance evaluation for phase-coded spread-spectrum multiple-access communication--part II: code sequence analysis," IEEE Transactions on Communications, vol. COM-25, pp. 800-803, August 1977b.

Reed, I. S., "On a moment theorem for complex Gaussian processes," IRE Transactions on Information Theory, vol. IT-8, pp. 194-195, April 1962.

Roefs, H. F. A., "Binary sequences for spread-spectrum multiple-access communication," Ph.D. Thesis, Department of Electrical Engineering, University of Illinois, (also Coordinated Science Laboratory Report R-785), August 1977.

Roefs, H. F. A., and Pursley, M. B., "Correlation parameters of random binary sequences," Electronics Letters, vol. 18, pp. 488-489, 1977.

Rummler, W. D., "A multipath channel model for line-of-sight digital radio systems," IEEE International Conference on Communications, Conference Record, vol. 3, pp. 47.5.1-47.5.4, June 1978.

Rummler, W. D., "A new selective fading model: application to propagation data," Bell System Technical Journal, vol. 58, pp. 1037-1071, May-June 1979.

Sarwate, D. V., and Pursley, M. B., "Crosscorrelation properties of pseudorandom and related sequences," submitted to Proceedings of the IEEE, June 1979.

Schneider, K. S., "Optimum detection of code division multiplexed signals," IEEE Transactions on Aerospace and Electronic Systems, vol. AES-15, pp. 181-185, January 1979.

Scholtz, R. A., "The spread spectrum concept," IEEE Transactions on Communications, vol. COM-25, pp. 748-755, August 1977.

Smith, E. G., "JTIDS: an update," IEEE Aerospace and Electronic Systems Society Newsletter, vol. 13, pp. 25-29, March 1978.

Spilker, J. J., Digital Communications by Satellite. Englewood Cliffs, N. J.: Prentice-Hall, 1977.

Stampfl, R. A., and Jones, A. E., "Tracking and data relay satellites," IEEE Transactions on Aerospace and Electronic Systems, vol. AES-6, pp. 276-289, May 1970.

Stein, S., "Fading communication media," Chp. 9 of Communication Systems and Techniques. New York: McGraw-Hill, 1966.

Stein, S., and Jones, J. J., Modern Communication Principles. New York: McGraw-Hill, 1967.

Stiffler, J. J., Theory of Synchronous Communications. Englewood Cliffs, N. J.: Prentice-Hall, 1971.

Stiglitz, I. G., "Multiple-access considerations--a satellite example," IEEE Transactions on Communications, vol. COM-21, pp. 577-582, May 1973.

Strohbehn, J. W., "Line-of-sight wave propagation through the turbulent atmosphere," Proceedings of the IEEE, vol. 56, pp. 1301-1318, August 1968.

Tobin, R. M., and Yao, K., "Upper and lower bounds for coherent phase-shift-keyed (CPSK) systems with cochannel interference," IEEE Transactions on Communications, vol. COM-25, pp. 281-287, February 1977.

Turin, G. L., "Error probabilities for binary symmetric ideal reception through nonselective slow fading and noise," Proceedings of the IRE, vol. 46, pp. 1603-1619, September 1958.

Van Trees, H. L., Detection, Estimation, and Modulation Theory, Part III. New York: Wiley, 1971.

Viterbi, A. J., "Optimum detection and signal selection for partially coherent binary communication," IEEE Transactions on Information Theory, vol. IT-11, pp. 239-246, April 1965.

Viterbi, A. J., "Spread spectrum communications--myths and realities," IEEE Communications Magazine, vol. 17, pp. 11-18, May 1979.

Wang, M. C., and Uhlenbeck, G. E., "On the theory of the Brownian Motion II," Reviews of Modern Physics, vol. 17, pp. 323-342, April-July, 1945.

Weber, W. J., "Performance of phase-locked loops in the presence of fading communication channels," IEEE Transactions on Communications, vol. COM-24, pp. 487-499, May 1976.

Welch, G. A., "Performance of direct sequence modulated spread spectrum multiple access communication systems in a Rayleigh fading environment," M.S. Thesis, Department of Electrical Engineering, University of Illinois, March 1978.

Wilde, D. J., Optimum Seeking Methods. Englewood Cliffs, N. J.: Prentice-Hall, 1964.

Wozencraft, J. M., and Jacobs, I. M., Principles of Communication Engineering. New York: Wiley, 1965.

Yan, T. Y., "Moment space error bounds for digital communication systems with intersymbol interference based on Nth moment," M.S. Thesis, System Science Department, University of California, Los Angeles, (also School of Engineering and Applied Science Technical Report ENG-7608, January 1976), Fall 1975.

Yao, K., "Error probability of spread spectrum multiple access communication systems," Proceedings of the 1976 Conference on Information Sciences and Systems, Johns Hopkins University, pp. 67-72, March 1976a.

Yao, K., "Performance bounds on spread spectrum multiple access communication systems," Proceedings of the 1976 International Telemetering Conference, pp. 317-325, September 1976b.

Yao, K., "Error probability of asynchronous spread-spectrum multiple access communication systems," IEEE Transactions on Communications, vol. COM-25, pp. 803-809, August 1977.

Yao, K., and Milstein, L. B., "Performance of PSK systems with bandpass limiters," Proceedings of the Sixteenth Annual Allerton Conference on Communication, Control, and Computing, pp. 423-431, October 1978.

Yao, K., and Tobin, R. M., "A new class of upper and lower bounds for digital communication systems with intersymbol interference," 1975 IEEE International Conference on Communications, Conference Record, pp. 35-11-35-15, June 1975.

Yao, K., and Tobin, R. M., "Moment space upper and lower error bounds for digital systems with intersymbol interference," IEEE Transactions on Information Theory, vol. IT-22, pp. 65-74, January 1976.

APPENDIX A

AVERAGE SIGNAL-TO-NOISE RATIO RESULTS FOR LARGE VALUES OF THE FADING POWER TRANSMISSION COEFFICIENT

In Chapter 2 we made mention, in passing, of the recent development of a three-path fading channel model for line-of-sight microwave channels ([Rummler, 1978], [Rummler, 1979]). In the literature describing this channel model, mention is made of several actual channels exhibiting fading to the extent that the fading power transmission coefficient γ^2 for these channels is on the order of $\gamma^2 = 0.5$. In Chapter 3, we have presented signal-to-noise ratio data for channels in which $\gamma^2 \leq 0.2$, primarily for the reason that it is believed that the effects of the synchronization subsystem on the communication system performance are no longer negligible for values of $\gamma^2 > 0.2$. For line-of-sight applications, however, other techniques (e.g. atomic clocks, auxiliary synchronization channels) may be used to obtain synchronization information so that reliable communications may be achieved. In this appendix we present additional SNR data for channels in which $\gamma^2 > 0.2$.

In Figure A1 we have plotted SNR as a function of the correlation duration of the channel for a time-selective fading channel with a triangular covariance function. In plotting Figure A1 we have used a maximal connected set of six m-sequences in their LSE/AO phases (see Chapter 3 for details). In Figure A2 we have plotted the corresponding results for a frequency-selective fading channel with a triangular covariance function. We see from these two plots that the increased amount of fading simply reduces the average SNR.

In Figure A3 we have plotted SNR versus correlation duration for single user DS/spread-spectrum and PSK systems operating over a frequency-selective fading channel with a triangular correlation function for two values of γ^2. Note that for these larger values of γ^2, the SNR at the output of the PSK system is so small as to make the PSK system virtually useless, while for values of correlation duration greater than 60 T_c, the degredation of the DS/spread-spectrum system from the ideal AWGN channel signal-to-noise ratio is less than 0.5 dB.

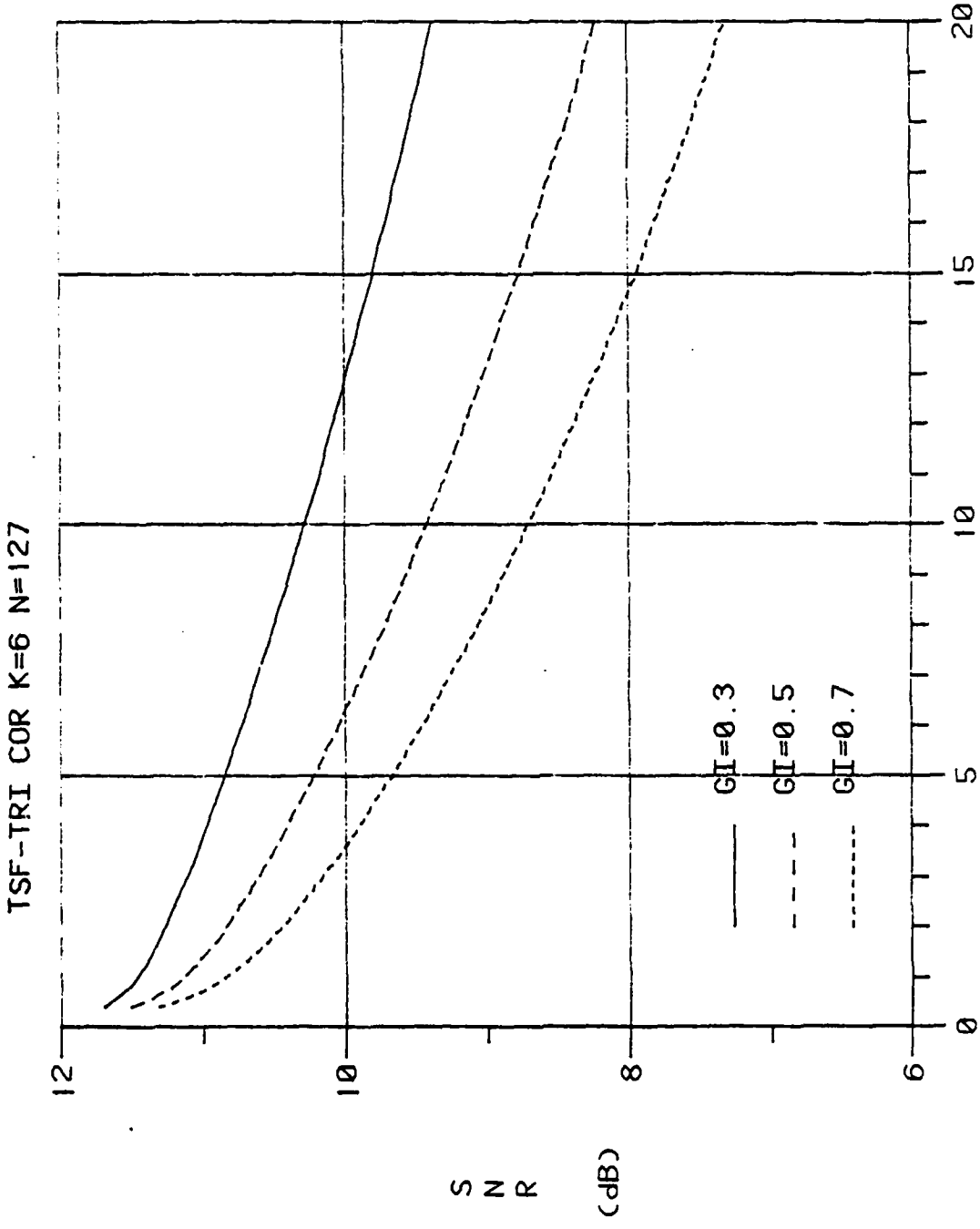

Figure A1. SNR vs. correlation duration for a time-selective fading channel with a triangular covariance function for three values γ^2 (N = 127, K = 6, $\mathcal{E}/N_0$ = 10dB, LSE/AO sequences).

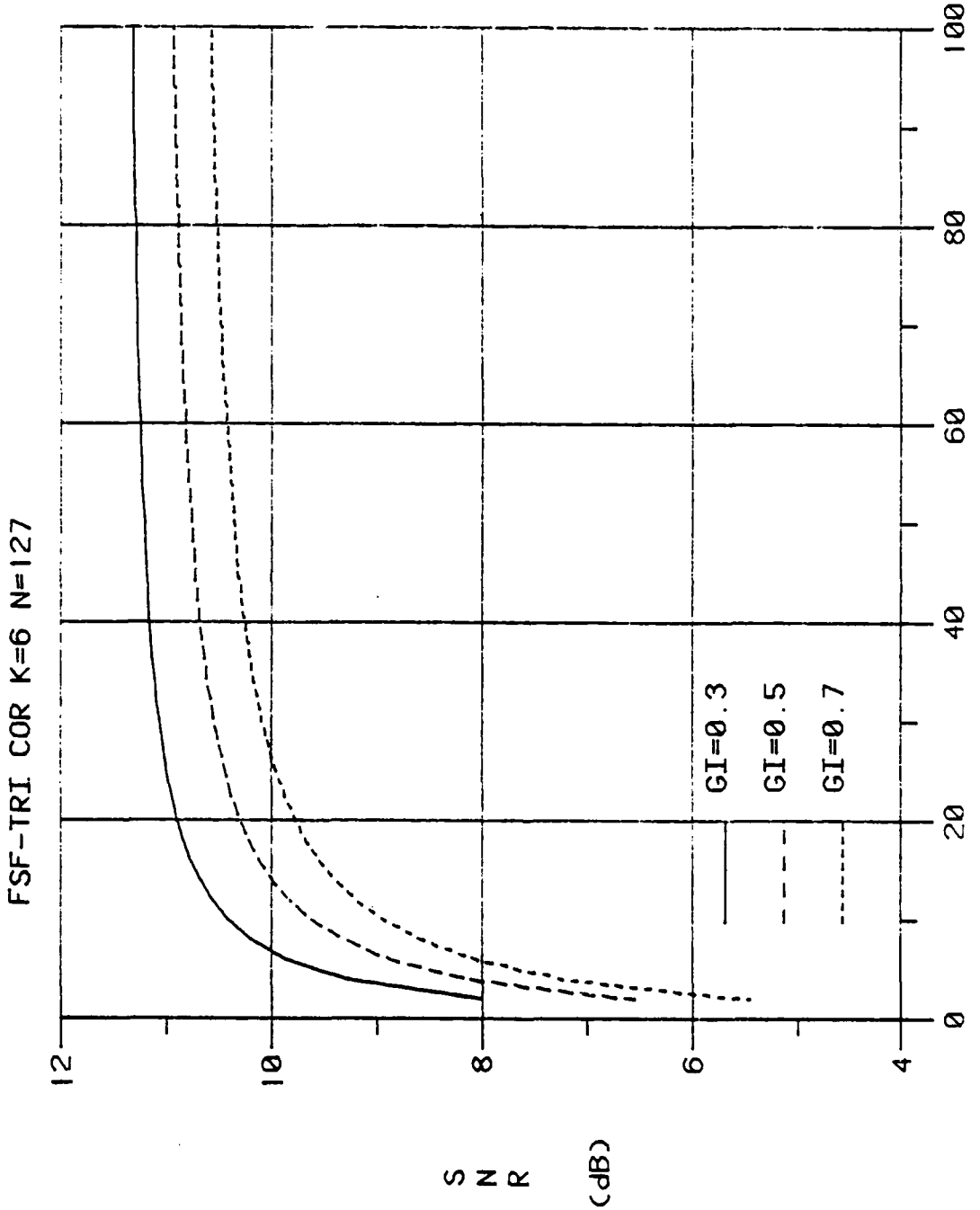

Figure A2. SNR vs. correlation duration for a frequency-selective fading channel with a triangular covariance function for single-user DS/spread-spectrum and biphase PSK systems (N = 127, K = 6, $\mathcal{E}/N_0$ = 10dB, LSE/AO sequences).

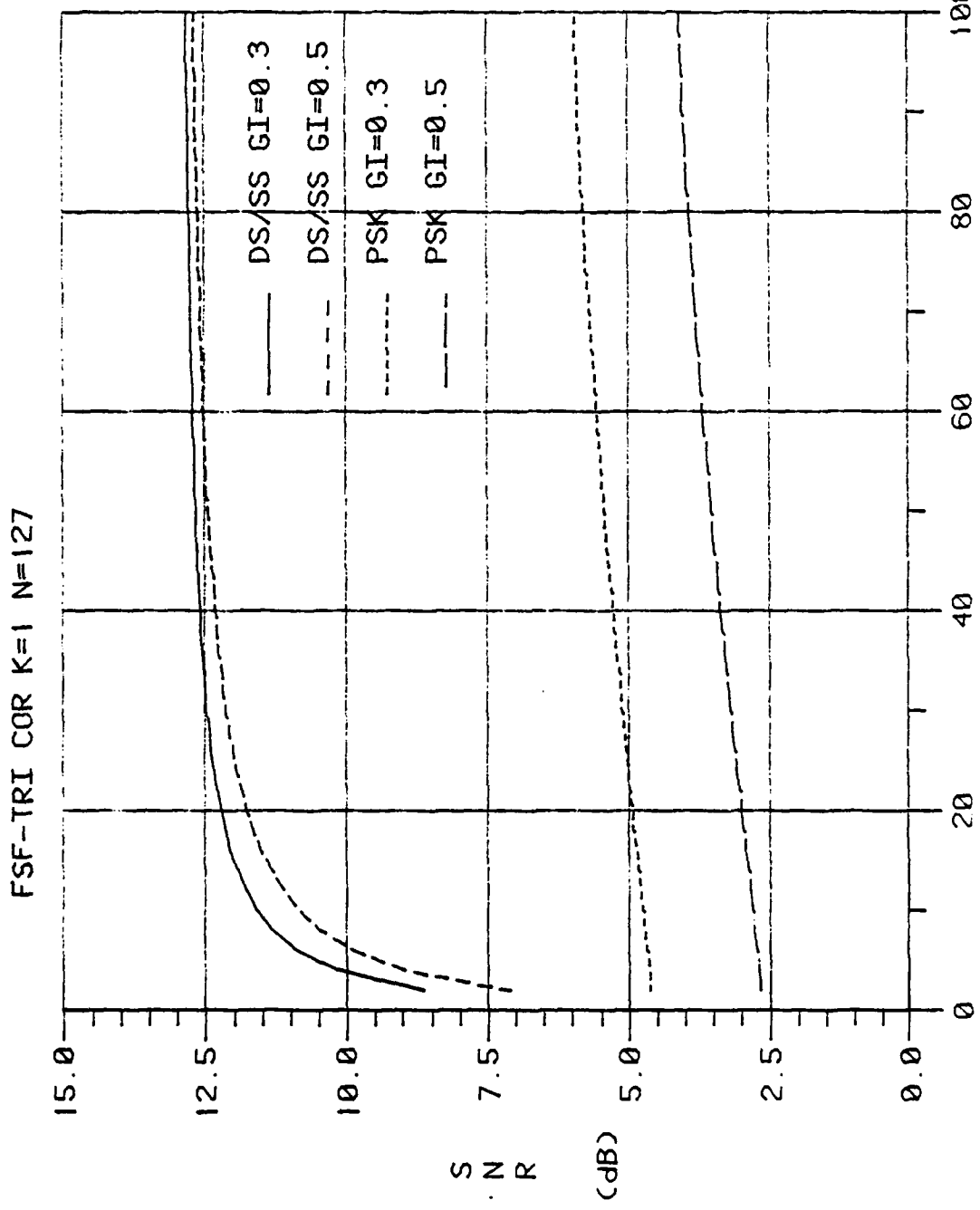

Figure A3. SNR vs. correlation duration for a frequency-selective fading channel with a triangular covariance function for single-user DS/spread-spectrum and biphase PSK systems ($N = 127$, $\mathcal{E}/N_o = 10$dB, LSE/AO sequence).

APPENDIX B

Nth MOMENT SPACE BOUNDS ON THE PROBABILITY OF ERROR

B.1 Introduction

In Chapter 4 we discussed the isomorphism theorem regarding relationships between arbitrary moments of random variables and showed how this theorem could be used to obtain bounds on the probability of error of a DS/SSMA system with a Rician fading channel. In using this theorem, we derived the Nth moments of the fading terms and then proceeded to plot the probability of error bounds directly. In this appendix we will derive analytical expressions for bounds on P_e from knowledge of the Nth moment of the fading terms and the normalized distortion D'. The resulting expressions for probability of error bounds were used in Chapter 4 to plot the actual error bounds. Many of the results to be presented were previously obtained by Yan (1975) but have been refined here for use with fading channels.

To begin with, instead of concerning ourselves with the details of a DS/SSMA system with a fading channel, we shall use a simpler (but more general) model of a digital communication system with interference and noise in deriving the moment space error bounds. The modifications necessary to treat DS/SSMA systems with fading channels are straightforward and will not be discussed here (see Chapter 4). For a transmitted data bit a_0, assumed to take on value $\{+1,-1\}$ with equal probability, the received signal at the output of the receiver at the decision instant $t = T$ is given by

$$y = a_0 h + z + n \tag{B.1}$$

where h may be thought of as the response of the channel, sampled at time $t = T$ due to the transmission of data bit a_0, z is the interference component,

and n is an additive Gaussian noise component with variance σ^2. The interference component is assumed to have an unknown distribution function with finite distortion D such that

$$|z| \leq D. \tag{B.2}$$

The probability of error at the output of the receiver is given by

$$\begin{aligned} P_e &= \tfrac{1}{2} \Pr\{y \leq 0 | a_0 = +1\} + \tfrac{1}{2} \Pr\{y \geq 0 | a_0 = -1\} \\ &= E\{ \tfrac{1}{2} Q(\tfrac{h+z}{\sigma}) + \tfrac{1}{2} Q(\tfrac{h-z}{\sigma})\} \end{aligned} \tag{B.3}$$

where the expectation is over the interference term z.

To derive Nth moment space bounds on the probability of error of this digital communication system, we will let $k_1(z) = z^n$ and let $k_2(z) = \frac{1}{2} Q(\frac{h+z}{\sigma}) + \frac{1}{2} Q(\frac{h-z}{\sigma})$. Furthermore, we will assume that the moment $m_1 \triangleq E\{k_1(z)\}$ is known. Noting that $m_2 = E\{k_2(z)\} = P_e$, we may use the isomorphism theorem of Chapter 4 to derive bounds on P_e. In order to apply this theorem, however, we first need to evaluate the convex hull $\mathcal{K}$ of the curve $\mathcal{C}$ of $k_2(z)$ versus $k_1(z)$. From calculus, we have the following results:

(i) A function f(x) is convex $\cup$ iff $f''(x) \geq 0$.

(ii) A function f(x) is convex $\cap$ iff $f''(x) \leq 0$.

Hence, in order to evaluate the convex hull of $\mathcal{C}$, we need to evaluate the first and second derivatives of $r(z) \triangleq k_2(k_1(z))$. Simple differentiation shows that

$$r'(z) = \frac{1}{2n\sigma\sqrt{2\pi}} \frac{e^{-\frac{(h-z)^2}{2\sigma^2}} - e^{-\frac{(h+z)^2}{2\sigma^2}}}{z^{n-1}} \triangleq K \frac{u(z)}{z^{n-1}} \tag{B.4}$$

$$r''(z) = \frac{K}{n} \{ \frac{zu'(z) - (n-1)u(z)}{z^{2n-1}} \} \tag{B.5}$$

where

$$K \triangleq [2n\sigma\sqrt{2\pi}]^{-1} \tag{B.6}$$

and

$$u(z) \triangleq e^{-\frac{(h-z)^2}{2\sigma^2}} - e^{-\frac{(h+z)^2}{2\sigma^2}} . \tag{B.7}$$

If we collect identical terms appearing inside the brackets of (B.5), r"(z) becomes

$$r''(z) = P(z)F(z) \tag{B.8}$$

where

$$P(z) = \frac{K}{n\sigma^2 z^{2n-1}} e^{-\frac{(h+z)^2}{2\sigma^2}} \tag{B.9}$$

and

$$F(z) = [zh + z^2 + (n-1)\sigma^2] + e^{\frac{2zh}{\sigma^2}} [zh - z^2 - (n-1)\sigma^2] . \tag{B.10}$$

An alternative form of writing F(z) is to expand the exponential term into a Taylor series expansion, multiply by the appropriate powers of z appearing within the square brackets and then collect identical terms. If we do this, (B.10) becomes

$$F(z) = F_1(z) + F_2(z) \tag{B.11}$$

where

$$F_1(z) = 2(2-n)[zh + \frac{h^2 z^2}{\sigma^2}] \tag{B.12}$$

$$F_2(z) = z^2 \sum_{k=1}^{\infty} \frac{(\frac{2zh}{\sigma^2})^k}{k!} C(k,n,\frac{h}{\sigma}) \tag{B.13}$$

$$C(k,n,\frac{h}{\sigma}) =)-1) + \frac{h^2}{\sigma^2} [\frac{2(k-2n+4)}{(k+1)(k+2)}] . \tag{B.14}$$

As we will see in the next two sections, depending upon the value of n, either (B.8) and (B.10) or (B.8) and (B.11) is more convenient to use in valuating the convexity of $\mathcal{C}$.

Finally we will need to know the following results on the limiting values of r'(z) and r''(z):

$$r'(z) \geq 0 \text{ for } z \geq 0 \tag{B.15}$$

$$\lim_{z \to \infty} r'(z) = 0 \tag{B.16}$$

$$\lim_{z \to 0} r''(z) = \begin{cases} \dfrac{h}{6n\sigma^4\sigma\sqrt{2\pi}} \left[\dfrac{h^2}{\sigma^2} - 3 \right] e^{-h^2/2\sigma^2}, & n = 2 \\ \infty, & n \geq 3 . \end{cases} \tag{B.17}$$

All of these results may be derived from the defining equations for r'(z) and r''(z) and L'Hopital's rule. In the next two sections we will consider in detail the convexity of $\mathcal{C}$ for n = 2 and for n ≥ 3, respectively. We will then use these results to obtain analytical expressions for bounds on P_e in terms of the Nth moment of z and the distortion D.

B.2 Second Moment Error Bounds

In the previous section we noted that we could write an expression for r''(z) as either P(z)F(z) or P(z)[$F_1(z) + F_2(z)$]. Because of the form of $F_1(z)$ it is more expedient to use the latter expression for r''(z) for n = 2. Hence for n = 2, we have that

$$\begin{aligned} r_2'(z) &= P(z)F_2(z) \\ &= P(z)z^2 \sum_{k=1}^{\infty} \frac{\left(\frac{2zh}{\sigma^2}\right)^k}{k!} C\left(k,2,\frac{h}{\sigma}\right). \end{aligned} \tag{B.18}$$

Because $k_1(z)$ and $k_2(z)$ are both symmetric about z = 0, in applying the isomorphism theorem to bound P_e, we need only let I = [0,D], i.e., only positive values of z need be considered in evaluating the convexity of $\mathcal{C}$. From (B.9) and (B.18), we see that for n = 2 and z ≥ 0, the sign of r''(z)

is completely determined by $C(k,2,\frac{h}{\sigma})$, which is a monotonically decreasing function of k with a maximum occurring at k = 1. Hence we note that

$$C(k,2,\tfrac{h}{\sigma}) = (-1) + \frac{h^2}{\sigma^2}\left[\frac{2k}{(k+1)(k+2)}\right] \begin{cases} \le 0, \ \frac{h}{\sigma} \le \sqrt{3}, \ \forall k \\ \ge 0, \ \frac{h}{\sigma} \ge \sqrt{3} \text{ for some } k < k_1 \end{cases} \tag{B.19}$$

where k_1 is the smallest integer such that

$$(-1) + \frac{h^2}{\sigma^2}\left[\frac{2k_1}{(k_1+1)(k_1+2)}\right] \le 0. \tag{B.20}$$

From (B.18) and (B.19) we have the result that if $\frac{h}{\sigma} < \sqrt{3}$, $\mathcal{C}$ is convex $\cap$ for all values of z. For $\frac{h}{\sigma} \ge \sqrt{3}$, using (B.18) and (B.20) we see that for small values of z, $\mathcal{C}$ is convex $\cup$. For larger values of z, however, and for $k \ge k_1$, C is negative and hence r''(z) may be less than zero. From (B.17) we see that, in fact, for large enough z and for $\frac{h}{\sigma} \ge \sqrt{3}$, r''(z) is negative. Consequently for $\frac{h}{\sigma} \ge \sqrt{3}$, $\mathcal{C}$ is initially convex $\cup$ and then becomes convex $\cap$.

In Figures B1 and B2 we have plotted $\mathcal{C}$ for $\frac{h}{\sigma} < \sqrt{3}$ and $\frac{h}{\sigma} \ge \sqrt{3}$, respectively for n = 2 and for arbitrary values of D. In plotting these two figures we have used the results of the previous paragraph to determine the convexity of $\mathcal{C}$. In Figure B2 we have labeled four points on $\mathcal{C}$ to aid in determining the moment space probability of error bounds. The point z_1 is defined to be the point satisfying the equation

$$r''(z_1) = 0 \ . \tag{B.21}$$

The point z_2 is the point on $\mathcal{C}$ such that a line drawn from the point $(k_1(0),k_2(0))$ is tangent to $\mathcal{C}$ at z_2, i.e., z_2 is the solution to the equation

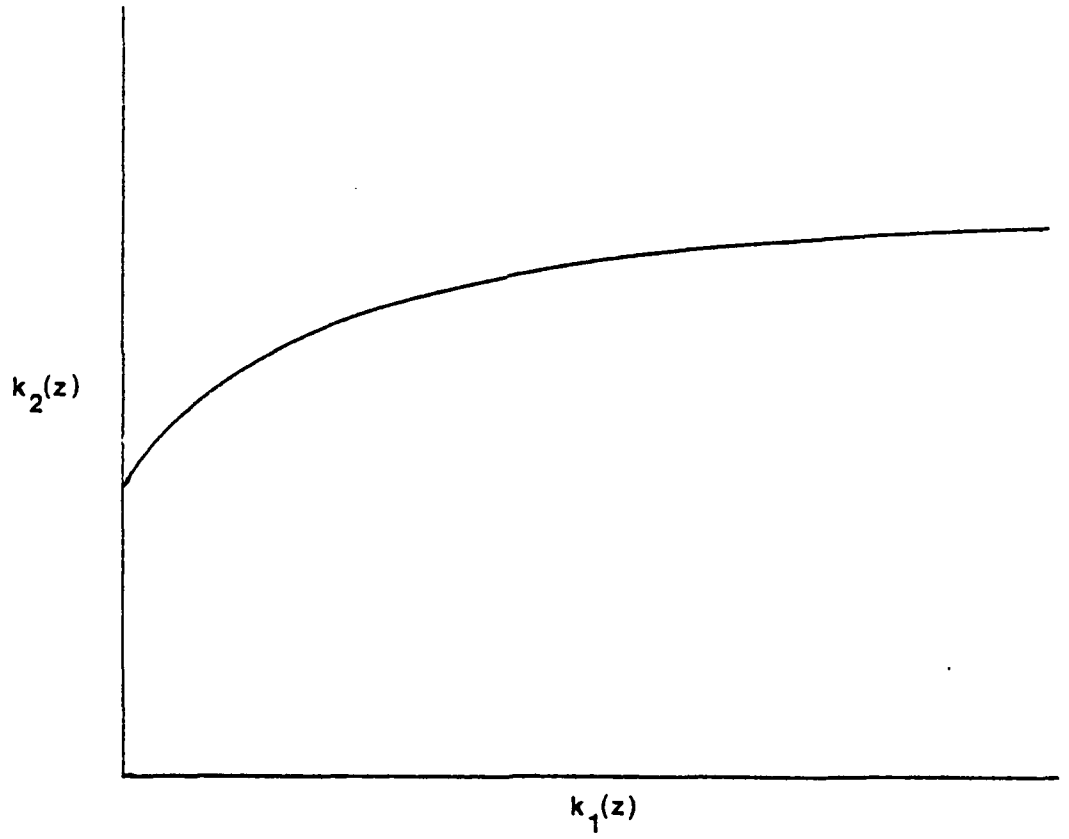

Figure B1, Plot of $\mathcal{C}$ for second moment space bounds ($\frac{h}{\sigma} < \sqrt{3}$).

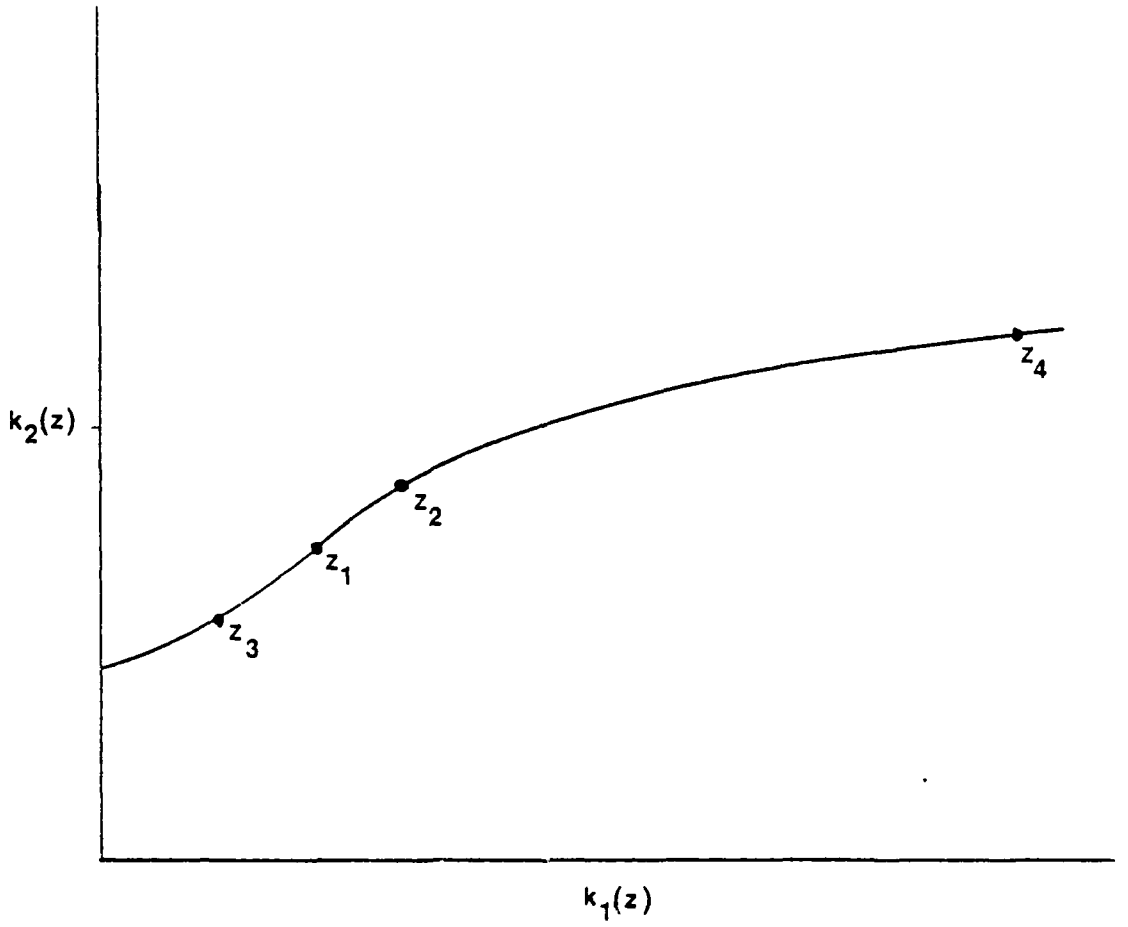

Figure B2. Plot of $\mathcal{C}$ for second moment space bounds ($\frac{h}{\sigma} \geq \sqrt{3}$).

$$\frac{1}{2z_2^2}\{Q(\frac{h+z_2}{\sigma}) + Q(\frac{h-z_2}{\sigma}) - 2Q(\frac{h}{\sigma})\} =$$

$$= \frac{1}{4\sigma z_2\sqrt{2\pi}}\{e^{-\frac{(h-z_2)^2}{2\sigma^2}} - e^{-\frac{(h+z_2)^2}{2\sigma^2}}\} . \qquad (B.22)$$

The point z_3 is defined to be the point on $\mathcal{C}$ such that a line drawn from $(k_1(D),k_2(D))$ is tangent to $\mathcal{C}$ at z_3, i.e., z_3 is the solution to the equation

$$\frac{1}{2(D^2-z_3^2)}\{Q(\frac{h+D}{\sigma}) + Q(\frac{h-D}{\sigma}) - Q(\frac{h+z_3}{\sigma}) - Q(\frac{h-z_3}{\sigma})\} =$$

$$= \frac{1}{4\sigma z_3\sqrt{2\pi}}\{e^{-\frac{(h-z_3)^2}{2\sigma^2}} - e^{-\frac{(h+z_3)^2}{2\sigma^2}}\} . \qquad (B.23)$$

Finally point z_4 is the point on $\mathcal{C}$ which intersects with a line tangent at $(k_1(0),k_2(0))$, i.e., z_4 is the solution to the equation

$$\frac{1}{2z_4^2}\{Q(\frac{h+z_4}{\sigma}) + Q(\frac{h-z_4}{\sigma}) - 2Q(\frac{h}{\sigma})\} = \frac{1}{2\sigma\sqrt{2\pi}}\frac{h}{\sigma^2}e^{-\frac{h^2}{2\sigma^2}} . \qquad (B.24)$$

In (B.24) we have used the fact that $r'(0)$ is equal to the right-hand side of (B.24), which follows from (B.4) and a simple application of L'Hopital's rule for derivatives.

Note that all of the four points z_1 through z_4 are solutions to single variable nonlinear equations. Hence they may be solved by any number of methods including the bisection method, the false-position method, or Newton's method. Once these points are determined, we may directly write down

equations for the moment space lower and upper bounds on the probability of error through the use of the isomorphism theorem. In Tables B1 and B2 we summarize these equations for lower and upper bounds, respectively. Note that in general, these bounds are functions of h/σ, D, and m_1.

B.3 Nth Moment Error Bounds

We may easily extend the results for second moment error bounds to Nth moment error bounds for n even and $n \geq 2$. However since $F_1(z)$ is no longer identically zero for $n \geq 2$, we should not expect that the convexity of $\mathcal{C}$ be identical to that of the $n = 2$ case. In the following we will show that this is, in fact, the case.

For large values of z we will use the expression $r''(z) = P(z)F(z)$ in determining the convexity of $\mathcal{C}$. From the observations made in the previous section we need only consider $z \geq 0$ in determining the convex regions of $\mathcal{C}$. From (B.15) and (B.16) we may conclude that for large z, $r''(z)$ is negative and hence $\mathcal{C}$ is convex $\cap$ for large z. For smaller values of z we will use the expression $r''(z) = P(z)[F_1(z) + F_2(z)]$ to determine the convexity of $\mathcal{C}$. Since we are only considering non-negative values of z, from (B.9), $P(z) \geq 0$ and thus the sign of $r''(z)$ is determined by the sign of the sum $F_1(z) + F_2(z)$. For $n > 2$, $F_1(z)$ is always negative and from (B.14) we see that <u>at least</u> the first 2n-4 terms of $F_2(z)$ are negative. Thus for small enough z and $\frac{h}{\sigma}$, the sum $F_1(z)$ is negative and hence $r''(z)$ is negative for small values of z. For larger values of z and $\frac{h}{\sigma}$ it may be possible that the $k > 2n-4$ terms of $F_2(z)$ will dominate the $k \leq 2n-4$ terms of $F_2(z)$ as well as $F_1(z)$ so that $F_1(z) + F_2(z) > 0$ for large values of z and $\frac{h}{\sigma}$. We may conclude from this that, depending upon the value of $\frac{h}{\sigma}$, $\mathcal{C}$ is either

SNR	P_e^L	m_1	D
$\frac{h}{\sigma} < \sqrt{3}$	$\frac{1}{2D^2}[Q(\frac{h+D}{\sigma}) + Q(\frac{h-D}{\sigma}) - 2Q(\frac{h}{\sigma})]m_1 + Q(\frac{h}{\sigma})$	all	all
$\frac{h}{\sigma} > \sqrt{3}$	$\frac{1}{2}[Q(\frac{h+\sqrt{m_1}}{\sigma}) + Q(\frac{h-\sqrt{m_1}}{\sigma})]$	all	$D \le z_1$
	$\frac{1}{2}[Q(\frac{h+\sqrt{m_1}}{\sigma}) + Q(\frac{h-\sqrt{m_1}}{\sigma})]$	$\sqrt{m_1} \le z_3$	$z_1 \le D \le z_2$
	$\frac{1}{2}[Q(\frac{h+D}{\sigma}) + Q(\frac{h-D}{\sigma}) - Q(\frac{h+z_3}{\sigma}) - Q(\frac{h+z_3}{\sigma})]$ $\cdot[\frac{m_1-z_3^2}{D^2-z_3^2}] + \frac{1}{2}[Q(\frac{h+z_3}{\sigma}) + Q(\frac{h-z_3}{\sigma})]$	$z_3 \le \sqrt{m_1} \le D$	$z_1 \le D \le z_4$
	$\frac{1}{2D^2}[Q(\frac{h+D}{\sigma}) + Q(\frac{h-D}{\sigma}) - 2Q(\frac{h}{\sigma})]m_1 + Q(\frac{h}{\sigma})$	all	$D \ge z_4$

Table B1. Second moment lower bounds on P_e.

SNR	P_e^U	m_1	D
$\frac{h}{\sigma} < \sqrt{3}$	$\frac{1}{2}[Q(\frac{h+\sqrt{m_1}}{\sigma}) + Q(\frac{h-\sqrt{m_1}}{\sigma})]$	all	all
$\frac{h}{\sigma} \geq \sqrt{3}$	$\frac{1}{2D^2}[Q(\frac{h+D}{\sigma}) + Q(\frac{h-D}{\sigma}) - 2Q(\frac{h}{\sigma})]m_1 + Q(\frac{h}{\sigma})$	all	$D \leq z_2$
	$\frac{1}{2z_2^2}[Q(\frac{h+z_2}{\sigma}) + Q(\frac{h-z_2}{\sigma}) - 2Q(\frac{h}{\sigma})]m_1 + Q(\frac{h}{\sigma})$	$\sqrt{m_1} \leq z_2$	$z_2 \leq D \leq z_4$
	$\frac{1}{2}[Q(\frac{h+\sqrt{m_1}}{\sigma}) + Q(\frac{h-\sqrt{m_1}}{\sigma})]$	$z_2 \leq \sqrt{m_1} \leq D$	$D \geq z_4$

Table B2. Second moment upper bounds on P_e.

convex $\cap$ for all values of z or $\mathcal{C}$ is initially convex $\cap$, then convex $\cup$, and finally convex $\cap$ as z varies from zero to infinity.

In order to determine the critical value of $\frac{h}{\sigma}$ (SNR_c) at which the second case occurs, we will again consider the equation $r''(z) = P(z)F(z)$. Note that the second case results from the first case when the maximum of $F(z)$ is greater than zero. In equation form this condition is equivalent to requiring that

$$\frac{dF(z_p)}{dz} = 0 \text{ when } F(z_p) = 0 \tag{B.25}$$

where z_p is the point at which the convexity of $\mathcal{C}$ changes. From (B.10) we have

$$\frac{dF(z_p)}{dz} = [h + 2z_p] + [h-2z_p + \frac{2h}{\sigma^2}(z_p h - z_p^2 - (n-1)\sigma^2)]e^{\frac{2z_p h}{\sigma^2}} = 0 \tag{B.26}$$

and

$$F(z_p) = [z_p h^2 + z_p^2 + (n-1)\sigma^2] + e^{\frac{2z_p h}{\sigma^2}}[z_p h - z_p^2 - (n-1)\sigma^2] = 0 . \tag{B.27}$$

Solving for $e^{\frac{2z_p h}{\sigma^2}}$ in (B.26) and (B.27) and equating the two results, we find that z_p is the solution to the quartic equation

$$z_p^4 + [(2n-1)\sigma^2 - h^2]z_p^2 + \sigma^4(n-1)(n-2) = 0 . \tag{B.28}$$

Note that (B.28) is actually a quadratic equation in the variable z_p^2 and hence has a solution given by

$$z_p^2 = \frac{\sigma^2}{2}\{[\frac{h^2}{\sigma^2} - (2n-1)] \pm [(\frac{h^2}{\sigma^2} - (2n-1))^2 - 4(n-1)(n-2)]^{\frac{1}{2}}. \quad (B.29)$$

In order for a solution to exist, z_p^2 must be real, i.e.

$$\frac{h^2}{\sigma^2} \geq (2n-1) + \sqrt{4(n-1)(n-2)}\ . \quad (B.30)$$

Note that (B.30) is just the condition on $\frac{h}{\sigma}$ for $\mathcal{C}$ to be both convex $\cap$ and convex $\cup$. Alternatively, if we define SNR_c as

$$SNR_c \triangleq [(2n-1) + \sqrt{4(n-1)(n-2)}\ ]^{\frac{1}{2}}, \quad (B.31)$$

then $\mathcal{C}$ is convex $\cap$ for all values of z if $\frac{h}{\sigma} < SNR_c$; otherwise $\mathcal{C}$ has both convex $\cap$ and convex $\cup$ regions.

In Figure B3 we have plotted $\mathcal{C}$ for various values of $\frac{h}{\sigma}$ and D. Using these plots and the value of $m_1 = E\{k_1(z)\}$, we may easily write down equations for lower and upper bounds on P_e and have done so in Tables B4 and B5, respectively. Note that the error bounds are dependent upon the values of the points z_1 through z_7 depicted in Figure B3. The points z_2 and z_4 are the solutions to the equation

$$r''(z) = 0 \quad (B.32)$$

for $\frac{h}{\sigma} \geq SNR_c$. The point z_3 is the point on $\mathcal{C}$ such that a line drawn from the point $(k_1(0),k_2(0))$ is tangent to $\mathcal{C}$ at z_3, i.e., z_3 is the solution to the equation

$$\frac{1}{2z_3^n}\{Q(\frac{h+z_3}{\sigma}) + Q(\frac{h-z_3}{\sigma}) - 2Q(\frac{h}{\sigma})\} = r'(z_3)\ . \quad (B.33)$$

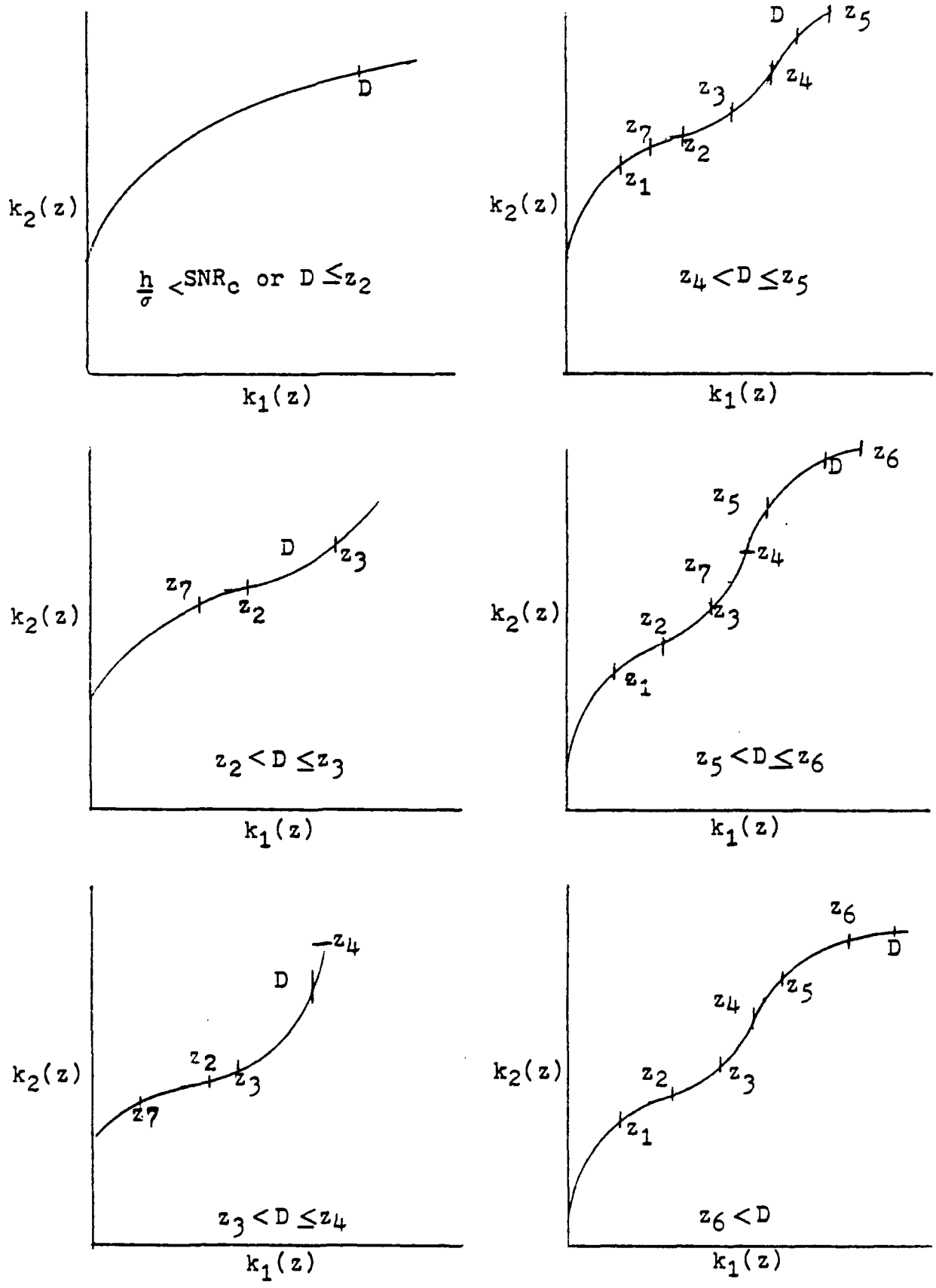

Figure B3. Plot of $\mathcal{C}$ for Nth moment space bounds.

SNR	P_e^L	m_1	D
$SNR < SNR_c$	$[Q(\frac{h+D}{\sigma}) + Q(\frac{h-D}{\sigma}) - 2Q(\frac{h}{\sigma})][\frac{m_1}{2D^n}] + Q(\frac{h}{\sigma})$	all	all
$SNR \geq SNR_c$	$[Q(\frac{h+D}{\sigma}) + Q(\frac{h-D}{\sigma}) - 2Q(\frac{h}{\sigma})][\frac{m_1}{2D^n}] + Q(\frac{h}{\sigma})$	all	$D \leq z_3$
	$[Q(\frac{h+z_3}{\sigma}) + Q(\frac{h-z_3}{\sigma}) - 2Q(\frac{h}{\sigma})]\ \frac{m_1}{2z_3^n} + Q(\frac{h}{\sigma})$	$\sqrt[n]{m_1} \leq z_3$	$z_3 < D \leq z_4$
	$\frac{1}{2}[Q(\frac{h+\sqrt[n]{m_1}}{\sigma}) + Q(\frac{h-\sqrt[n]{m_1}}{\sigma})]$	$z_3 \leq \sqrt[n]{m_1} \leq D$	
	$[Q(\frac{h+z_3}{\sigma}) + Q(\frac{h-z_3}{\sigma}) - 2Q(\frac{h}{\sigma})]\ \frac{m_1}{2z_3^n} + Q(\frac{h}{\sigma})$	$\sqrt[n]{m_1} \leq z_3$	$z_4 < D \leq z_6$
	$\frac{1}{2}[Q(\frac{h+\sqrt[n]{m_1}}{\sigma}) + Q(\frac{h-\sqrt[n]{m_1}}{\sigma})]$	$z_3 < \sqrt[n]{m_1} \leq z_7$	
	$[Q(\frac{h+D}{\sigma}) + Q(\frac{h-D}{\sigma}) - Q(\frac{h+z_7}{\sigma}) - Q(\frac{h-z_7}{\sigma})]$ $\cdot [\frac{m_1 - D^n}{2(D^n - z_7^n)}] + \frac{1}{2}[Q(\frac{h+D}{\sigma}) + Q(\frac{h-D}{\sigma})]$	$z_7 < \sqrt[n]{m_1} \leq D$	
	$[Q(\frac{h+D}{\sigma}) + Q(\frac{h-D}{\sigma}) - 2Q(\frac{h}{\sigma})]\ \frac{m_1}{2D^n}$ $+ Q(\frac{h}{\sigma})$	all	$D > z_6$

Table B3. Nth moment lower bounds on P_e.

SNR	P_e^U	m_1	D
$SNR < SNR_c$	$\frac{1}{2}[Q(\frac{h+\sqrt[n]{m_1}}{\sigma}) + Q(\frac{h-\sqrt[n]{m_1}}{\sigma})]$	all	all
$SNR \geq SNR_c$	$\frac{1}{2}[Q(\frac{h+\sqrt[n]{m_1}}{\sigma}) + Q(\frac{h-\sqrt[n]{m_1}}{\sigma})]$	$\sqrt[n]{m_1} \leq z_7$	$z_1 \leq D \leq z_5$
	$[Q(\frac{h+D}{\sigma}) + Q(\frac{h-D}{\sigma}) - Q(\frac{h+z_7}{\sigma}) - Q(\frac{h-z_7}{\sigma})]$ $\cdot[\frac{m_1-D^n}{2(D^n-z_7^n)}] + \frac{1}{2}[Q(\frac{h+D}{\sigma}) + Q(\frac{h-D}{\sigma})]$	$z_7 \leq \sqrt[n]{m_1} \leq D$	
	$\frac{1}{2}[Q(\frac{h+\sqrt[n]{m_1}}{D}) + Q(\frac{h-\sqrt[n]{m_1}}{D})]$	$\sqrt[n]{m_1} \leq z_1$	$D > z_5$
	$\frac{1}{2}[Q(\frac{h+z_5}{\sigma}) + Q(\frac{h-z_5}{\sigma}) - Q(\frac{h+z_1}{\sigma}) - Q(\frac{h-z_1}{\sigma})]$ $\cdot[\frac{m_1-z_1^n}{2(z_5^n-z_1^n)}] + \frac{1}{2}[Q(\frac{h+z_1}{\sigma}) + Q(\frac{h-z_1}{\sigma})]$	$z_1 < \sqrt[n]{m_1} \leq z_5$	
	$\frac{1}{2}[Q(\frac{h+\sqrt[n]{m_1}}{\sigma}) + Q(\frac{h-\sqrt[n]{m_1}}{\sigma})]$	$z_5 \leq \sqrt[n]{m_1} \leq D$	

Table B4. Nth moment upper bounds on P_e.

The point z_6 is defined to be the point on $\mathcal{C}$ such that the line drawn from the point $(k_1(0),k_2(0))$ through the point $(k_1(z_3),k_2(z_3))$ intersects $\mathcal{C}$ at z_6, i.e., z_6 is the solution to the equation

$$r'(z_3) = \frac{1}{2z_6^n}\left\{Q\left(\frac{h+z_6}{\sigma}\right) + Q\left(\frac{h-z_6}{\sigma}\right) - 2Q\left(\frac{h}{\sigma}\right)\right\} . \tag{B.34}$$

The point z_7 is the point on $\mathcal{C}$ such that a line drawn from $(k_1(D),k_2(D))$ is tangent at z_7, i.e., z_7 is the solution to

$$r'(z_7) = \frac{Q\left(\frac{h+D}{\sigma}\right) + Q\left(\frac{h-D}{\sigma}\right) - Q\left(\frac{h+z_7}{\sigma}\right) - Q\left(\frac{h-z_7}{\sigma}\right)}{2[D^n - z_7^n]} . \tag{B.35}$$

Finally the points z_1 and z_5 are defined to be those points on $\mathcal{C}$ such that a line drawn from z_1 on $\mathcal{C}$ to z_5 on $\mathcal{C}$ is tangent at both points and that $\mathcal{C}$ does not intersect the connecting line, i.e., z_1 and z_5 are the solutions to the equations

$$r'(z_1) = r'(z_5) \tag{B.36}$$

and

$$r'(z_1) = \frac{Q\left(\frac{h+z_1}{\sigma}\right) + Q\left(\frac{h-z_1}{\sigma}\right) - Q\left(\frac{h+z_5}{\sigma}\right) - Q\left(\frac{h-z_5}{\sigma}\right)}{z_1^n - z_5^n} . \tag{B.37}$$

Because (B.32) through (B.35) are one variable nonlinear equations, they may be solved using any of the methods listed in the previous section. Equations (B.36) and (B.37) however are two variable nonlinear equations. One method of solving this set of equations is to use a Fibonacci search ([Aoki, 1971], [Wilde, 1964]) to search over z_5 while holding z_1 fixed, where we are trying to minimize the quantity

$$d = \left| r'(z_5)z_5^n - r'(z_1)z_1^n + \tfrac{1}{2}\left[Q\left(\frac{h+z_1}{\sigma}\right) + Q\left(\frac{h-z_1}{\sigma}\right) - Q\left(\frac{h+z_5}{\sigma}\right) - Q\left(\frac{h-z_5}{\sigma}\right)\right]\right| . \qquad (B.38)$$

Further details on finding z_1 and z_5 may be found in [Yan, 1975] for the fourth moment case.

VITA

David Edward Borth was born in Hinsdale, Illinois on June 17, 1952. He received the B.S. (with highest honors) and M.S. degrees, both in electrical engineering, from the University of Illinois at Urbana-Champaign in 1974 and 1975, respectively. From January 1974 to June 1975 he was a graduate research and teaching assistant in the Department of Electrical Engineering. He held a National Institutes of Health Fellowship in 1975.

In 1975 he joined the Systems Division of Watkins-Johnson Company, Palo Alto, California as a Member of the Technical Staff and was involved in the analysis and design of computer-controlled microwave receiving systems. In 1977 he returned to the University of Illinois as a research assistant in the Coordinated Science Laboratory. During the academic year 1977-1978 he held a University of Illinois Graduate Fellowship. Since September 1979 he has been an Assistant Professor in the School of Electrical Engineering, Georgia Institute of Technology, Atlanta Georgia.

Mr. Borth is co-author of the papers

1. D. E. Borth and C. A. Cain, "The generation of acoustic signals in materials irradiated with microwave pulses," Proceedings of the Microwave Power Symposium 1975, University of Waterloo, Waterloo, Ontario, Canada, pp. 95-98, May 28-30, 1975.
2. C. A. Cain and D. E. Borth, "The microwave hearing effect--a theoretical analysis," Abstracts of the USNC/URSI Meeting, University of Illinois, Urbana, Illinois, p. 103, June 3-5, 1975.

3. D. E. Borth and C. A. Cain, "Theoretical analysis of acoustic signal generation in materials irradiated with microwave energy," IEEE Transactions on Microwave Theory and Techniques, vol. MTT-25, pp. 944-954, November 1977.

4. D. E. Borth and M. B. Pursley, "Direct-sequence spread-spectrum multiple-access communication for a class of Rician fading channels," Proceedings of the National Telecommunications Conference, vol. 3, pp. 35.2.1-35.2.6, December 1978.

5. D. E. Borth and M. B. Pursley, "Spread-spectrum communication via fading channels," Abstracts of the 1979 IEEE International Symposium on Information Theory, Grignano, Italy, June 25-29, 1979.

6. D. E. Borth and M. B. Pursley, "Analysis of direct-sequence-spread-spectrum multiple-access communication over Rician fading channels," IEEE Transactions on Communications, vol. COM-27, October 1979.

7. D. E. Borth, M. B. Pursley, D. V. Sarwate, and W. E. Stark, "Bounds on error probability for direct-sequence spread-spectrum multiple-access communications," 1979 MIDCON Conference Proceedings, Chicago, Illinois 1979.

Mr. Borth is a member of Phi Eta Sigma, Phi Kappa Phi, Eta Kappa Nu, and Tau Beta Pi and is a student member of the Institute of Electrical and Electronics Engineers.

END